COPPER SCAVENGING IN PATHOGENIC MYCOBACTERIA

by

AHMED FATHY HIKAL

(Under the direction of Russell Karls)

ABSTRACT

Pathogenic mycobacteria require copper to survive within their host. As this essential mineral is toxic in abundance, both pathogen and host have evolved mechanisms to control levels of free copper ions. Nutritional immunity refers to host processes to restrict availability of copper and other trace metals in some niches while greatly increasing their concentrations in others to defend against invading microbes. How the human pathogen *Mycobacterium tuberculosis* acquires copper from its host has not been elucidated. Herein, we demonstrate that a nonribosomal peptide synthase (NRPS) operon conserved in this agent of tuberculosis and in the related fish pathogen *Mycobacterium marinum* is required for scavenging copper from low-copper environments through production of copper-binding chalkophores. Outer membrane protein PPE1 encoded in the same operon and required for copper scavenging is not involved in export of chalkophores to the surface, which suggests function in import of copper-chalkophore adducts. Cytoplasmic membrane P-type ATPase CtpB is also required for growth in low-copper environments, but a *M. tuberculosis* CtpB null strain is hypervirulent in mouse infection studies, in contrast to NRPS operon mutants which are highly attenuated. CtpB is herein proposed to export copper to the periplasm for production of copper-dependent respiration complexes required for growth and energy generation by these obligate aerobic bacteria. This work identifies important copper

trafficking processes that enable pathogenic intracellular mycobacteria to counters host copper nutritional immunity mechanisms.

INDEX WORDS: *Mycobacterium,* tuberculosis, *marinum*, nonribosomal peptide synthase, copper, chalkophore, CtpB, P-type ATPase

COPPER SCAVENGING IN PATHOGENIC MYCOBACTERIA

by

AHMED FATHY HIKAL

B.V.Sc., Sadat University, Egypt, 2003

M.V.Sc, Benha University, Egypt, 2009

A Dissertation Submitted to the Graduate Faculty of The University of Georgia in Partial Fulfillment of the Requirements for the Degree

DOCTOR OF PHILOSOPHY

ATHENS, GEORGIA

2022

COPPER SCAVENGING IN PATHOGENIC MYCOBACTERIA

by

AHMED FATHY HIKAL

Major Professor:	Russell Karls
Committee:	Eric Lafontaine
	Ellen Neidle
	David Peterson
	Fredrick Quinn

Electronic Version Approved:

Ron Walcott
Vice Provost for Graduate Education and
Dean of the Graduate School
The University of Georgia
August 2022

DEDICATION

With genuine gratitude, I dedicate this work to my wife (Shaimaa Ballouz) and my children (Huda, Rahma, Habiba, and Albaraa) for their outpouring of support and love.

This thesis is also dedicated to the memory of my beloved parents (Fathy Hikal and Huda Elsheikh), who have been the source of inspiration and strength throughout my education journey.

Lastly, this study is also wholeheartedly dedicated to the memory of my teacher and Master's advisor, Dr. Adel Khalid (professor of microbiology), for his endless guidance and encouragement.

ACKNOWLEDGMENTS

First, words cannot express my recognition to my advisor, Dr. Russell Karls, for his invaluable patience and feedback. His sincerity, motivation, and talent in teaching have deeply inspired me. Dr. Karls was an integral part of me during my Ph.D. journey. Without his support, guidance in developing my methodology, and the emotional support he gave me, I wouldn't have made it. Dr. Karls has taught me the fundamentals of research and how to present my research as clearly as possible. In addition to his guidance throughout the study, Dr. Karls supported my family and me, especially in the first week we arrived in Athens, and facilitated the admission of my children to school. It was a privilege to work under his supervision.

Next, this endeavor would not have been possible without Dr. Fredrick Quinn, the head of the department and a committee member, for allowing me to join his laboratory to work under Dr. Karls' supervision and providing me with priceless advice throughout my Ph.D. program. He also coordinated with my embassy in the USA and the University of Georgia Graduate School to ease the admission process. Dr. Quinn and his family, particularly his daughter (Sarah Quinn) and his son-in-law (Mustafa Ezzarghani), gave my family and me a warm welcome when we arrived in the USA and picked us up from the airport.

I also could not have undertaken this milestone without my committee members: Dr. Ellen Neidle, Dr. Eric Lafontaine, and Dr. David Peterson, for their time, encouragement, and insightful comments. Their suggestions made my research so much richer. Furthermore, I am grateful to the

Ministry of Higher Education in Egypt and the University of Georgia for funding my Ph.D. program.

I would also like to express my deepest gratitude to my friend and former lab-mate, Dr. Oliver Shey-Njila, for providing several plasmids used in this study, sharing ideas, and fruitful discussions about our projects. I am also extremely grateful to Dr. Tuhina Gupta for conducting the animal study which underscores the significance of my research. She is also very kind and helpful. Dr. Gupta has cared about me and my project by providing new ideas and teaching me the methodology of animal infection. I would also like to reveal my profound appreciation to Dr. Hind Yahyaoui Azami, Dr. Wendy Watford, and Dr. Kaori Sakamoto for their help in conducting the animal study and histopathological examination of the animal tissues. Many thanks also go to Shelly Helms for spending so many hours training me in the BSL3 lab and guiding me in the lab before she left. Special thanks to my former lab-mate, Dr. Lauren Essler, for teaching me murine cell infection in BSL3 and sharing reagents. I am also grateful to Jamie Barber for teaching me how to use the confocal microscope. Further, I would like to thank Dr. Asif Shajahan for performing the mass spectrometry analyses to detect chalkophores signatures in Dr. Azadi's lab at the Complex Carbohydrate Research Center-UGA. Next, I express my gratitude to Dr. Anna Karls for the bright-field microscope used in my research and allowing me to use her qPCR machine.

To the rest of my former and current lab-mates, thank you for the fun and support. I had a fantastic experience in the lab in your presence. I hope our paths cross again, and I wish you the best in your careers.

Further, I would like to recognize my colleague, Dr. Ashraf Awad (professor and head of the Bacteriology, Immunology, and Mycology Department, College of Veterinary Medicine,

Benha University, Egypt), for his unwavering support and encouragement. He took care of all paperwork needed for extending my stay in the USA until my Ph.D. program was completed. Moreover, I would also like to articulate my deepest gratitude to my colleagues in Egypt, Drs. Fatma El-Hofy, Amira Rizk, Enas Soliman, and Manar Elkhayat, for their help during my Ph.D. scholarship application process and encouragement through phone calls and messages.

My close friends - Wasseem Khattab and Ahmed Abdeen, thank you for dealing with the long process of my leave extension in Egypt and for being there for me. You are such incredible friends.

I am also thankful to my parents (Fathy Hikal and Huda Elsheikh), siblings (Naglaa, Seham, Faten, Mohamed, and Reham Hikal), mother-in-law (Omiama Mosallam), and father-in-law (Elsayed Ballouz). Their belief in me, support, prayers, and motivation have uplifted my spirit throughout my education.

Lastly, I would be neglectful in not mentioning my wife and children for their love, sacrifices, understanding, prayers, enduring this long journey, and continuing support to complete my Ph.D. program.

TABLE OF CONTENTS

LIST OF TABLES

Page

LIST OF FIGURES

Page

CHAPTER 1

INTRODUCTION

Mycobacterium tuberculosis, the causative agent of tuberculosis (TB), is one of the deadliest infectious diseases [1]. The World Health Organization estimated 9.9 million cases of active TB disease and 1.3 million TB-related deaths in 2020 [1]. The emergence of multiple drug-resistant and extensively drug-resistant TB complicates treatment efforts. *Mycobacterium bovis* BCG is the only available vaccine. However, its efficacy against pulmonary TB ranges from 0 to 80% [2]. A better understanding of *M. tuberculosis* physiology will aid drug and vaccine development.

Copper is an essential trace element that functions in several enzymes involved in diverse biological reactions [3]. In *M. tuberculosis*, this metal provides a vital role as a cofactor of the Qcr-Cta aerobic respiration supercomplex and the SodC copper-zinc superoxide dismutase which protects the bacteria from superoxide radicals generated by macrophages and neutrophils [4][5][6]. Heterologous expression of outer membrane porin protein MspA from the soil saprophyte *Mycobacterium smegmatis* in *M. tuberculosis* increased sensitivity to exogenous copper [7]. Although *M. tuberculosis* lacks a MspA homolog, treatment of either species with spermine, an inhibitor of porin activity, increased tolerance to copper suggesting the potential for porins contributing to copper transport in *M. tuberculosis* [7]. Transcription sigma factor SigC in *M. tuberculosis* was shown to be required for growth in copper-deficient medium and for virulence in mice [8]. Artificial induction of *sigC* resulted in increased transcription of nonribosomal peptide synthase (NRPS) operon genes *Rv0096-Rv0101* and the *ctpB* gene encoding a copper-transporting

P-type ATPase [8]. Transposon-mediated disruption of the *Rv0097* homolog (*Mb0100*) in *Mycobacterium bovis* attenuated virulence and survival of the bovine TB agent in guinea pigs and prevented synthesis of virulence lipids; phthiocerol and phthiodiolone dimycocerosate esters (PDIMs) [9]. Expression of *Rv0097-Rv0101* homologs from *Mycobacterium marinum* in *E. coli* enabled synthesis of isonitrile lipopeptides (INLPs) if provided C10 or C12 fatty acids [10]. The *Mtb* NRPS operon was reported to synthesize zincophores (Kupyaphores) which are secreted extracellularly to warrant zinc uptake [11]. Unraveling the roles of *Rv0096-Rv0101* and *ctpB* in copper acquisition by *M. tuberculosis* are the main foci of this dissertation.

CHAPTER 2

LITERATURE REVIEW

2.1. Overview

In 1882, *M. tuberculosis* bacteria were determined by Robert Koch to be the causative agent of tuberculosis (TB) in humans [12]. The *M. tuberculosis* Complex includes tuberculous *Mycobacterium* species such as: *M. tuberculosis*, *M. bovis*, *M. africanum* and *M. microti* [13]. In humans, *M. tuberculosis* and *M. africanum* are the main causes of TB, however, *M. africanum* is generally restricted to west Africa [14]. The World Health Organization reported that *M. tuberculosis* is the leading cause of death from a single infectious agent and in 2020, 1.3 million humans died from TB [1]. Co-infection of HIV and *M. tuberculosis,* which represents 8% of TB cases worldwide, is a huge impediment to control and preventive measures for both diseases [1]. Drug-resistant TB also complicates TB eradication efforts; an estimated 2.2 million rifampicin-resistant TB and multidrug-resistant TB cases are resistant to rifampicin or isoniazid (first-line TB drugs) [1].

Humans can be infected when *M. tuberculosis* enters the respiratory tract via inhalation of aerosol droplets. When the *M. tuberculosis* bacilli reach the lower respiratory tract, they may be taken up by alveolar macrophages via receptor-mediated phagocytosis [15]. Immune-evasion mechanisms enable *M. tuberculosis* to escape lysosomal toxicity through blocking the maturation of phagosomes [16]. This pathogen can also translocate from phagosomes into the cytosol via the *M. tuberculosis*-encoded ESAT-6 protein which self assembles under acidic conditions to form

pores in the phagosomal membrane [17]. Within alveolar macrophages or dendritic cells, *M. tuberculosis* bacilli can be transported to the mediastinal lymph nodes to initiate an adaptive immune response through the activation of $CD4^+$ T cells [18]. As adaptive immune response develops, *M. tuberculosis*-infected macrophages become surrounded by recruited cells that aggregate to form granulomas to reduce bacterial dissemination. Granulomas include multi-nucleated Langerhans cells located in the center surrounded by macrophages, lymphocytes, and fibroblasts [19].

Resistance of *M. tuberculosis* to antibiotics is either attributed to intrinsic or acquired resistance. The long outer membrane lipids reduce permeability of many drugs, while drug-efflux transporters have been shown to pump antibiotics outside of the cell [20][21]. Neither natural transposons nor plasmids have been reported to be associated with natural drug resistances in *M. tuberculosis* [22].

2.2 Metal acquisition in bacteria and host nutritional immunity

Transition metals such as iron, zinc, and copper are important co-factors in biological processes for all living organisms. To acquire essential metals, *M. tuberculosis* bacteria have developed multiple tools including: elemental metal import, siderophores, and mechanisms to release metals from host proteins [5]. To suppress bacterial infection, the host restricts access to essential transition metals by a term called “nutritional immunity” [23].

2.2.1. Iron uptake in extracellular bacteria

Iron is one of the most abundant transition metals in living microorganisms. It exists in two forms: Fe^{2+} (reduced) and Fe^{3+} (oxidized) which make it a useful as an electron carrier in several

catalytic or redox reaction enzymes [24]. Therefore, it plays a crucial role in a variety prokaryotic and eukaryotic biological processes such as the Krebs cycle, oxygen utilization, gene regulation and DNA replication [25]. To block bacterial replication, mammals have evolved mechanisms to restrict free iron availability. For respiration in humans, iron is bound to the heme moiety of hemoglobin. Hemoglobin is complexed with erythrocytes, rendering iron unavailable to invading pathogens [23]. Moreover, extracellular iron is bound with high affinity to transferrin or lactoferrin which aid in limiting the availability of iron to pathogens [26]. In addition, natural resistance-associated macrophage protein 1 (Nramp1) is expressed on the phagosomal membrane extrudes Fe^{+2} out of the phagosomal compartment limiting iron accessibility by bacteria in the phagosome [27][28]. To circumvent iron scarcity, invading pathogens have evolved strategies to acquire iron from the host. A wide range of pathogenic Gram-positive and-negative bacteria often produce siderophores which bind iron with higher affinity than does host transferrin [26]. Several Gram-positive bacteria directly acquire iron through heme cell-surface receptors; however, *Bacillus anthracis* secretes a specific iron-chelating protein, hemophore, to facilitate heme uptake [26]. Nevertheless, some Gram-negative bacteria, such as *Pseudomonas aeruginosa*, use both direct heme and extracellular hemophore uptake systems to scavenge iron from the host [29].

2.2.2. Iron uptake by *M. tuberculosis*

Mycobacterium tuberculosis has two known strategies to obtain iron from the host: siderophore-mediated and direct heme utilization. Under low-iron conditions, *M. tuberculosis* generates two forms of siderophores: a bacterial membrane-associated mycobactin and an extracellular, soluble exochelin (carboxymycobactin) [30][31][32]. Unlike mycobactin, which has a long lipid membrane anchor, carboxymycobactin has a short alkyl side chain which ends with a

carboxylic acid [32]. Since carboxymycobactin is water-soluble, it can compete with host transferrin and lactoferrin and transfer the metal to the cell wall-associated mycobactin [33]. Synthesis and transport of carboxymycobactin relies on the inner membrane proteins MmpL4, MmpL5, MmpS4, and MmpS5 and interaction between those proteins is required for the full siderophores export [34][35]. Nonetheless, the mechanism for export of carboxymycobactin across the outer membrane has not been fully elucidated.

How does *M. tuberculosis* acquire iron? In deficient-iron conditions, carboxymycobactin binds ferric iron to produce ferric-carboxymycobactin that is imported across the outer membrane into the periplasm by an unknown mechanism [36]. Subsequently, an inner membrane ABC transporter, IrtA/IrtB, transports ferric-bound siderophores into the cytoplasm [37]. The IrtA N-terminal region has a flavin adenine dinucleotide domain that is proposed to functions as a flavin/ferric reductase, which reduces Fe^{+3} to Fe^{+2} to be utilized by the cell for various biological processes [38]. *Mycobacterium tuberculosis* can also use heme as a source of iron as it has been reported that the diminished growth of *ΔmbtD*, a siderophore-deficient mutant of *M. tuberculosis,* was rescued by addition of 1 μM or 10 μM hemin [39]. Supporting this data, Tullius and colleagues have identified *M. tuberculosis* Rv0203 as a hemophore-secreted protein, which binds free heme or heme-bound hemoglobin and is transported into the cytoplasm via protein MmpL11 or MmpL3 [40].

How does *M. tuberculosis* handle excess iron in the cytoplasm? At high concentration, iron generates free radicals that can damage macromolecules. Thus, *M. tuberculosis* must develop a system to store excess iron to avert its damaging effect. This concept was established by Pandey and Rodriguez who found that in iron replete conditions *M. tuberculosis* generates iron storage bacterioferritin proteins BfrB and BfrA under control of the IdeR transcriptional regulator [41].

Deletion of *bfrB* rendered the bacteria sensitive to iron toxicity and the mutant failed to persist in mice signifying the importance of iron storage for *M. tuberculosis* virulence [41].

2.2.3. Zinc homeostasis in *M. tuberculosis*

Zinc is important in all living organisms. Because zinc has a single oxidation state (+2) in solution, it is not involved in electron transfer; however, it is incorporated in protein structures such as zinc fingers or functions in enzyme catalysis [42]. Zinc is a structural element or co-factor in a wide variety of *M. tuberculosis* enzymes including: zinc metallo-peptidases, the helicase RqlH, fructose bisphosphate aldolase, carbonic anhydrase, cytidine deaminase, superoxide dismutase, and the Esx-3 secretion system substrate EsxG-EsxH complex [43]. Although zinc is essential, it is toxic when present in excess. To overcome zinc toxicity, *M. tuberculosis* encodes CtpC, a P-type ATPase zinc-efflux pump [44]. Mutation of *ctpC* resulted in impaired growth in host macrophages [44]. In addition to its role in counteracting zinc toxicity in *M. tuberculosis*, CtpC also functions as a P_{1B}-type Mn^{2+}-transporting ATPase for Mn^{2+} homeostasis, and participates in uploading Mn^{2+} into secreted bacterial metalloproteins [45]. The same study showed that CtpC has greater ATPase activity in the presence of Mn^{2+} than Zn^{2+}. Intriguingly, the *ctpC* mutant exhibited Mn^{2+} accumulation in the cytoplasm, supporting the hypothesis that CtpC is a Mn^{2+}-efflux pump [45]. More recently, *M. marinum* CtpC was shown to be involved in zinc detoxification in professional phagocytes [46]. Deletion of *ctpC* led to growth defects in zinc-supplemented medium, supporting the role of CtpC in protecting mycobacteria from toxic levels of zinc [46].

Mycobacterium tuberculosis encodes zinc uptake regulator, Zur, which was identified as a zinc-sensitive transcriptional repressor that regulates 32 genes in the same operon [47]. The same

study did not observe growth defects when *zur* mutant was grown in zinc-deficient medium, which suggest that *M. tuberculosis* use another mechanism to obtain zinc when it is restricted [47]. Zinc-binding molecules, termed kupyaphores, were recently reported to be synthesized by a nonribosomal peptide synthase (NRPS) operon to scavenge zinc and protect *M. tuberculosis* from zinc starvation [11]. These molecules consist of diacyl-diisonintrile lipopeptides with an ornithine-phenylalaninol core [11]. The authors reported detection of these molecules in the lungs of mice infected for 6-15 days, but not after 28 days, which suggested that *M. tuberculosis* may encounter nutrient deprivation during infection [11].

2.2.4. Copper homeostasis in bacteria

Copper is needed for all living aerobic organisms. Its ability to cycle between Cu (II) and Cu (I) forms under physiological conditions underlies its essentiality in single electron cuproenzymes such as: superoxide dismutase, cytochrome oxidase, nitrate reductase, nitric oxide reductase, and NADH dehydrogenase [48]. Cuproproteins that involved copper storage and Cu-chaperones also bind copper temporarily and deliver it to cuproenzymes [49]. Excess copper is toxic to bacteria; unbound copper in the cell can react with hydrogen peroxide to generate hydroxyl radicals that damage DNA, protein, and lipids [50]. In abundance, Cu (I) was also shown to replace iron ions in iron-sulfur cluster enzymes such as isopropyl malate dehydratase and fumarase, leading to the inactivation of branched-chain amino acid biosynthesis in *E. coli* regardless of the presence of oxygen [51].

2.2.4.1. Mechanisms of copper homeostasis in bacteria

Copper homeostatic mechanisms have been extensively studied in several pathogenic and non-pathogenic bacteria. The *Enterococcus hirae cop* operon encodes CopA, CopB, CopY, and CopZ, which are known to control copper levels inside the bacteria [52]. Among these proteins, CopA and CopB, the P-type ATPases, are predicted copper-transport proteins [52]. Odermat and colleagues demonstrated that the CopA is a Cu (I) importer, whereas CopB exports Cu (I) to the periplasm [53]. When *E. hirae* is grown in a copper-deficient medium, CopA imports copper across the cytoplasmic membrane [54]. In addition to CopA, *E. hirae* encodes copper chaperone protein, CopZ, which binds and transfers two copper atoms to the Zn^{2+}-bound CopY where the two Cu (I) atoms displace Zn^{2+}, leading to the release of CopY from its promoter, allowing the expression of the *cop* operon [52]. To circumvent the adverse effect of copper, the *E. hirae* chaperone protein CopZ transports Cu (I) to the copper-efflux ATPase CopB for export from the cell [52][55][54].

Copper tolerance in *E. coli* is controlled mainly by the Cue system, which includes the P-type ATPase copper-efflux protein CopA that exports Cu (I) from the cytoplasm to the periplasm where the periplasmic-multicopper oxidase CuO converts Cu (I) to the less toxic Cu (II) form [56][57][58]. Disruption of *copA* resulted in a severe growth defects in copper-supplemented medium [58]. In addition to the Cue system, tolerance to high levels of copper (400 μM) in *E.coli* is controlled by the copper-responsive two-component system CueRS [57]. More specifically, this system is pivotal to *E. coli* when grown under anaerobic conditions, where copper accumulation reaches to an extremely high levels as opposed to aerobic cells [57]. Uropathogenic *E. coli,* however, are protected from copper toxicity by chelating the host-derived Cu (II) using a soluble catecholate siderophore, yersiniabactin (Ybt) [59]. The Cu^{2+}-Ybt complex was detected by LC-

MS/MS in urine samples of humans with urinary tract infection (UTIs) demonstrating the important role of Ybt during infection [59].

2.2.4.2 Copper homeostasis in *Mycobacterium tuberculosis*

As an obligate pathogen, *M. tuberculosis* bacteria have evolved strategies to counteract copper toxicity in macrophages. It has been estimated that *M. tuberculosis* bacteria encounter a high- copper (up to 426 μM) environment inside phagosomes one hour post-infection [60]. In response to elevated copper (500 μM) *in vitro*, *M. tuberculosis* upregulate 30 genes, including genes *csoR* and *ctpV* encoding CsoR and CtpV, the first identified proteins in the *M. tuberculosis csoR* copper toxicity-response operon reported to function in copper tolerance [61][62][63]. In the absence of copper, CsoR represses transcription of the *csoR* operon; however, in the presence of excess copper, CsoR binds a single copper ion and de-repress the operon allowing the transcription of the *cso* operon genes [61]. Of genes in this operon, *ctpV,* which encodes CtpV, the P-type ATPase, exports copper across the inner membrane and is required to maintain copper homeostasis in M. tuberculosis during infection [62]. Even though deletion of *ctpV* did not result in a significant virulence defect in guinea pigs or BALB/c mice, *M. tuberculosisΔctpV* showed a growth defect after exposure to 500 μM copper chloride [62]. This pathogen also uses another strategy to resist copper toxicity. Festa and colleagues identified *lpqS, Rv2963, mymT, socAB* and *ricR* as a regulon controlled by the regulated-in-copper repressor, RicR [64]. The authors observed that deletion of *ricR* resulted in constitutive expression of the regulon genes and the mutant was highly resistant to copper toxicity. Intriguingly, the *mymT* (mycobacterial metallothionein) gene was the most-expressed gene in the RicR regulon [64]. Localized in the cytoplasm, MymT sequesters excess copper by binding up to six copper atoms to facilitate copper resistance [65]. Disruption of *mymT*

did not result in attenuation in mice which may suggest that *M. tuberculosis* uses additional Cu^{+}-detoxification systems in the host [65]. Since CtpV only pumps Cu ions across the inner membrane to the periplasm, an outer membrane protein is likely required to export Cu ions from the bacteria [62]. Wolschendorf and colleagues showed that the MctB (Rv1698) protein is an outer membrane protein that prevents cuprous ion accumulation in the periplasm [66]. That study tested the effect of metals including Cu^{2+}, Fe^{3+}, Zn^{2+}, Mn^{2+}, and Ni^{2+} on *M. tuberculosisΔmctB* growth; only copper impaired growth of the mutant. Additionally, the *M. tuberculosisΔmctB* strain was also significantly attenuated in guinea pigs suggesting the pivotal role of the MctB in copper tolerance [66]. Like *E.coli*, *M. tuberculosis* also use a similar multicopper oxidase protein, the membrane-associated mycobacterial multicopper oxidase, MmcO, to oxidizes toxic Cu (I) to Cu (II) in the periplasm [67]. Deletion of *M. tuberculosis mmco* severely inhibited growth in medium supplemented with 50 μM copper demonstrating a role for MmcO in copper tolerance [67]. Although the copper-efflux mechanism has been identified in *M. tuberculosis*, the copper-import system is still not fully understood. The *M. smegmatis* porin protein, MspA, has been ascribed to be involved in copper uptake, which was confirmed by *ΔmspA* tolerance to toxic levels of copper (100μM) [7]. Since *M. smegmatis* belongs to non-tuberculous mycobacteria, its copper uptake system is most likely not conserved in pathogenic mycobacteria; the latter are predicted to use a sophisticated mechanism to obtain copper from the host.

2.2.4.3. Metallophores in bacteria and their roles in copper uptake

To fulfil the high demand of copper that is needed in metalloenzymes, which perform aerobic oxidation of methane to methanol as a carbon source for energy, *Methylosinus trichosporium*, a Gram-negative methanotrophic bacterium, secretes high-affinity copper-chelators [68]. In a low-copper environment, methanotrophs express particulate methane

monooxygenase enzymes (pMMO) and soluble monooxygenase (sMMO) [69]. The first complete crystal structure of copper-binding molecule methanobactin was resolved in 2004; this molecule is secreted when *M. trichosporium* OB3b or *Methylococcus capsulatus* are grown in a copper-starved media [70]. The core structure of the copper-methanobactin (Cu-mb) chromopeptide of *M. trichosporium* OB3b mainly consists of imidazole rings that coordinate copper [70]. Metallophores are not defined only in methanotrophs but also in other bacteria, such as Streptomyces [71]. Wang and colleagues identified a *Streptomyces thioluteus* diisonitrile product (SF2768), synthesized in part by a nonribosomal peptide synthase (NRPS) gene cluster (*sfa*), that functions as a chalkophore by aiding copper import through binding extracellular copper and delivering it to the ABC transporter Orf19 for transport into the cytoplasm [71]. Genes in the *sfa* gene cluster have homology to genes in the NRSP operon in *Mycobacterium marinum*, suggesting the possibility of a conserved copper-uptake mechanism [71].

2.3. Nonribosomal peptide synthase operons in mycobacteria

Nonribosomal peptide synthase (NRPS) operons are conserved in several pathogenic *Mycobacterium* species [10][71]. In *M. tuberculosis,* the NRPS operon consists of genes *Rv0096-Rv0101*. These genes are conserved to varying degrees in *Mycobacterium bovis, Mycobacterium leprae, Mycobacterium marinum, Mycobacterium abscessus, and Mycobacterium ulcerans* [10].

The first gene in the *M. tuberculosis* NRPS operon, *Rv0096* encodes PPE1*,* a member of PE/PPE protein family [72]. This family is named for the conserved proline-glutamate and proline-proline-glutamate residues in the N-terminal region of the encoded proteins [73]. Cole and colleagues noted that approximately 10% of the *M. tuberculosis* genome encodes PE/PPE proteins [72]. The PPE family consists of 68 members that have ~180 amino-acid residues conserved in the

N-terminal region and categorized into 3 classes [73]. The first is the **m**ajor **p**olymorphic **t**andem **r**epeat (MPTR) class, characterized by multiple copies of the Asn–X–Gly–X– Gly–Asn–X–Gly motif [73]. The second class is defined by the presence of a conserved motif at position 350, whereas the third does not have well-characterized proteins other than the conserved 180 amino acids of the PPE domain [73]. Some of the PPE family members have been detected on the bacterial surface, suggesting potential functions in *M. tuberculosis* virulence [74]. Members of the PE/PPE family are highly expressed during infection suggesting the important role they play inside the host [75]. Although the exact functions of PE/PPE proteins are unknown, they are polymorphic and associated with the bacterial surface or secreted [74][76]. There is a link between secretion of PPE proteins and the ESX-5 (ESAT-6-like) secretion system in pathogenic mycobacteria; PE_PGRS and PPE-MPTR proteins were shown to be secreted via ESX-5 secretion systems in *M. tuberculosis* [77][78]. Although transposon insertion into *PPE1* indicated the gene was non-essential for *M. tuberculosis* growth *in vitro*, the mutation hindered bacteria replication in murine macrophages [79][80] Detection of the PPE1 protein in the lungs of guinea pigs 90 days after *M. tuberculosis* infection suggests a role in virulence [75], however, the specific function of PPE1 has yet to be established.

The second gene in the *M. tuberculosis* NRPS operon, *Rv0097*, encodes a putative oxidoreductase with a cytochrome c oxidase subunit I copper-binding signature [81]. Sequence analysis of Rv0097 shows 98% conservation in the *M. tuberculosis* complex, which suggest that Rv0097 plays an important role in pathogenic mycobacteria [82]. Expression of *Rv0097* was reported to be higher (1.43 fold) in immunocompetent BALB/c mice compared to severe-combined immunodeficient (SCID) mice at 21 days post-infection [83]. In the cattle agent of tuberculosis, *M. bovis*, transposon insertion into *Mb100*, the *Rv0097* homolog, resulted in

attenuation in guinea pigs and loss of production of virulence lipids: phthiocerol and phthiodiolone dimycocerosate esters (PDIMs), further indicating the crucial role of Rv0097 in virulence [9]. It is worth noting that transposon insertion caused polar effects on the transcription of genes downstream from *Mb100* [9]. Additionally, sera of *M. tuberculosis*-infected guinea pigs recognized Rv0097 in extracts from stationary pellicle cultures but not from shaking cultures of the pathogen and was detected by mass spectrometry in *M. tuberculosis* strain H37Rv cultured in a defined minimal medium, Sauton medium which shows that Rv0097 is produced under metal deprivation condition [82][84].

The third genes in the *M. tuberculosis* NRPS operon, *Rv0098*, was initially identified as a type III fatty acyl-coenzyme A (CoA) thioesterase (FcoT) that hydrolyzes fatty acyl-CoA to free fatty acid and coenzyme A [85]. A later study has showed that Rv0098 catalyzes the Michael addition of glycine to the β-position of an α,β-unsaturated fatty acyl-Acyl Carrier Protein (ACP) to generate N-carboxymethyl-3-aminoacyl-ACP, an intermediate product in an isonitrile lipopeptide synthesis (INLP) pathway [10][11].

The fourth gene in the *Rv0096-Rv0101* operon, *Rv0099*, encodes a fatty acyl-AMP ligase (FAAL) which activates fatty acids by adenylation and subsequently transfers the fatty acyl group to the ACP domain of Rv0100, the fifth encoded protein in the same operon [86]. The same study has revealed by electrospray ionization-quadrupole time of flight (ESI-QTOF) mass spectrometry that the holo-acyl carrier protein Rv0100 is acylated after incubation with Rv0099 and fatty acids of different lengths to be further processed to generate INLPs [86][10].

The last gene of the *Rv0096-Rv0101* operon is the 7.5 kb *Rv0101* encoding a nonribosomal peptide synthase [87]. By two-dimension liquid chromatography (2DLC) mass spectrometry, Rv0101 has been identified in *M. tuberculosis* cell wall, cell membrane, and cytosol fractions [88].

Like *Rv0097*, *Rv0101* was reported as nonessential for growth in vitro, but is required for survival *in vivo* [89][90][91]. Rv0101 has seven catalytic domains; two condensation domains (C), two adenylation domains (A), two thiolation domains (T), and a reductase domain (R) that act in assembly-line through condensation of a monomeric unit to generate INLP [92]. The R domain of Rv0101 was shown to release an acyl chain after forming an aldehyde intermediate [92]. Rv0101 functions to link two INLP chains through incorporation of two amino acids resulting in a final diisonitrile dilipopeptide linked by and ornithine-phenylalaninol dipeptide [11]. Deletion of *Rv0101* resulted in impaired growth in zinc-chelated medium [11]. Also, Harris and colleagues reported a decrease in intracellular zinc pool after deletion of the *Rv0096-Rv0101* homolog in *M. marinum*, suggesting a role in metal transport [10]. A proposed function of the Rv0097-Rv0101 enzymes was discussed in a recent study [11] which suggested that fatty acyl AMP ligase Rv0099 attaches a long-chain fatty acid to acyl carrier protein Rv0100. Thioesterase Rv0098 then incorporates a glycine at the carbon-carbon double bond. Next, oxidoreductase Rv0097 modifies the glycyl group to an isonitrile. Nonribosomal peptide synthase Rv0101 has multiple domains: two sets of condensation (C), adenosylation (A), and transferase (T) domains followed by a reductase (R) domain. The first C-A-T set links two isonitrile lipid chains with amino acid ornithine. The second C-A-T set adds a phenylalaninol. Finally, the reductase releases the di-isonitrile dilipopeptide product from the enzyme complex [11].

2.4. Regulation of the nonribosomal peptide synthase operon

To date, there are at least four regulators for the *Rv0096-Rv0101* operon in *M. tuberculosis.* 1) This operon is negatively regulated by the SenX3–RegX3 two-component regulatory system as all six genes of this operon are highly upregulated in a *senX3–regX3* mutant [93]. 2) SigM was

found to positively regulate the *Rv0096-Rv0101* operon among other genes in *M. tuberculosis*, such as *esxU* and *esxT* (components of EsX-4 secretion proteins) [94]. 3) The *Rv0096-Rv0101* operon is positively regulated by Rip1 and negatively regulated by the PdtaRS two-component system; Rip 1 triggers transcription of the PPE1-5′ (the start site of *PPE1* to 277 nucleotides after the *PPE1* translation initiation site), then PPE1-5′ mRNA binds to PdtaR, thereby derepressing the expression of the NRPS cluster [95]. 4) Our laboratory has revealed that transcription of the *Rv0096-Rv0101* operon requires sigma factor C (SigC) in copper-limited Sauton medium and when free copper is depleted from Sauton medium by using the copper (II)-specific chelator ammonium tetra-thiomolybdate (TTM) [8].

In chapter 3, I discuss the role of the inner membrane P-type ATPase, CtpB, in copper transport and virulence in mice. This work is a continuation of a research that had been performed by Dr. Oliver Shey-Njila, a former graduate student in the laboratory [96]. In chapter 4, I describe a mechanism of copper scavenging utilizing the *M. tuberculosis Rv0096-Rv0101* operon or the homologous operon in *M. marinum* and examine the impacts of deleting *Rv0097* on virulence and replication of *M. tuberculosis* in mice.

CHAPTER 3

ROLES FOR COPPER-TRANSPORTING PROTEIN CTPB IN *MYCOBACTERIUM TUBERCULOSIS* REPLICATION IN LOW-COPPER NICHES *IN VIVO*[1]

[1]The work presented in this chapter was a portion of the following article: Hikal AF, Shey-Njila O, Gupta T, Sakamoto K, Yahyaoui Azami H, Watford WT, Quinn FD, and Karls RK. CtpB facilitates *Mycobacterium tuberculosis* growth in copper-limited niches. *International Journal of Molecular Sciences*. 2022 May 20;23(10):5713. doi: 10.3390/ijms23105713 [97]. Portions reprinted here with permission of publisher.

ABSTRACT

Copper is a required trace metal for bacterial pathogens and their eukaryotic hosts as it catalyzes single electron-transfer reactions in the catalytic sites of important cuproenzymes. The high reactivity of copper (I) ions can result in toxicity from damage to key enzymes. Thus, copper levels must be carefully controlled. As an evolutionary response to infection, host cells developed nutritional immunity mechanisms to alternately starve invading microbes of essential metals and subsequently deluge them with toxic concentrations of heavy metals. Successful pathogens circumvent host nutritional immunity processes. Here, we show that *ctpB*, which encodes CtpB, a cytoplasmic membrane P-type ATPase in the highly-successful human pathogen *Mycobacterium tuberculosis* is an important virulence factor. Deletion of *ctpB* resulted in hypervirulence in the DBA/2 mouse infection model. In contrast, a *ctpB* mutant replicated poorly in adipose cells, but growth was restored to wildtype levels with copper supplementation. Transcription of *ctpB* was upregulated when wildtype *M. tuberculosis* was cultured in copper-chelated medium and within infected adipocytes, but not when the medium was supplemented with copper. Based on the available data, CtpB is proposed to either function in copper acquisition in copper-limited niches or efficiently traffics the metal to the cyt *aa3-bc1* respiration supercomplex to facilitate respiration by this obligate aerobic pathogen.

INTRODUCTION

The fundamental role of copper in single electron transfer in cuproenzymes in all living organisms and toxicity of this metal in abundance requires regulated transport across biological membranes in eukaryotes and prokaryotes. For transport of charged metals across the hydrophobic

cytoplasmic membrane, energy is required. For P-type ATPases, the energy comes from ATP hydrolysis.[98] Members of this metal transporter family have three cytoplasmic domains (actuator, nucleotide-binding, and phosphorylation) and two inner-membrane domains (class-specific support and transport) [99]. For *Mycobacterium tuberculosis*, eleven cation transporter P-type ATPases were identified by in-silico analysis [100]. The functions of these putative P-type ATPases remain to be fully elucidated; however, some have been characterized to transport specific metals. For example, a homolog of CtpE has been reported to import Ca^{2+} across the inner membrane in *Mycobacterium smegmatis* [101]. López and colleagues have reported that CtpG is involved in cadmium and/or copper export across the *M. tuberculosis* plasma membrane [102]. The same study showed that despite the ATPase activity of CtpG when supplemented with different heavy metals, CtpG preferentially bound cadmium, which suggest a role for CtpG in cadmium detoxification [102]. CtpG has also been reported to be activated by zinc and play a role in zinc detoxification in *M. bovis* [103]. CtpV was identified as an efflux pump which exports copper ions from *M. tuberculosis* in response to a toxic level of copper [104]. CtpA contributed somewhat to copper resistance when expressed in *M. smegmatis* [105]. León-Torres et al. showed that even though Cu (I) increases ATPase activity in membranes enriched for CtpB, deletion of *ctpB* from *M. tuberculosis* did not impact survival after exposure to toxic levels of copper, suggesting that CtpB is not a copper-detoxification efflux pump [106].

Eukaryotic cells tightly limit abundance of free essential trace metals, such as copper, in some compartments to minimize availability to invading microbes, but flood others to intoxicate the invaders in a term known as “nutritional immunity” [107]. Some pathogens have evolved mechanisms to scavenge copper from their host. Our laboratory has demonstrated that artificial induction of *sigC* encoding transcription sigma factor C (SigC), required for growth in a copper-

starved environment, leads to 3-fold upregulation of *ctpB*, suggesting a possible role for CtpB in copper transport [8]. Deletion of *ctpB* in *Mycobacterium bovis* BCG and *M. tuberculosis* led to growth defects in copper-starved medium [97]. The same study showed that *M. smegmatis* expressing *M. tuberculosis ctpB* could not tolerate high levels of copper salts. In the work presented in this chapter, transcription of *ctpB* is induced when *M. tuberculosis* encounters limited-copper conditions *in vitro* and *in vivo*. Growth of a *ctpB* mutant is impaired in a naturally copper-limiting host cell type, but surprisingly the same mutant is more virulent than wild type in a immune competent mouse model. These findings support CtpB function in response to host copper nutritional immunity.

RESULTS

Copper depletion induces expression of *ctpB in vitro*

Because a *M. tuberculosis* mutant lacking *ctpB* replicated poorly in copper-starved medium, [97] we sought to assess the transcriptional response of *ctpB i*n copper-chelated medium. Quantitative reverse-transcription PCR was employed to measure *ctpB* expression in wild type *M. tuberculosis* strain Erdman cultured in a copper-deficient minimal medium (SMT) containing or lacking 20 μM of a copper (II) chelator, tetrathiomolybdate (TTM). After normalization of expression to housekeeping gene *sigA*, transcription of *ctpB* was found to be upregulated 7-fold in SMT containing the chelator (Fig. 3.1 A). These results indicate that elevated *ctpB* transcription is part of the stress response to copper starvation.

Replication of *M. tuberculosis* in adipocytes requires *ctpB*

While it was previously shown that *ctpB* is needed for *M. tuberculosis* growth in copper-limited conditions *in vitro*, we hypothesized that loss of the gene would impact replication in an *in vivo* copper-deficient cell type. To test this hypothesis, murine 3T3-L1 adipocytes were employed because the parent NIH 3T3 fibroblast cell line was reported to contain a low concentration of copper [108]. Multiple studies support adipocytes as possible sanctuaries for *M. tuberculosis* during infection where the bacilli may persist for years undetected by the host immune system [109][110][111]. In our study, 3T3-L1 pre-adipocytes were differentiated to adipocytes and then infected in parallel with *M. tuberculosis* wildtype (Erdman), *ΔctpB,* the complemented *ctpB* mutant (*ΔctpB*-comp). At day 12 post-infection, *ΔctpB* showed a significant replication defect in adipocytes compared to strain Erdman and *ΔctpB*-comp (Fig. 3.2). Supplementation of *ΔctpB*-infected cells with 0.1 mM $CuCl_2$ significantly improved growth (Fig. 3.2). Together, these data demonstrate the pivotal role of *ctpB* in the replication of *M. tuberculosis* within copper-restricted host cells.

Copper decreases *ctpB* expression in 3T3-L1 adipocytes

As available copper in 3T3-L1 adipocytes is low, we hypothesized that supplementation of 3T3-L1 adipocytes with copper would lead to downregulated expression of *ctpB*. Transcription of *ctpB* was compared in adipocytes infected with *M. tuberculosis* Erdman and grown in basal medium (DMEM + 10% FBS) or basal medium supplemented with 0.1 mM $CuCl_2$ for ten days. As anticipated, *ctpB* expression was significantly lower (reduced by one-third) in adipocytes supplemented with copper relative to the expression in basal medium (Fig. 3.1 B). To assess the possibility that intracellular zinc levels in adipocytes might have an impact on *ctpB* expression, 0.1 mM $ZnSO_4$ supplementation was assayed in parallel. Transcription of *ctpB* in basal medium

supplemented with zinc was not significantly different from expression in basal medium alone (Fig.3.1 B). Thus, elevated *ctpB* expression in adipocytes is in response to a low-copper environment rather than one low in zinc.

Deletion of *ctpB* increases *M. tuberculosis* virulence in immune-competent mice

We assessed the importance of *ctpB* in replication and potential virulence of *M. tuberculosis* in immune-competent DBA/2 mice. Groups of mice were infected by tail vein injection with 1-2 x 10^5 CFU of strain Erdman, *ΔctpB,* or *ΔctpB*-comp and euthanized when moribund. Survival studies revealed that mice infected with the *ctpB* deletion mutant died earliest. The mean survival time of this group was 100 days. In contrast, the mean survival time of mice of infected with parent strain Erdman was 142 days, and 124.5 days for those infected with the complemented mutant (Fig. 3.3). Analysis of the lungs at the time of death revealed no differences in gross pathology regardless of the infecting strain [97]. Histopathological analysis of lung tissue sections confirmed extensive infiltration of polymorphonuclear cells in all groups and no significant differences between groups by various assessments of disease pathology [97]. Homogenization and plating of organ sections did not result in statistically-significant differences in the mycobacterial burdens between the mutant, complemented mutant, and parent strain. All had high mycobacterial colony counts. Approximate loads were: 8 x 10^6 CFU in the lungs, 3 x 10^5 CFU in the spleens, and 2 x 10^5 CFU in the livers, regardless of infecting strain [97]. Together, this data indicates that the *ctpB* mutant replicated more effectively than the other strains in this animal model resulting in more rapid progression to a terminal disease state.

Conservation of CtpB is limited to intracellular pathogenic mycobacteria

To assess the conservation of CtpB among mycobacteria species, phylogenetic analysis was performed. The phylogenetic tree shows that *M. tuberculosis* CtpB is very highly conserved (99-100% identity) among *M. tuberculosis* complex species (MTC) and has high conservation with mycolactone (ML)-producing species *M. ulcerans*, *M. marinum* (82% identity, 90% similarity) and the etiological agent of leprosy, *M. leprae* (78% identity, 87% similarity) (Fig. 3.4). No close homologs are detected in any other mycobacterial groups with indicates it is conserved only among intracellular pathogenic mycobacteria. Interestingly, CtpB has homology to the previously defined copper-transporting P-type ATPase, CtpA (68-69% identity, 78-80% similarity) (Fig. 3.4), which suggests that both CtpB and CtpA may have critical roles in combating nutritional immunity.

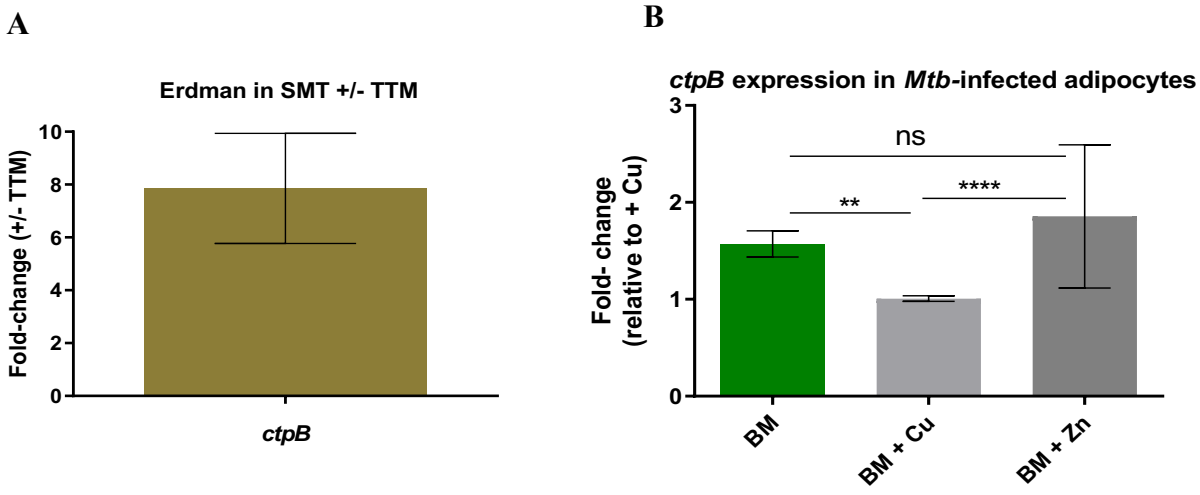

Figure 3.1. Transcription of *ctpB* in *M. tuberculosis* Erdman increases in response to copper limitation. Gene expression of *ctpB* was examined after culture of strain Erdman in A) SMT +/- 20 μM TTM or B) after infection of 3T3-L1 adipocytes cultured DMEM-FBS (basal medium, BM) or BM supplemented with 0.1 mM $CuCl_2$ or $ZnCl_2$. Gene expression was normalized to *sigA*. Figure and legend reproduced from Shey-Njila *et al*. [97]. (CC BY 4.0).

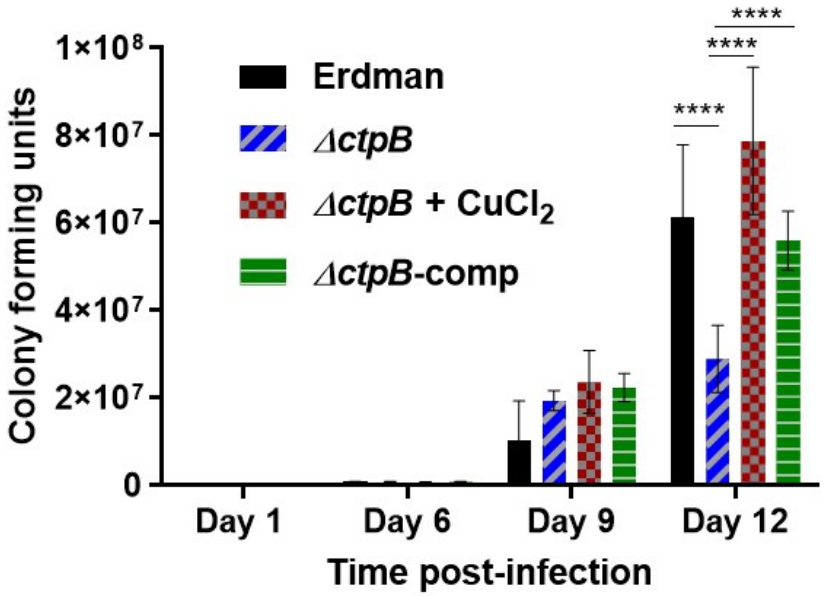

Figure 3.2. *ctpB* is required for replication and copper acquisition by *M. tuberculosis* in adipocytes. 3T3-L1 adipocytes were infected for 24 hours at MOI = 1 with the indicated strains were cultured in DMEM-FBS (basal medium, BM) or BM supplemented with 0.1 mM $CuCl_2$. At the indicated time-points, cells were lysed with 1% Triton X-100 and viable bacteria enumerated by plating on 7H10tgADS agar. Results shown are the average with standard error from two experiments performed in triplicate. ANOVA with multiple comparisons between groups was used to assess significant differences between groups (****$p<0.0001$). Figure and legend reproduced from Shey-Njila *et al*. [97]. (CC BY 4.0).

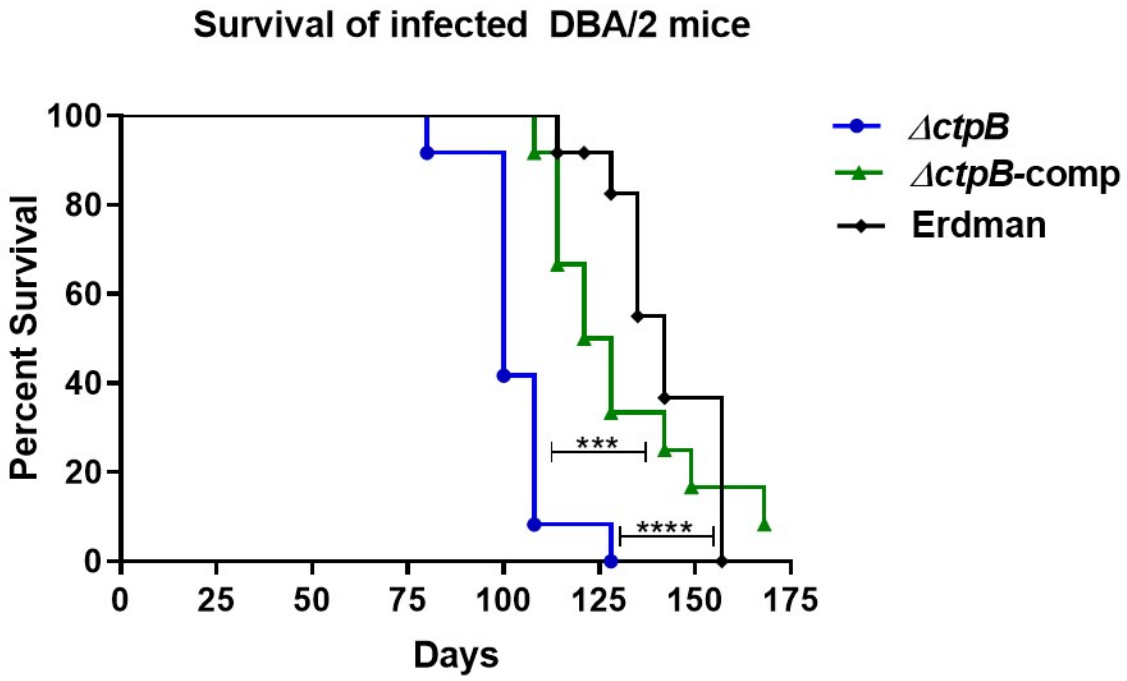

Figure 3.3. Loss of *ctpB* increases *M. tuberculosis* virulence in DBA/2 mice. Shown is relative survival of DBA/2 mice intravenously-infected with the *M.tuberculosis ctpB* mutant (Δ*ctpB*), parent strain Erdman, or complemented mutant (Δ*ctpB*-comp). Significant differences between groups was determined by applying the Mantel-Cox test (***p<0.001, ****p<0.0001). Figure reproduced from Shey-Njila *et al*. [97]. (CC BY 4.0).

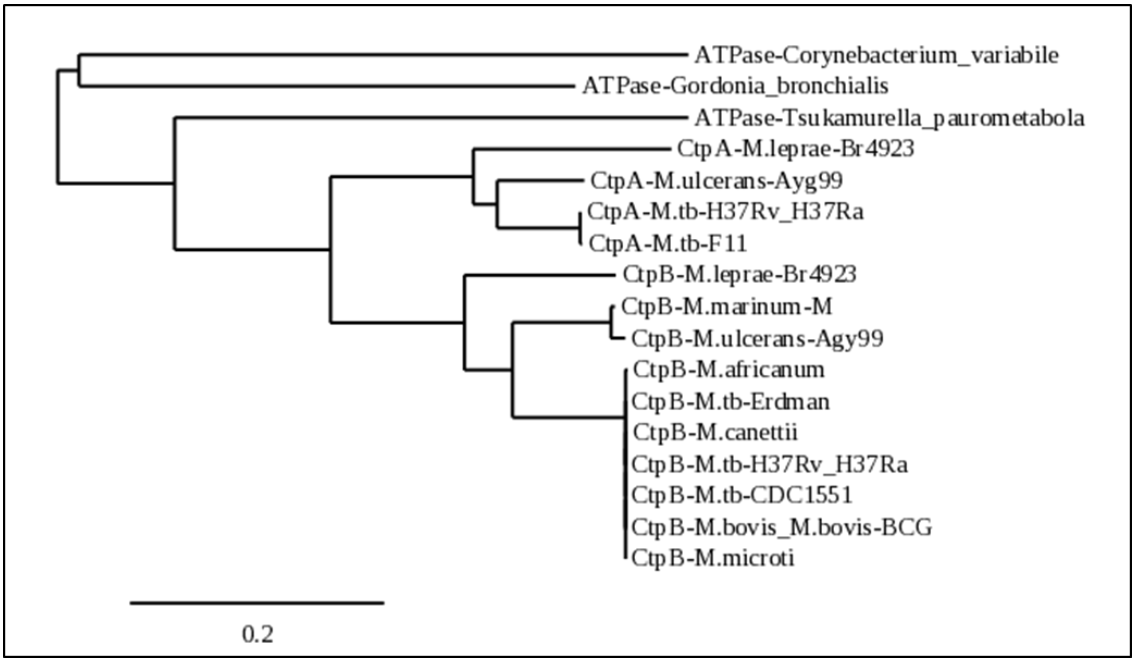

Figure 3.4. CtpB conservation among intracellular pathogenic *Mycobacterium* species. The phylogenetic tree was rendered with Phylogeny (http://www.phylogeny.fr/) alignment of CtpB homologs from mycobacterial strains of interest and top hits of homologs obtained through the Mycobrowser precomputed nonredundant protein BLAST search results for the *M. tuberculosis* H37Rv CtpB. Representative homologs for the *M. tuberculosis* (M.tb) complex, *M. marinum*/*M. ulcerans*, and *M. leprae* clades are shown. Branches with support value less than 50% are collapsed. GenBank entries used: NP_214617.1, WP_003400797.1, YP_004743591, CCC25178.1, WP_012392262.1, WP_011742338.1, CAR72097.1, CAA86363.1, WP_011961619.1, NP_214606.1, MWP_003400679.1, WP_014000034.1, WP_012392258.1, YP_908222.1, CAR72084.1, ACY21849.1, ADG76735.1. Figure and legend reproduced from Shey-Njila et al. [97]. (CC BY 4.0).

DISCUSSION

Because of its paramount importance in several biological processes inside living cells, regulated copper acquisition is imperative by pathogens that replicate in their hosts. One of the aspects of nutritional immunity is binding free copper by storage and chaperone proteins to deprive invading microbes of this critical element. In response to copper scarcity inside host cells, pathogens have developed mechanisms to obtain this metal [52]. Aerobic pathogens, such as *M. tuberculosis* must overcome host mechanisms that restrict available copper. In environments with ample quantities, copper ions may enter the *M. tuberculosis* outer membrane through undefined porin-like protein channels [7] and be imported across the cytoplasmic membrane by undefined transporters, but most likely members of the major facilitator superfamily of transport proteins [49]. Since free copper is toxic in abundance, storage in the cytoplasm of *M. tuberculosis* includes MymT, a metallothionin protein that binds up to six Cu^{+} ions [65]. In addition to copper-storage in the cytoplasm, *M. tuberculosis* limits intracellular copper levels through CtpV, a cytoplasmic-membrane P-type ATPase, to export copper from the cytoplasm into the periplasm to aid in copper detoxification [104]. Further, MctB serves as an efflux pump that exports copper ions across the outer membrane [66].

How does *M. tuberculosis* obtain copper ions or provide it to the respiratory complex when free levels of the metal are restricted? Current data is consistent with two possible roles for CtpB. Either it aids copper uptake in copper-deficient niches or it exports copper to the periplasm to be incorporated in the cyt *aa3-bc1* respiration supercomplex. Chelation of Cu^{2+} from SMT minimal medium induced expression of *ctpB* 7-fold in *M. tuberculosis* strain Erdman relative to transcription in SMT alone. Addition of Cu^{2+} to adipocytes significantly decreased transcription of *ctpB,* indicating that this gene is part of the bacterial response to copper limitation. We also

determined that replication of *M. tuberculosis ΔctpB* in adipocytes was limited due to copper scarcity as the growth defect was not evident when copper salts were added to the medium. These *in vivo* observations further indicate the important role of *ctpB* in copper transport when *M. tuberculosis* encounters naturally copper-restricted host cells. Our transcriptional data are consistent with a previous study which noted that *ctpB* may be downregulated in *M. tuberculosis* in response to supplementation with a toxic level (0.5 mM) of Cu^{2+} ions, [62] suggesting that CtpB may not function in copper detoxification [104].

As CtpB is highly conserved in pathogenic mycobacterial groups that include *M. tuberculosis*, *M. marinum*, *M. ulcerans*, and *M. leprae*, [97] this copper-transporting protein appears to have evolved exclusively in intracellular pathogenic mycobacteria to survive in copper-deprived host niches, most likely through aiding import of the metal or by efficiently directing copper to respiration complexes needed by these obligate aerobic pathogens. Intriguingly, the same pathogens have a highly-conserved P-type ATPase, CtpA, which has been shown to function as a Cu^{+} exporter in *M. tuberculosis* [97], suggesting both CtpB and CtpA function in optimizing copper trafficking. Taking into consideration the *in vitro* data that support the need for CtpB under in low-copper environments, we expected that deletion of *ctpB* would impair *M. tuberculosis* replication virulence in experimentally-infected mice. Surprisingly, the *ctpB* deletion mutant was more virulent than either its wildtype parent strain Erdman or the complemented *ctpB* mutant, resulting in earlier time-to-death of mice infected with the strain lacking *ctpB* in a long-term survival study (Fig.3.3). There were no significant differences in the lung pathology or bacterial organ burdens in mice infected with any of the strains when each animal reached a humane endpoint score and was euthanized, which is consistent with the mutant replicating more quickly than the other strains in this model system.

How can hypervirulence of *ΔctpB* be explained*?* Bacteria import a variety of metals, when present in abundance using low-specificity major-facilitator superfamily (MFS) transporters which use the energy from electrochemical potential across the membrane to import metals and other small molecules [112]. During infection, microbes encounter various stresses, including copper starvation, copper overload, and reactive oxygen and nitrogen species. When *M. tuberculosis* encounters a low-copper environment, CtpB function is clearly required and an abundance of CtpB may be synthesized. If CtpB is needed for copper import and the bacteria encounter a rapid shift to a toxic-copper intracellular environment, perhaps copper is imported through both the MFS and CtpB routes resulting in in toxification of wildtype bacteria, but not *ΔctpB* with only the MFS system. Alternatively, if CtpB functions to efficiently direct copper to the essential cyt *bc1-aa3* respiration supercomplex, then a rapid shift from low to high copper might result in excess metallation of the aerobic respiratory complexes resulting in production of reactive oxygen radical. This question is revisited in Chapter 4 in light of results of studies that examine function of the *Rv0096-Rv0101* operon. Finally, survival and virulence of the *ctpB* mutant needs to be examined in an animal model such as rabbits, guinea pigs, or nonhuman primates which, unlike mice, develop hypoxic lung granulomas, a hallmark of human tuberculosis for containing the spread of *M. tuberculosis*, [113] where increased copper-dependent respiration capacity may be required for survival of the pathogen.

Methods

Strains and growth conditions

Strains of *M. tuberculosis* used in this study included a *ctpB* deletion mutant (*ΔctpB*), the complemented *ΔctpB* mutant (*ΔctpB*-comp), and wildtype parent strain Erdman. The *ctpB* mutant

was generated by replacing *ctpB* with a hygromycin-resistance [97]. For complementation, the *ctpB* gene with upstream promoter region was introduced into the mutant on an integrative plasmid conferring resistance to gentamicin [97]. Strains of *M. tuberculosis* were first cultured in Middlebrook 7H9 broth or 7H10 agar supplemented with 10% albumin-dextrose-saline (ADS), 0.5% glycerol, and 0.05% Tween 80 (7H9tgADS and 7H10tgADS, respectively). For copper studies, bacteria were passaged at least three times in Sauton medium with cell dispersant 0.05% tyloxapol (SMT) and stored in 1 mL aliquots upon reaching OD_{600} = 1 at -80°C [97]. To determine the bacterial titers for the frozen stocks, aliquots were thawed at 37°C and cells were collected by centrifugation (10,000 x *g*, 5 min). Pellets were resuspended in 1 mL phosphate-buffered saline (PBS) and sonicated twice for 30 seconds in an ultrasonic water bath. Serial dilutions of each strain were made in PBS + 0.05% tween 80 and plated onto 7H10ADSgt agar. Plates were incubated at 37°C for 3 weeks and then colonies were counted to determine the number of colony forming units (CFU).

RNA isolation and RT-qPCR

For transcription studies *in vitro*, *M. tuberculosis* strain Erdman was cultured in 7H9tgADS, passaged three times in fresh SMT medium, and seeded into replicate cultures in SMT to OD_{600} = 0.05. Cells were incubated at 37°C with shaking (70 rpm) until OD_{600} = 0.35, at which point copper (II) chelator ammonium tetrathiomolybdate (TTM) was added to a final concentration of 20 μM to half of the cultures, and all cultures were incubated until each reached OD_{600} = 0.45, then the cells were harvested by centrifugation (10,000 x g, 5 min) and pellets stored at -80°C. Total RNA was extracted using Trizol with methodology previously described [8]. For *in vivo* transcription studies, murine 3T3L1 adipocyte cells were infected with *M. tuberculosis* strain

Erdman at a multiplicity of infection (MOI) of 1 three different flasks and incubated 10 days at 37°C in DMEM + 10% FBS, DMEM + $CuCl_2$ (100 μM) or DMEM + 10% FBS + $ZnSO_4$ (100 μM), at which time, cells were lysed in 4 M guanidine isothiocyanate and bacteria harvested by centrifugation (10,000 x *g*, 45 min). Total bacterial RNA was isolated as described previously [8].

Cell line infection studies

Murine adipocyte cell line 3T3-L1 were cultured as described [97]. Briefly, cells were cultured in DMEM + 10% bovine calf serum (BCS) and differentiated into adipocytes in DMEM-FBS (10%) containing 0.25 μM dexamethasone, 0.5 mM 3-isobutyl-1-methylxanthine (IBMX), 2 μM rosiglitazone, and 1 μg/ml insulin for 48 hours at 37°C, 5% CO_2, then medium was replaced with DMEM-FBS (10%) + 1 μg/ml insulin and cells incubated 48 hours at 37°C, 5% CO_2. Cells were maintained in DMEM-FBS (10%) until fully differentiated into adipocytes. Adipocytes were counted from three wells on the day of infection to determine the amount of bacteria to add to obtain the specific MOI. Adipocytes were infected in parallel with *M. tuberculosis* strain Erdman, *ΔctpB,* and *ΔctpB*-comp at MOI = 1 and cultured over a 12-day period. At the indicated times, cells were washed with PBS and lysed with 1% triton X-100. Serial dilutions of the lysed cells were plated onto 7H10ADSgt and plates incubated at 37°C for 3 weeks for CFU enumeration.

Murine infection studies

Female DBA/2J mice, 6-8 weeks of age. were purchased from Jackson Laboratories and injected intravenously with 1-2 x 10^5 CFU *M. tuberculosis* strain Erdman, *ΔctpB*, or *ΔctpB*-comp. Animals were euthanized upon demonstrating signs of morbidity. Necropsy, gross pathology,

histopathology, and bacterial loads in the indicated organs were performed as described previously [97].

Statistical analysis

For bacterial growth curves and transcriptional analysis, statistically-significant differences between groups was calculated using ANOVA with pair-wise comparisons. The log-rank (Mantel-Cox) test was used for the Kaplan-Meier curves to assess the significant differences in the animal survival study. GraphPad Prism software was used to plot the data and for statistical comparisons between groups.

CHAPTER 4

NONRIBOSOMAL PEPTIDE SYNTHASE OPERON FUNCTION IN COPPER ACQUISITION BY PATHOGENIC MYCOBACTERIA [1]

[1]Hikal AF, Shey-Njila O, Gupta T, Shajahan A, Sakamoto S, Yahyaoui Azami H, Watford WT, Barber JP, Azadi P, Quinn FD and Karls RK. *To be submitted to Journal of Bacteriology.*

Abstract

Copper is an essential micronutrient for *Mycobacterium tuberculosis*, but this etiological agent of tuberculosis must overcome host nutritional immunity mechanisms to replicate and cause disease. Herein, we report that the nonribosomal peptide synthase (NRPS) operon of this pathogen functions in copper scavenging and replication in copper-starved niches. Perturbation of the operon impaired growth in copper-chelated medium and in an adipose cell line that naturally restricts copper diffusion. Genes in the NRPS operon are upregulated in response to copper starvation and within adipocytes. Deletion of NRPS gene *Rv0097* led to reduced *M. tuberculosis* replication and pathology in the lungs of infected mice. We further show that the NRPS in *Mycobacterium marinum* also functions in copper scavenging. The *PPE1* gene immediately upstream of the NRPS genes in either species is also required for copper acquisition. Supernatants from a *M. tuberculosis PPE1* mutant cultured in copper-chelated medium enhanced growth of a *M. marinum Rv0097* homolog deletion mutant similarly cultured suggesting the presence of a soluble copper-binding factor which is supported by detection of mass spectroscopy peak of identical size to a known copper-binding isonitrile molecule. Conservation of this NRPS operon among various mycobacteria suggests that evolution of this metal scavenging system aids these microbes in acquiring copper, including the obligate pathogens.

Introduction

Copper is an essential mineral in all living organisms. The redox-active properties of this metal enable cuproenzymes such as cytochrome c oxidase and superoxide dismutase to catalyze single electron-transfer reactions [54]. Eukaryotic defenses against microbes include nutritional immunity mechanisms to restrict availability of trace minerals in some locales, but provide them in toxic concentrations in others [114]. In response, pathogens evolve mechanisms to obtain essential metals needed for replication from their hosts. For example, the human pathogen *Mycobacterium tuberculosis* synthesizes the siderophores mycobactin and carboxymycobactin to chelate and facilitate iron acquisition [30][31][32]. Mechanisms of copper assimilation by this pathogen remain to be fully elucidated.

Nonribosomal peptide synthase (NRPS) genes are conserved among multiple *Mycobacterium* species as well as non-mycobacterial actinomycetes and function in metal transport is an emerging theme [10]. *Mycobacterium marinum* NRPS genes *MMAR0260-MMAR0256* expressed on a multi-copy plasmid in *E. coli* enabled production of soluble isonitrile lipopeptides (INLPs) if supplied C10 or C12 fatty acids, while deletion of the region from *M. marinum* decreased the level of intracellular zinc [10]. The corresponding NRPS gene cluster, *Rv0097-Rv0101*, in *M. tuberculosis* is required for synthesis of diacyl-diisonitrile lipopeptides proposed to aid zinc uptake and growth in zinc-deficient medium and in the lungs of infected mice [11]. Expression of *M. tuberculosis* NRPS genes *Rv0096-Rv0101* is in part regulated by SigC, a transcription sigma factor that promotes transcription of the operon and growth in copper-restricted medium [8]. The related *sfa* gene cluster in *Streptomyces thioluteus* mediates synthesis of a copper-binding diisonitrile molecule that functions as a chalkophore in copper import [71]. The present study examines the hypothesis that the conserved NRPS operon in intracellular pathogenic

mycobacteria encodes enzymes that synthesize chalkophores that aid growth in copper-starved niches. Results confirm this hypothesis and demonstrate that loss of NRPS operon function highly attenuates the pathogen.

Results

M. marinum nonribosomal peptide synthase (NRPS) genes function in copper acquisition

Mycobacterium marinum, a pathogen that causes tuberculosis-like fish infections and human skin lesions encodes genes *MMAR0261* through *MMAR0256* which are homologs of *M. tuberculosis* genes *Rv0096* through *Rv0101*, respectively (Fig. 4.1). Hygromycin-resistant transposon mutants with insertions in the *MMAR0261–MMAR0256* genomic region kindly provided by the Ramakrishnan lab (University of Cambridge) [115] were subsequently unmarked (Fig. 4.2). Sequencing the insertion site of one of the unmarked mutants revealed that 212 bp of residual transposon element sequence remains in the chromosome, thus shifting the reading frame of the encoded protein. To elucidate if genes *MMAR0260-MMAR0256* function in copper acquisition, *M. marinum* strains were initially cultured in Middlebrook 7H9tgADS broth and then passaged three or more times in Sauton medium containing 0.05% Tyloxapol (SMT). Growth of the mutants was then examined in stationary microplate SMT cultures. Mutants with disruptions of *MMAR0260*, *MMAR0259*, *MMAR0258*, or *MMAR0256* grew indistinguishable from parent strain M in SMT (Fig. 4.3). Growth was also examined in SMT containing the copper (II) chelator tetrathiomolybdate (TTM) at 15 μM. Under these conditions, each of the mutants failed to grow as well as wild type unless the medium was also supplemented with 15 μM $CuCl_2$ (Fig. 4.4). Complementation of each of the mutants with a plasmid encoding the *MMAR0259-MMAR0256* genomic region under control of promoter $P_{myctetO}$ reversed the growth inhibition by TTM (Fig.

4.4). Additionally, mutants harboring a plasmid encoding *M. tuberculosis Rv0097-Rv0101* controlled from $P_{myctetO}$ partially to fully reversed the growth inhibition by TTM (Fig. 4.4 A-D). In contrast, a *MMAR0260* mutant carrying a plasmid encoding *MMAR0260* without downstream operon genes was unable to reverse growth inhibition by TTM (Fig. 4.4 A), which is consistent with the 212-bp insertion in *MAR0260* exerting a polar effect on transcription of downstream genes. Similarly, if the *MMAR0260* mutant carried a plasmid encoding only *MMAR0260* homolog *Rv0097*, reversal of the TTM growth inhibition did not occur (Fig. 4.4 A). Because we were not able to obtain a stable *E. coli* clone with *MMAR0260-MMAR0256* together on a single plasmid, the *MMAR0260* mutant was complemented with two plasmids: an integrative plasmid that carries *MMAR0260* with native upstream regulatory sequences and a replicating plasmid encoding *MMAR0259-MMAR0256* genes under control of promoter $P_{myctetO}$. The results showed a significant increase in growth in TTM-treated SMT medium (Fig. 4.4 A). Chelation of copper (I) using chelator bathocuproinedisulfone (BCS) did not prevent growth of any of the mutants (Fig. 4.5). Consistent with the liquid culture data, the *MMAR0260*, *MMAR0259*, *MMAR0258* and *MMAR0256* mutants spotted onto 7H10tgADS agar + 25 μM TTM exhibited reduced growth relative to wildtype, whereas introduction of 75 μM $CuCl_2$ or a plasmid encoding *MMAR0259-MMAR0256* or *Rv0097-Rv0101* reversed the growth defects of the mutants (Fig. 4.6 A-D). After 3 weeks of incubation, each of the mutants had substantially smaller colonies relative to strain M or to the mutants carrying a plasmid expressing *MMAR0259-MMAR0265* or *Rv0097-Rv0101* (Fig. 4.7). These data were corroborated by growing the *MMAR0260* mutant in SMT treated with Chelex-100 which removes divalent metals. Without supplementation with of 25 μM $CuSO_4$, the mutant grew significantly slower than wildtype, while supplementation with 25 μM $ZnSO_4$ had no

significant effect (Fig. 4.8). Thus, the *MMAR0260* mutant is much more sensitive to lack of copper rather than zinc.

Impacts of low copper on *M. marinum* mutants was also examined by AlamarBlue assay. Mutants with insertions into *MMAR0260, MMAR0259, MMAR0258,* or *MMAR0256* exhibited growth inhibition (blue color) in microplate SMT cultures with 15 μM TTM added, while growth was not impaired if 9 or 18 μM $CuCl_2$ was also present (Fig. 4.9). If mutants harbored a plasmid encoding $P_{myctetO}$*Rv0097-Rv0101*, growth was restored (pink color) in SMT + 20 μM TTM (Fig. 4.9). Together, these data support that genes *MMAR0260, MMAR0259, MMAR0258*, and *MMAR0256* are necessary for growth in copper (II) -chelated medium and that the *Rv0097-Rv0101* genomic region from *M. tuberculosis* can complement these *M. marinum* mutants.

Rv0097 is required for *M. tuberculosis* growth in copper-chelated medium

To further explore the role of *M. tuberculosis* NRPS operon genes in essential metal acquisition, the *Rv0097* gene in *M. tuberculosis* strain Erdman was deleted by mycobacterial recombineering (Fig. 4.10) [116]. Growth of a *ΔRv0097* strain carrying an empty vector and *ΔRv0097* complemented with a plasmid encoding $P_{myctetO}$*Rv0097-Rv0101* was compared with strain Erdman. Strains were first cultured in Middlebrook 7H9tgADS broth and passaged three or more times in SMT prior to assessing phenotypes associated with metal limitation [8]. Growth was examined in slowly-shaking cultures containing SMT medium and 25 μM TTM. The mutant complemented with NRPS operon genes and parent Erdman grew significantly faster than the empty-vectored mutant (Fig. 4.11). Supplementation of the *Rv0097* mutant strain with 50 μM $CuCl_2$ restored the growth rate to that of strain Erdman (Fig. 4.11).

By alamarBlue assay, stationary microplate cultures of the *ΔRv0097* empty vector strain grew as well as parent Erdman in SMT, whereas addition of 15 or 20 μM TTM inhibited growth of the mutant (Fig. 4.12 A). Growth inhibition of the mutant by TTM was largely reversed by addition of 9 or 18 μM $CuCl_2$, but growth was less robust at higher concentrations of the metal (Fig. 4.12 A). When cultured in SMT with 15 μM of copper (I) chelator BCS, growth of strain Erdman was unimpaired, while the *ΔRv0097* strain was only mildly impacted, indicating that the mutant is much more sensitive to the copper (II) chelator TTM than BCS (Fig. 4.12. A).

To test that the growth defect of *ΔRv0097* in SMT + 15 μM TTM reflects copper depletion rather than a reduction in available zinc ions, supplementation with 9 – 72 μM $ZnCl_2$ was examined. The mutant failed to grow regardless of the amount of zinc added (Fig. 4.12 B), which supports that the growth defect by TTM is the result of chelation of copper rather than zinc. Introduction of a plasmid encoding *Rv0097-Rv0101* to *ΔRv0097* reversed the growth defect (Fig. 4.12 C) Together, the stationary microplate culture data confirm the shaking-culture results demonstrating that *Rv0097* is required for growth in copper-restricted conditions.

PPE1 **is required for growth under copper-starved conditions**

Genes *MMAR0261* and *Rv0096* encode PPE1 homologs in *M. marinum* and *M. tuberculosis*, respectively, with 65% identity and 75% similarity. In *M. tuberculosis*, *Rv0096* is the first gene in the *Rv0096-Rv0101* operon; however, in *M. marinum* a 175 bp intergenic region is located between *MMAR0261* and the *MMAR0260-MMAR0256* genes (shown to aid growth in copper-starved medium). A SigC promoter was previously identified upstream of *Rv0096* [117]. In *M. marinum*, identical SigC -35 and -10 promoter elements are located upstream of *MMAR0261*, but another set of SigC promoter elements is located in the 175-bp region between *MMAR0261*

and *MMAR0260*. Since SigC homologs in *M. tuberculosis* and *M. marinum* are 100% conserved and SigC is required for transcription of *Rv0096-Rv0101* genes under copper-starved conditions [8], we hypothesized that the PPE1 homologs facilitate copper acquisition. Growth analysis reveals that a *MMAR0261* mutant exhibits a growth defect in SMT + 20 μM TTM relative to wildtype parent strain M and growth of the mutant can be restored by 20 μM $CuCl_2$ or complementation with a plasmid encoding *MMAR0261* (Fig. 4.13 A). Growth of the mutant is also largely restored by introducing a plasmid encoding *Rv0096* (Fig. 4.13 A). When plated on copper-deficient solid medium, the *MMAR0261* mutant produced much smaller colonies than wildtype or the mutant complemented with either *MMAR0261* or *Rv0096* (Fig. 4.13 B and C). As expected, addition of Cu^{2+} to the medium reversed the growth defect of the mutant (Fig. 4.13 B and C). AlamarBlue analysis confirm growth of a *MMAR0261* null mutant in SMT medium and inhibition by addition of 15 or 20 μM TTM (Fig. 4.9 A and B). Growth was restored by addition of 9 or 18 μM $CuCl_2$ (Fig. 4.9 A). Growth was not restored by introduction of a plasmid encoding $P_{myctetO}$*Rv0097-Rv0101* (Fig. 4.9 B), which was expected since this plasmid does not include a *PPE1* homolog. Similarly, a *M. tuberculosis Rv0096* deletion mutant did not grow well compared to strain Erdman in SMT supplemented with 15 μM TTM (Fig. 4.14). Addition of 10 or 20 μM $CuCl_2$, but not $ZnCl_2$ restored growth (Fig. 4.14).

Rv0097 **is required for** ***M. tuberculosis*** **replication in adipocytes**

We next examined whether the NRPS operon has a functional role in a natural copper-limited environment encountered by obligate pathogenic mycobacteria. Adipocytes have been reported to provide a lipid-rich niche for *M. tuberculosis* [118]. Bacilli of *M. tuberculosis* have also been detected within adipose tissue of experimentally-infected mice [109]-[111]. Depletion of

murine adipose tissue was reported to exacerbate lung pathology and increase *M. tuberculosis* replication in the lungs, which suggests this pathogen accesses adipose tissue during infection [111]. Subcellular copper levels in the murine NIH 3T3 fibroblast cell line was reported to be extremely low when grown in basal DMEM medium [108]. This strain is the progenitor of the pre-adipocyte cell line 3T3-L1 (ATCC CL-173). To test whether the lipid-rich environment of 3T3-L1 adipocytes models a natural copper-limited niche utilized by *M. tuberculosis*, we first infected 3T3-L1 pre-adipocytes with *M. tuberculosis* strains. At day 12 post-infection, a mutant lacking *Rv0097* yielded significantly-reduced bacterial CFUs relative to parent Erdman or the mutant complemented with $P_{myctetO}$*Rv0097-Rv0101* (Fig. 4.15 A). In cells supplemented with 100 μM $CuCl_2$, growth of the mutant did not significantly differ from that of strain Erdman at the same time point (Fig. 4.15 A). Next, 3T3-L1 pre-adipocytes were differentiated into adipocytes (Fig. 4.16) and infected with the same *M. tuberculosis* strains. At days 9 and 12 post-infection, the *Rv0097* mutant replicated significantly slower than Erdman or the mutant encoding *Rv0097-Rv0101* on a plasmid, and the mutant cultured in cells supplemented with 100 μM $CuCl_2$ (Fig. 4.15 B). Infection of adipocytes in medium supplemented with 100 μM $ZnSO_4$ failed to reverse the growth defect of the *Rv0097* mutant (Fig. 4.15 C). Together, these data support that *Rv0097* is necessary for replication in this natural *in vivo* copper-restricted niche.

To assess whether infection leads to host cell killing, cells were stained with fluorescent dye Zombie Red, which permeates dead cells, and nuclear stain DAPI. Red staining of pre-adipocytes was very sparse at 6 days post-infection with strain Erdman, *ΔRv0097*, or *ΔRv0097* complemented with $P_{myctetO}$*Rv0097-Rv0101* (Fig. 4.17 A). However, by day 12, cell death was significantly higher in cells infected with either Erdman or the complemented mutant (Fig. 4.17 A). Quantification of cell death (Zombie Red fluorescence) at day 12 post-infection showed that

cells infected with strain Erdman have significantly-higher staining than *ΔRv0097,* while an intermediate was observed for the complemented mutant (Fig 4.17 B). Thus, presence of an intact *Rv0097-Rv0101* region results in more effective killing by *M. tuberculosis* in adipocytes.

Infection of 3T3-L1 pre-adipocytes was also monitored by light microscopy (Fig. 4.18). Cell debris is evident at 12 days post-infection with either Erdman or the *Rv0097-Rv0101*-complemented mutant, but not with *ΔRv0097.* Signs of host cell debris in infections with the *Rv0097* mutant appear at day 18, while cells cultured in medium supplemented with 50 μM $CuCl_2$ infected for the same length of time with this mutant exhibited more areas of cell debris. At day 24 post-infection, the accumulation of cell debris was greatest in cells infected with Erdman followed by cells infected with the complemented mutant, then those infected with the *Rv0097* mutant in copper-containing medium, and lastly in cells infected with the *Rv0097* mutant in medium without copper supplementation. Thus, the defect in host cell killing correlates with a defect in the ability of the *Rv0097* mutant to acquire copper in adipocytes.

As *M. tuberculosis* bacilli can survive in unactivated phagocytes, we examined whether *Rv0097* influences replication or survival in unactivated and IFN-γ-activated THP-1 macrophages. No significant differences in bacterial counts were observed between an *Rv0097* mutant and Erdman or the *Rv0097-Rv0101*-complemented *Rv0097* mutant (Fig. 4.19 A and B). In a study of murine peritoneal macrophages, Wagner and colleagues reported average phagosomal copper concentrations of 426 μM and 49 μM at 1 and 24 hours, respectively, following *M. tuberculosis* infection [119]. They also reported phagosomal copper levels of 17 μM after 24-hour infection with *Mycobacterium avium* with the level rising to 82 or 177 μM in cells treated with IFN-γ 24 hours before or after *M. avium* infection, respectively. Together, these data support that the internal

environment of the macrophages studied are not sufficiently copper limited to result in a replication defect of the *Rv0097* null strain.

Copper limitation induces expression of *Rv0096-Rv0101* operon genes *in vitro*

Transcriptional analyses were performed to examine the effects of limiting copper availability on expression of genes in the *M. tuberculosis Rv0096-Rv0101* operon. We have previously demonstrated that genes in this operon require *sigC* for elevated transcription in copper-restricted medium and that copper supplementation ablates transcriptional differences in this operon in strains containing or lacking *sigC* [8]. In the current study, we examined expression of representative *Rv0096-Rv0101* operon genes in strain Erdman cultured in SMT containing or lacking 20 μM TTM and normalized expression to housekeeping gene *sigA*. The presence of the copper chelator resulted in elevated expression of *Rv0096* (5-fold), *Rv0097* (12-fold), and *Rv0101* (4-fold) (Fig. 4.20). This fits with the hypothesis that the *Rv0096-Rv0101* region encodes proteins required for copper-scavenging when *M. tuberculosis* encounters a copper-starved niche.

Expression of *Rv0096-Rv0101* operon genes in 3T3-L1 adipocytes is down-regulated by exogenous copper

As we have shown that growth of an *Rv0097* null strain within 3T3-L1 adipocytes is improved by copper supplementation, we anticipated that expression of genes in the *Rv0096-Rv0101* operon to correlate inversely with exogenous copper in this cell type. Transcription of *Rv0096*, *Rv0097*, and *Rv0101* was examined 10 days after *M. tuberculosis* Erdman infection of adipocytes (MOI = 1) cultured in basal medium or in the same medium supplemented with either 0.1 mM Cu^{2+} or Zn^{2+}. Expression of all three genes was downregulated in adipocytes cultured in copper-supplemented basal medium (Fig. 4.21). In zinc-supplemented cells, *Rv0096* and *Rv0097*

appeared slightly elevated, while *Rv0101* was elevated approximately 3-fold (Fig. 4.21). Together, these data indicate that genes in the *Rv0096-Rv0101* operon are elevated within adipocytes in the absence of exogenous copper supplementation which supports function of this operon in copper acquisition or utilization by *M. tuberculosis*.

PPE1 may function in NRPS-associated copper import

As several PPE family proteins are surface localized, we investigated whether PPE1 encoded upstream of mycobacterial NRPS genes required for synthesis of isonitrile lipopeptides (INLPs)[11] or related isonitrile molecules from streptomyces [71] functions in export of isonitrile molecules. If these INLPs are chalkophores (i.e. facilitate copper acquisition) and PPE1 functions in their export, then a *M. tuberculosisΔPPE1* strain harboring a plasmid encoding $P_{myctetO}$*Rv0097-Rv0101* should be capable of making chalkophores, but not secreting them out of the bacteria. In contrast, if PPE1 instead functions to import copper-bound INLPs, then INLPs should be secreted. To test this hypothesis, supernatants were obtained from this strain cultured in SMT medium containing 25 μM TTM and applied to a strain defective in INLP production to assess for improved growth in copper-chelated SMT medium. Because the supernatant was obtained from a *ΔPPE1* strain cultured with antibiotic to ensure plasmid maintenance, the recipient strain tested also carried a plasmid conferring resistance to the antibiotic. Results indicate that while growth of recipient strain *MMAR0260*$^{-}$/p*MMAR0260* is slowed when TTM is present in the SMT medium, addition of the *ΔPPE1*/p$P_{myctetO}$*Rv0097-Rv0101* supernatant reversed the TTM-associated growth defect as did supplementation with 25 μM $CuCl_2$ indicating chalkophores are present in the supernatant (Figure 4.22). Importantly, growth was not restored by supernatant from *ΔPPE1*

carrying an empty vector (Figure 4.22). Together, the data indicate that chalkophore production requires *Rv0097-Rv0101* and that PPE1 is not required for chalkophore export.

Detection of a chalkophore signature

To screen for unique chemical profiles in NRPS mutants, culture supernatants were examined from strains *M. marinum MMAR0261*$^{-}$ carrying plasmid $pP_{myctetO}$*Rv0097-Rv0101* and *M. marinum MMAR0260*$^{-}$ carrying plasmid $pP_{myctetO}$*Rv0097* grown in SMT treated with TTM. By LC-MS/MS, a peak of 365.2167 Daltons was present only in extract from the first strain (Fig. 4.23). This peak mass is identical (to two decimal places) to that of an isonitrile chalkophore from *Streptomyces thioluteus* reported to bind copper (Fig. 4.23) [71].

***Rv0097* is required for virulence and replication in mice**

To assess if loss of *Rv0097* impacts virulence, intravenous infections of DBA/2 mice with strains Erdman, an *Rv0097* deletion mutant, or the mutant complemented with $P_{myctetO}$*Rv0097-Rv0101* were compared. In an animal survival study, all mice infected with strain Erdman died within the 175-day study, while none infected with the *Rv0097* mutant succumbed during the same period, and 30% of those infected with the complemented mutant died (Fig. 4.24 A). After euthanizing all remaining animals at the end of the study, gross pathology revealed no visible granulomas in lungs of mice infected with the mutant, some granulomas in the complemented group, and large granulomatous regions in most infected with strain Erdman (Fig. 4.24 B). Histopathology indicated significantly less necrosis, immunopathology, and percent of area affected in the lungs of mice infected with the mutant relative to Erdman or the complemented mutant as well as ~10-fold fewer acid-fast bacilli in the mutant (Fig. 4.25). Mycobacterial burdens

at the time of death indicated significantly fewer CFUs in the lungs, spleen, and liver of mice infected with the mutant versus the complemented mutant or strain Erdman (Fig. 4.26). The load in the lung for the mutant was at least ten-fold lower than for Erdman, but dissemination to the spleen and liver was reduced by more than 100 and 1000-fold, respectively. Thus, loss of capacity for chalkophore synthesis significantly reduces the ability of *M. tuberculosis* to replicate, induce granuloma formation, disseminate, and cause disease in the infection model system.

Discussion

Nonribosomal peptide synthases (NRPSs) are multi-domain protein complexes in bacteria and fungi that have evolved to link and modify amino acids to produce peptide secondary metabolites such as antibiotics, toxins, immunosuppressants, and pigments [120]. Nonribosomal products sometimes facilitate bacterial metal acquisition [121][122] or abrogate toxicity of a specific metal, such as copper [59]. Five NRPS genes required for synthesis of isonitrile lipopeptides (INLPs) are conserved to varying degrees in Actinobacteria [10][71]. A mutation in one of these genes in *M. marinum* resulted in reduced intracellular zinc levels [10], whereas NRPS genes in *Streptomyces thioluteus* isonitrile enabled production of nonlipidated isonitriles capable of binding Cu^{+} or Cu^{2+} [71]. Functional roles for the conserved NRPS operon in pathogenic mycobacteria remained to be elucidated.

In the present study, we demonstrate that NRPS operon genes are required for copper acquisition by *M. tuberculosis* and *M. marinum*, but only in conditions where the metal is scarce. We revealed that disruption of the operon in *M. tuberculosis* impairs replication in adipocytes, but growth was restored with copper supplementation. In contrast, loss of NRPS function failed to significantly impact replication in THP-1 macrophages. These observations are consistent with adipocytes, but not THP-1 cells, having copper-deficient niches. The severe attenuation of an

Rv0097 deletion mutant in murine infections, particularly in impairment to induce granulomas in the lungs and significantly-reduced *M. tuberculosis* dissemination to the spleen and liver underscores the importance of the NRPS operon to the fitness of this pathogen. Increased transcription of NRPS operon genes in copper-chelated medium and in adipocytes relative to copper-replete medium support the capacity of *M. tuberculosis* to sense and respond to copper deficiency by upregulating expression of a mechanism to acquire this metal. We discuss these data in the context of published studies below.

The data are consistent with pathogenic mycobacteria responding to redox stress utilizing the conserved NRPS operon to produce chalkophores to scavenge and import copper to prioritize metallation of the Qcr-Cta aerobic respiration supercomplexes that deliver electrons to oxygen and concomitantly pump protons across the cytoplasmic membrane to increase the proton-motive force. A model is presented to help visualize how chalkophores may participate in *M. tuberculosis* copper homeostasis (Fig. 4.27). Although mycobacterial copper trafficking systems have yet to be fully elucidated, in a copper-replete environment, copper ions may enter the periplasm via outer membrane porin-like proteins and be pumped into the cytoplasm by low-affinity major facilitator superfamily (MFS) transporters [49][123]. In the bacterial cytoplasm, Cu^{2+} is reduced by glutathione and other reductants [124]. The highly-reactive free Cu^{+} ions are bound by cytoplasmic metallothioneins, such as MymT, to minimize toxicity [65]. Membrane and periplasmic cuproenzymes studied in detail are metallated in the periplasm, often with the copper ions originating from the cytoplasm via copper-exporting P-type ATPases that may direct the metal to specific cuproenzymes [49]. This may be due to a need for Cu^{+} for metal insertion or that facilitated delivery minimizes free Cu^{+} ions in the periplasm with potential to inactivate important enzymes containing iron-sulfur centers [51]. When copper levels increase, copper-efflux P-type ATPase

CtpV exports excess Cu^{+} to the periplasm [104][125], where the metal can be oxidized to the less-reactive Cu^{2+} form by mycobacterial multicopper oxidase MmcO [67]. Excess copper ions are exported across the outer membrane by mycobacterial copper transport protein MctB [126]. In response to oxidative stress, copper-transporting P-type ATPase CtpA [105] is the logical choice to export Cu^{+} for targeted metallation of the periplasmic Cu, Zn superoxide dismutase SodC given that both *ctpA* and *sodC* are required for survival in macrophages [80][127] (Fig. 4.27).

In low-copper locales, nonspecific copper uptake systems are unlikely to import adequate amounts of the metal. In response to copper starvation, transcription of *M. tuberculosis* NRPS operon genes is directed by transcription sigma factor SigC [8]. The NRPS complex synthesizes chalkophores that are exported to the surface via an undefined mechanism which likely includes a mycobacterial membrane protein large (MmpL) transporter localized in the cytoplasmic membrane as this family exports multiple outer membrane and capsule lipids as well as the lipidated and nonlipidated iron chelators, mycobactin and carboxymycobactin, respectively [128]. Periplasmic and outer membrane proteins that complete the chalkophore export system also remain to be identified.

By analogy to mycobactin forms, mycobacteria may produce both lipidated and soluble isonitrile peptides that function as chalkophores. This is supported by our detection of a molecule in culture supernatant from a *M. marinum MMAR0260* mutant encoding *Rv0097-Rv0101* that had the identical mass of a nonlipidated diisonitrile peptide produced from *E. coli* expressing *Streptomyces coeruleorubidus* NRPS genes *scoA-E* [10]. Recently, Mehdiratta and colleagues reported NRPS operon-dependent INLP production by *M. tuberculosis* required for growth in response to zinc starvation [11]. The NRPS protein conserved in many actinomyces has single condensation, adenylation, and thiolation domains for incorporation of a single amino acid linking

two lipidated isonitrile chains synthesized by the four enzymes encoded immediately upstream of the *Rv0101* gene in the operon. The products from *M. marinum* or *S. coeruleorubidus* NRPS genes expressed in *E. coli* preferentially incorporated a lysine linking the isonitrile chains [10]. When the corresponding genes from *Streptomyces thioluteus* were expressed in *Streptomyces lividans*, lysine was also incorporated and subsequently cyclized [71]. In contrast, *M. tuberculosis* and other tuberculous mycobacteria NRPS homologs have duplicate sets of condensation, adenylation, and thiolation domains suggesting the capacity to link INLPs with a chain consisting of two modified amino acid. In the Mehdiratta et al. zinc study, an ornithine-phenylalaninol dipeptide core linked the INLP chains [11].

Our detection of a secreted product from *MMAR0261*$^{-}$ /pP$_{myctetO}$*Rv0097-Rv0101* with an identical mass of an isonitrile product generated from *S. coeruleorubus* genes was unexpected as it had a single amino acid linking two the isonitrile chains. This product may have been synthesized from the *M. marinum* operon since a SigC promoter is present immediately upstream *MMAR0260* which would have allowed some expression of *MMAR0260-MMAR0256* despite disruption of *MMAR0261*. An alternative hypothesis is that *Rv0101* is regulated to prevent expression of the full-length NRPS protein or that activity of the C-terminal half is blocked under a specific condition resulting in INLPs linked with a single amino acid. It remains to be determined if incorporating 1 versus 2 amino acids between INLP chains influences metal binding.

Different INLP forms participating in metal binding is possible interpretation from examining details of the study by Mehdiratta and colleagues [11]. Their conclusion that the NRPS operon is required for zinc acquisition is based on a *M. tuberculosis* mutant that lacked the last gene (*Rv0101*) in the NRPS operon. This *ΔRv0101* strain failed to grow in Chelex-treated Sauton medium, but grew when supplemented with zinc, but not copper, suggesting a defect only in zinc

scavenging. We demonstrated that a *ΔRv0097* deletion/insertion mutant is defective for growth under copper-starved conditions, but growth restoration only occurs if supplemented with copper or by complementation with *Rv0097-Rv0101*. Further, addition of zinc did not restore growth of the *M. marinum Rv0097* homolog mutant in Chelex-treated Sauton medium. Thus, *ΔRv0097* likely prevents production of any INLPs, while *ΔRv0101* clearly lacks the enzyme for linking INLP chains together, but should have the capacity to make unlinked INLPs. In the Medhiratta et al. report, addition of zinc did not fully restore *ΔRv0101* growth to the wildtype level, and transcription of NRPS operon genes were upregulated wildtype in chelated SMT regardless of whether low or high zinc was added, which would be consistent with the cultures remaining copper-deficient. Given that both copper and zinc are essential metals, growth should have not have been detected by supplementation with zinc alone unless the cultures had residual copper present. Trace amounts of copper were most likely introduced when their the Chelex-treated culture flasks were rinsed with double-distilled water, which may have contained leached copper from pipes that plumb their water system. After rinsing, the glassware was baked for an hour at 80°C, which would have reduced any Cu^{2+} to Cu^{+}. It is possible that *ΔRv0101* imported copper needed for respiration in the zinc-supplemented cultures by diffusion of Cu^{2+} reoxidized from Cu^{+}. Another possibility is that single INLP chains produced in the mutant are still able to bind and import Cu^{+}. Linking INLP chains in a wildtype strain would be expected to increase metal-binding capacity, particularly for divalent cations.

How chalkophores deliver captured copper remains to be elucidated. For *S. thioluteus*, it has been suggested that copper-bound SF2768 is imported into the cytoplasm via ABC transporter Orf19-21 where the metal is released and SF2768 is exported for re-use [71]. Metal-bound INLPs from *M. tuberculosis* are also proposed to be imported to the cytoplasm, but proteins that mediate

the process were not identified [11]. Our data indicates that PPE1 is dispensable for export of chalkophores, but not for growth in copper-chelated medium. As PPE family proteins are generally localized to the outer membrane, PPE1 may function as an outer membrane component for import of copper-chalkophore adducts.

How does chalkophore-mediated copper import support bacterial growth under copper starved conditions? As *M. tuberculosis* enters dormancy in response to hypoxia, replication cannot occur without functional Qcr-Cta respiration complexes. Under copper-starvation conditions, it is likely metallated by the copper-transporting P-type ATPase CtpB [106] given that *ctpB* transcription is increased and required for growth such conditions.[97] Additional support comes from sequence examination of the essential integral membrane protein Rv0102, encoded between the NRPS operon and *ctpB*. Precomputed BLAST results for Rv0102 on the Mycobrowser webserver (accessed on 20 June 2022) revealed homology to CtaG-like cytochrome c oxidase assembly factor proteins predicted to metallate the CuB site of subunit 1 of respiration complexes [129].

Another stress-response role for the NRPS operon has emerged. The *M. tuberculosis* NRPS operon was recently reported to function in response to nitric oxide (NO) sensing and resistance [95]. Deletion of *rip1* encoding protease Rip1 protease increases sensitivity to nitric oxide and toxic copper levels (0.2 or 0.5 mM), while introduction of genes *Rv0097-Rv0101* to the mutant restores resistance to NO, but not copper [95]. Additional regulation of the operon in response to NO is mediated by the PtadS/R two-component response regulatory system [95]. The authors suggest that chalkophores are needed not for copper-detoxification, but rather for delivery of copper to the periplasm to ameliorate or prevent NO toxicity. As it is known that NO inactivates

cytochrome oxidases [130], we predict the chalkophores are needed to supply copper to the periplasm for synthesis or repair Qcr-Cta respiration complexes.

We further demonstrated that copper uptake contributes to host cell killing by *M. tuberculosis*. Adipocytes were used to model a copper-restricted environment pathogenic mycobacteria encounters in the host. *Mycobacterium tuberculosis* have been detected within adipocytes and adapt their metabolism for the lipid-rich niches [118]. Adipose tissues appear to be a safe harbor for *M. tuberculosis* regardless the route of infection, while depletion of fat cells exacerbates lung pathology [111]. We surmised that copper is less available and less diffusible in lipid-rich environments. Deletion of *Rv0097* results in impaired replication in 3T3L1 adipocytes, which was reversed by supplementing adipocytes with Cu (II); this underscores the critical role of copper acquisition for bacterial replication during infection.

The soluble isonitrile hydratases in actinomycetes in metal acquisition warrant further study. The *sfaF* gene in *S. thioluteus* encodes an isonitrile hydratase that oxidizes isonitrile groups on SF2768 to formamides which blocked copper binding [131]. In *M. tuberculosis*, Rv0052, a homolog of SfaF, similarly modified the isonitriles of INLPs, and transcription of *Rv0052* was upregulated under low-zinc, but not high-zinc conditions, supporting a role in zinc acquisition [11]. In neither study were Cu or Zn isonitrile substrates tested to assess whether the hydratases function to release bound metal. An alternative hypothesis is that oxidation of isonitrile groups is required for zinc binding and uptake. If copper is the preferred substrate for INLP binding, but much more zinc was supplied to cultures, this may explain the detection of Zn-INLP adduct.

The inability of NRPS operon mutants of tuberculous mycobacteria to produce chalkophores for scavenging essential metals from their hosts helps explain animal infection data from multiple studies. Our long-term DBA/2 mouse survival study demonstrated that NRPS

operon mutant *ΔRv0097* remained highly attenuated over a 175-day period in which all mice infected with parent Erdman succumbed to infection. This is consistent with attenuation in guinea pigs by a *Mycobacterium bovis* mutant with transposon-disruption of *Mb0100* (the *Rv0097* homolog), which interestingly conferred short-term protection against WT *M. bovis* challenge equivalent to the BCG vaccine [132]. Deletion of the *Rv0101*/*nrp* from *M. tuberculosis* H37Rv was highly attenuated in immunocompetent (C57BL/6) and immunodeficient (SCID^{-},RAG2^{-}, and IFNγ^{-}) mice [91]. Additionally, C57BL/6 mice studies with a transposon-disrupted *Rv0097* Erdman strain revealed a persistence defect by the mutant where replication peaked in the lungs at 4 weeks post-infection reaching ~10^6 CFU and gradually declined ~1.5 $\log_{10}$ CFU over the next 8 weeks; interestingly, in isoniazid (INH)-treated animals, the mutant was largely resistant to INH killing by the drug over the same period but not when cultured *in vitro* [133]. By comparison, in untreated mice the WT strain reached peak lung burden (~2 x 10^6 CFU) by 2 weeks post-infection and loads remained at this level over the next 8 weeks, whereas in INH-treated mice, lung loads remained at the same level but then dropped 3 $\log_{10}$ units in the subsequent 8 weeks. In each of these studies, the NRPS mutants were defective at scavenging host copper, which may have reduced replication efficiency and resulting damage to the host due to inability to produce ample copper-dependent Qcr-Cta respiration complexes. In the INH study, it took more than 4 weeks for the drug levels in the lungs to reach an effective concentration since the WT burden did not decrease until week 6 [133]. The resistance of the mutant to INH after week 4 is consistent with copper-depletion by bacteria that entered lung-associated adipose tissue, resulting in cessation of growth and resistance to the drug.

While NRPS operon mutants and *ctpB* are required for growth in copper-starved niches, why are NRPS mutants highly attenuated, while a *ctpB* mutant is highly virulent? The difference

may lie in NRPS mutants being defective at importing copper in low-copper environments, while a *ctpB* mutant might accumulate higher intracellular Cu^+ levels than a NRPS mutant or wildtype. Sustained expression of NRPS genes for chalkophore import is expected without CtpB to efficiently metallate Qcr-Cta respiration complexes that restore redox balance in the cytoplasm and lead to downregulation of NRPS gene expression. A higher basal cytoplasmic Cu^+ level in a *ctpB* mutant should eventually lead to increased export via efflux pump CtpV; however, periplasmic MmcO and outer membrane efflux pump MctB may not be upregulated until sufficient Cu^+ builds in the periplasm to allow Qcr-Cta metallation by diffusion. Thus, the *ctpB* mutant may have elevated cytoplasmic and periplasmic Cu^+ levels in low-copper environments. These elevated stores may enable the mutant to quickly respond to oxidative and nitric oxide stresses to metallate SodC and respiration complexes, respectively. Given the importance of respiration to this pathogen, it remains to be determined if loss of CtpB correlates with improved fitness in models other than mice which lack complex hypoxic granuloma structures where CtpB function may be critical for survival of the pathogen. Importantly, while NRPS operons are conserved in pathogenic mycobacteria, CtpA and CtpB homologs are only conserved in obligate intracellular, granuloma-inducing, pathogenic mycobacteria. This suggests that this group of pathogens has evolved these copper transporters to efficiently metallate vital cuproenzymes to enhance survival in unique host niches.

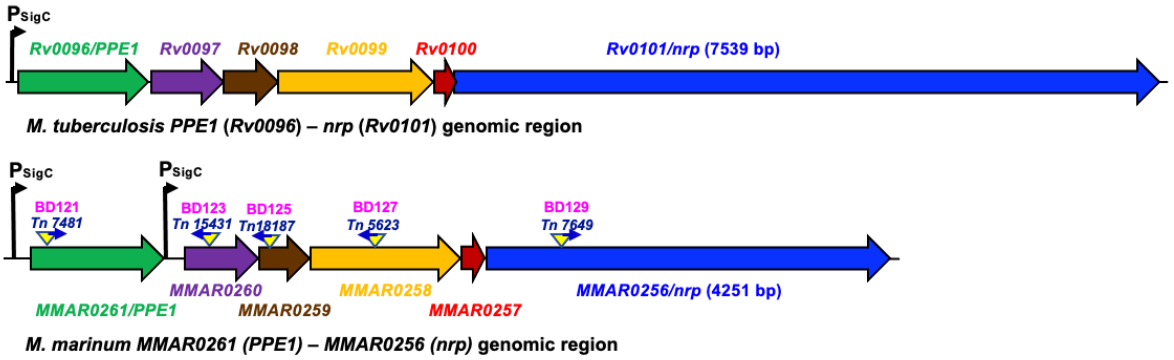

Fig. 4.1. Schematic of the conserved nonribosomal peptide synthase (NRPS) genomic region of *M. tuberculosis* and *M. marinum*. Homologous genes (thick arrows, same color) in the NRPS genomic regions of *M. tuberculosis* and *M. marinum* are shown (same color). Predicted sigma factor C promoter (P_{SigC}) sites upstream of *MMAR0261* and *MMAR0260* have identical recognition elements [-35 (GGGAAC) – 16 or 17 bp spacing – -10 (CGACT)] to those upstream of *M. tuberculosis Rv0096/PPE1* suggest that the *M. marinum PPE1* homolog may be transcribed independently from *MMAR0260-MMAR0256*. Transposon (Tn)-mediated gene-disruption mutants of *M. marinum* are indicated (yellow triangles). The orientation of the inserted hygromycin-resistance gene (*hyg*) flanked by γδ-resolvase sites in each mutant are shown (blue arrows). After *hyg* removed by introduction of the γδ-resolvase gene, 212-bp remains, and the mutants were renamed (BD numbers). Gene information shown is for *M. tuberculosis* strain H37Rv and *M. marinum* strain M obtained from Mycobrowser (mycobrowser.epfl.ch).

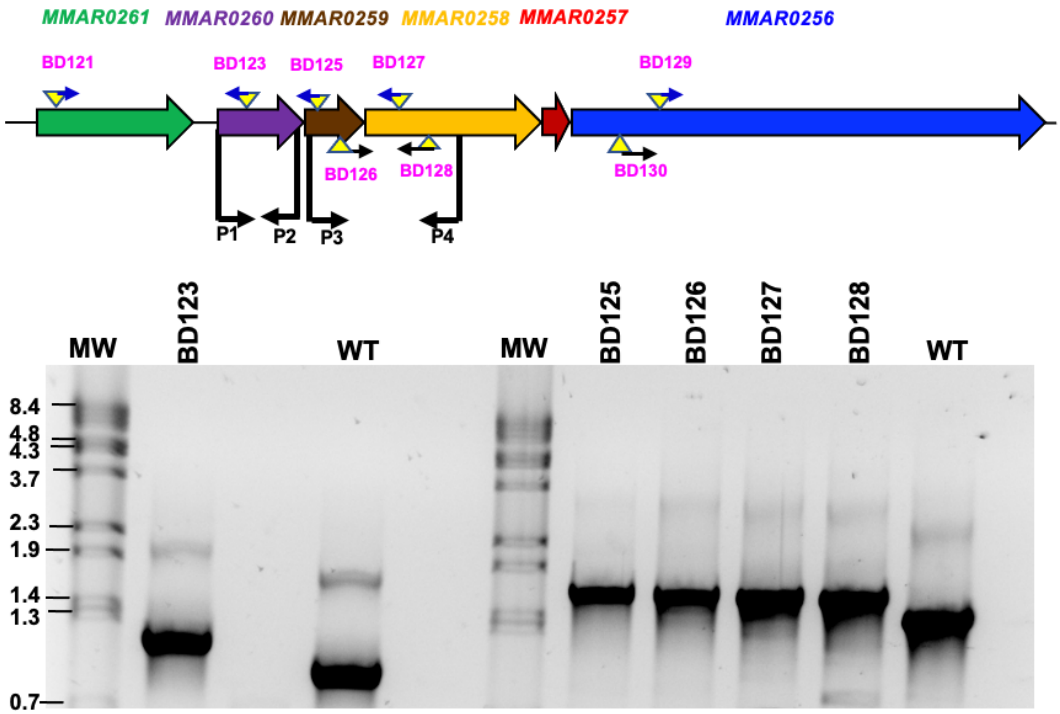

Fig. 4.2 Confirmation of unmarked *M. marinum* mutants. *M. marinum Tn5370*-mediated transposon mutants were PCR screened after transformation with plasmid pRK266 encoding γδ resolvase which catalyzes site-specific recombination at the resolvase sites flanking *hyg* in each mutant. Primers P1522 (P1) and P2261 (P2) were used to screen for unmarking of mutant Tn15431, while primers P1976 (P3) and P1874 (P4) were used to screen for unmarking of mutants Tn18187, Tn23984, Tn5623, and Tn21692. Strains deleted for *hyg* were renamed (BD numbers). The sizes (in kb) of lambda/*Bst*EII DNA size standards (MW) are shown. The expected amplicon for the native P1-P2 region of *M. marinum* strain M (WT) is 0.9 kb and that for the P3-P4 region is 1.4 kb. After excision of *hyg*, a residual 212-bp region remains in each of the mutants.

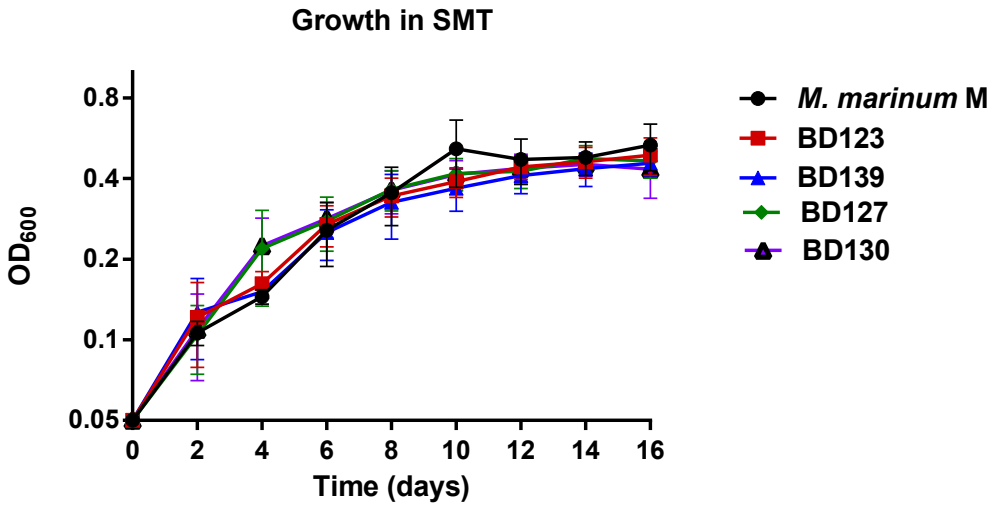

Fig. 4.3. *M. marinum* NRPS operon mutants are not impaired for growth in SMT. Growth of strains *M. marinum* M, BD123 (*MMAR0260*⁻), BD139 (*MMAR0260*⁻/pP$_{myctetO}$*Rv0097*), BD127 (*MMAR 0258*⁻), and BD130 (*MMAR0256*⁻) was monitored (OD$_{600}$) in SMT cultures incubated stationary at 30ºC. Data shown represent the mean +/- standard error of two independent experiments performed in triplicate.

A

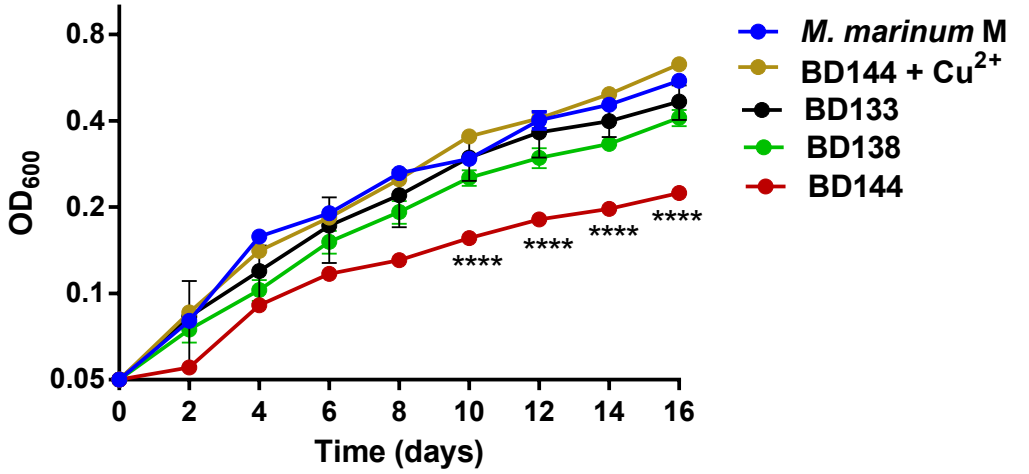
0.8
0.4
0.2
0.1
0.05
OD600
0
2
4
6
8
10
12
14
16
Time (days)
****
****
****
****
M. marinum M
BD144 + Cu2+
BD133
BD138
BD144

B

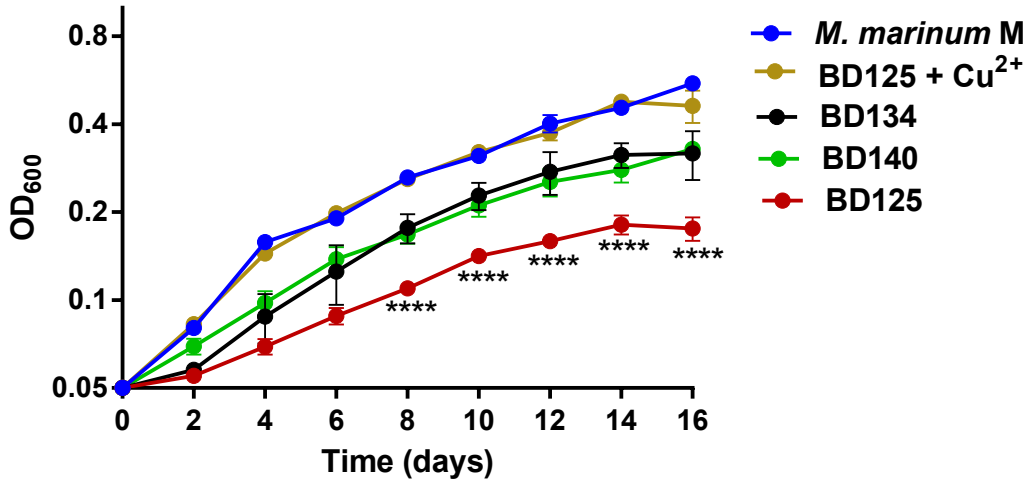
0.8
0.4
0.2
0.1
0.05
OD600
0
2
4
6
8
10
12
14
16
Time (days)
****
****
****
****
****
M. marinum M
BD125 + Cu2+
BD134
BD140
BD125

C

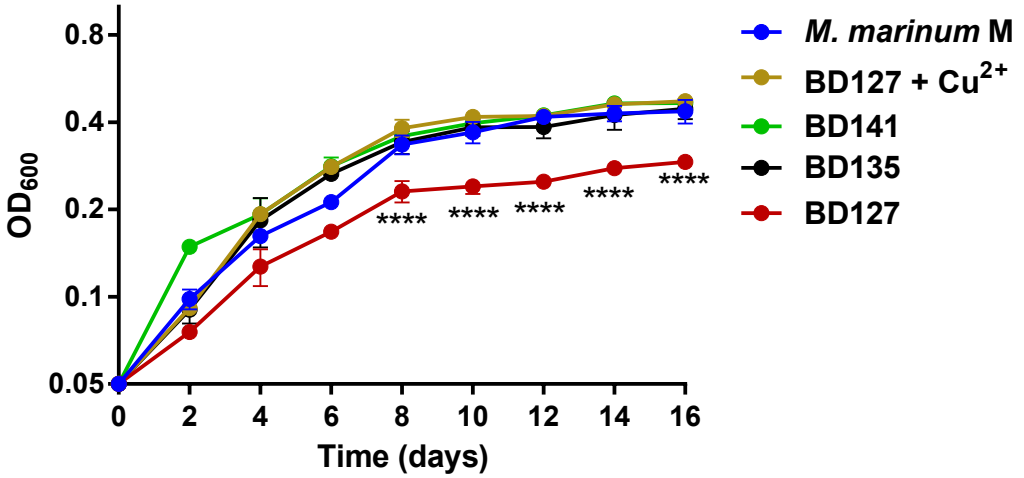
0.8
0.4
0.2
0.1
0.05
OD600
0
2
4
6
8
10
12
14
16
Time (days)
****
****
****
****
****
M. marinum M
BD127 + Cu2+
BD141
BD135
BD127

D

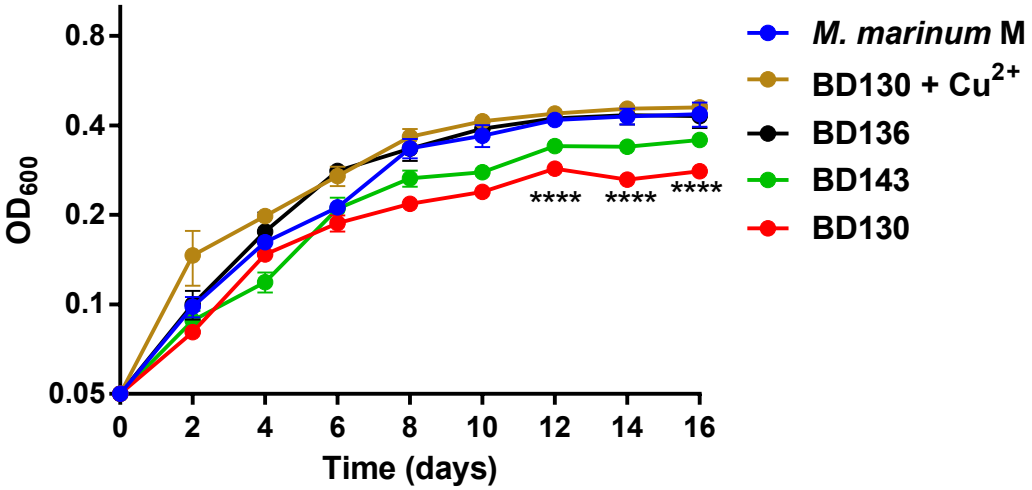
0.8
0.4
0.2
0.1
0.05
OD600
0
2
4
6
8
10
12
14
16
Time (days)
****
****
****
M. marinum M
BD130 + Cu2+
BD136
BD143
BD130

Fig. 4.4. *M. marinum* NRPS operon genes are required for copper uptake. Strains *M. marinum* M, BD144 (*MMAR0260*$^{-}$/*MMAR0260)*, BD138 (*MMAR0260*$^{-}$/pP$_{myctetO}$*Rv0097-Rv0101*), BD133 (*MMAR02060*$^{-}$::*MMAR0260*/pP$_{myctetO}$*MMAR0259-MMAR0256*), BD125 (*MMAR0259*$^{-}$), BD134 (*MMAR0259*$^{-}$/pP$_{myctetO}$*MMAR0259-MMAR0256*), BD140 (*MMAR0259*$^{-}$/pP$_{myctetO}$*Rv0097-Rv0101*), BD127 (*MMAR0258*$^{-}$), BD135 (*MMAR0258*$^{-}$/pP$_{myctetO}$*MMAR0259-MMAR0256*), BD141 (*MMAR0258*$^{-}$/pP$_{myctetO}$*Rv0097-Rv0101*), BD130 (*MMAR0256*$^{-}$), BD136 (*MMAR0256*$^{-}$/pP$_{myctetO}$*MMAR0259-MMAR0256*), and BD143 (*MMAR0256*$^{-}$/pP$_{myctetO}$*Rv0097-Rv0101*) were cultured stationary at 30ºC in SMT with 15 µM tetrathiomolybdate (TTM) without or with 15 µM $CuCl_2$ (Cu^{2+}). Growth curve data was separated into 3 graphs (A-C) to aid comparisons of each mutant with its complementing strain and parent strain M. Cell densities shown (OD_{600}) are the mean +/- standard error from two independent experiments in triplicate. Significant differences in growth of the indicated mutant strain relative to strain M and complemented mutants in the absence of added copper and to the mutant in copper-supplemented medium are shown (****p<0.0001).

A

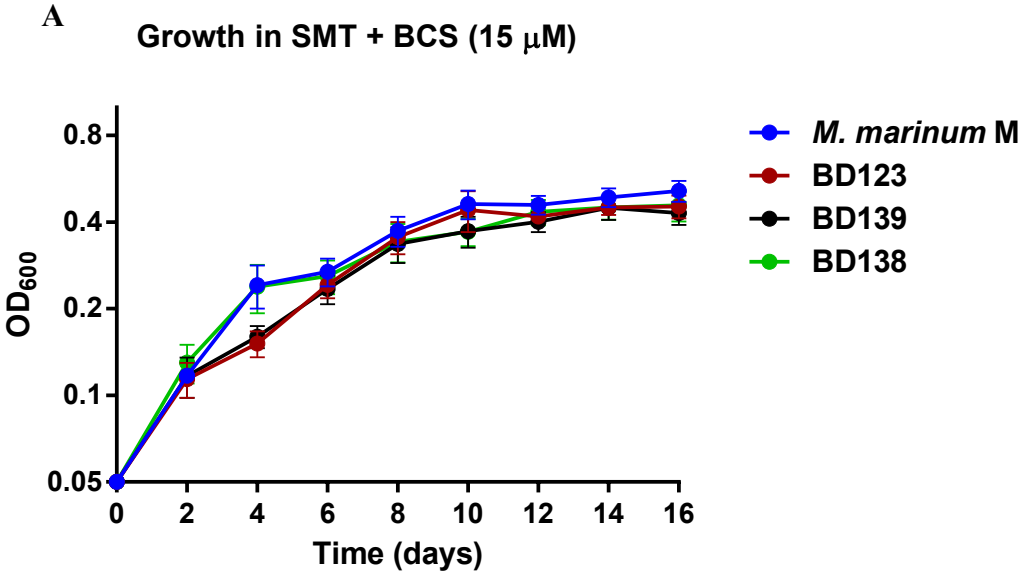
Growth in SMT + BCS (15 μM)
0.8
0.4
0.2
0.1
0.05
OD600
0
2
4
6
8
10
12
14
16
Time (days)
M. marinum M
BD123
BD139
BD138

B

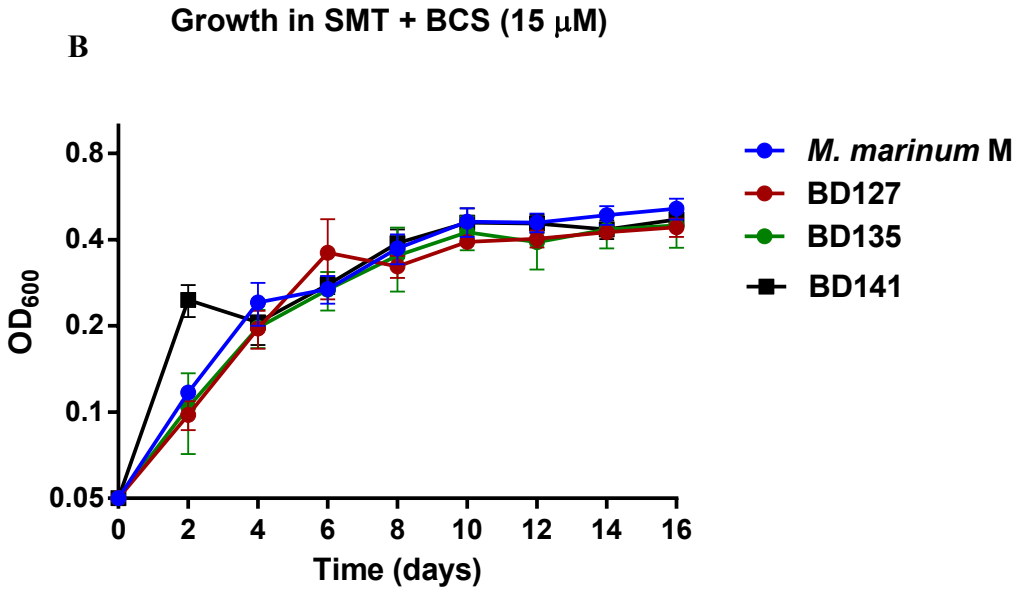
Growth in SMT + BCS (15 μM)
0.8
0.4
0.2
0.1
0.05
OD600
0
2
4
6
8
10
12
14
16
Time (days)
M. marinum M
BD127
BD135
BD141

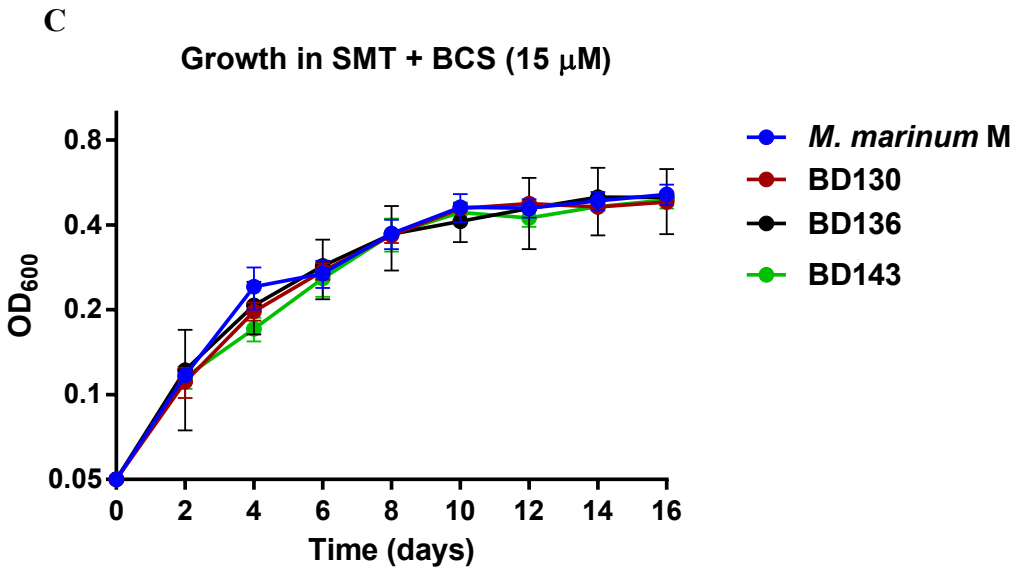

Fig. 4.5. Copper (I) chelation does not suppress growth of *M. marinum* NRPS operon mutants. Growth of *M. marinum* strains M, BD123 (*MMAR0260*$^{-}$), BD138 (*MMAR0260*$^{-}$/pP$_{myctetO}$*Rv0097-Rv0101*), and BD139 (*MMAR02060*$^{-}$/pP$_{myctetO}$*Rv0097*) (A); strains M, BD127 (*MMAR0258*$^{-}$), BD135 (*MMAR0258*$^{-}$/pP$_{myctetO}$*MMAR0259-MMAR0256*), and BD141 (*MMAR0258*$^{-}$/pP$_{myctetO}$*Rv0097-Rv0101*) (B); and strains M, BD130 (*MMAR0256*$^{-}$), BD136 (*MMAR0256*$^{-}$/pP$_{myctetO}$:*MMAR0259-MMAR0256*), and BD143 (*MMAR0256*$^{-}$/pP$_{myctetO}$:*Rv0097-Rv0101*) (C) was compared in SMT cultures containing 15 μM bathocuproinedisulfone (BCS) at 30ºC without shaking. Data shown indicate the mean optical density (OD_{600}) with standard error at each time point from two independent experiments in triplicate.

A

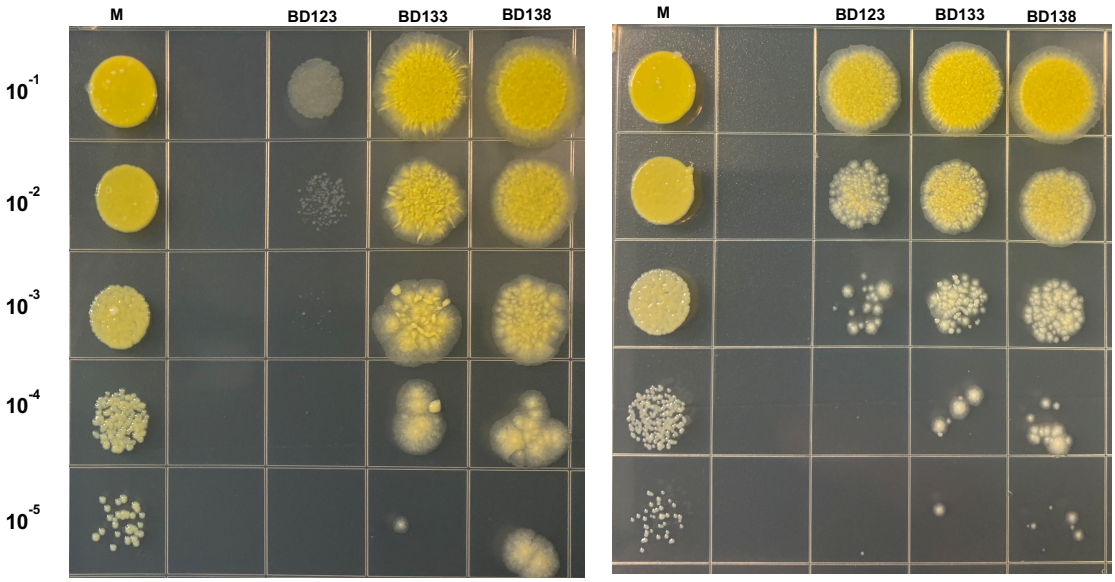

7H10 + TTM | 7H10 + TTM + $CuCl_2$

B

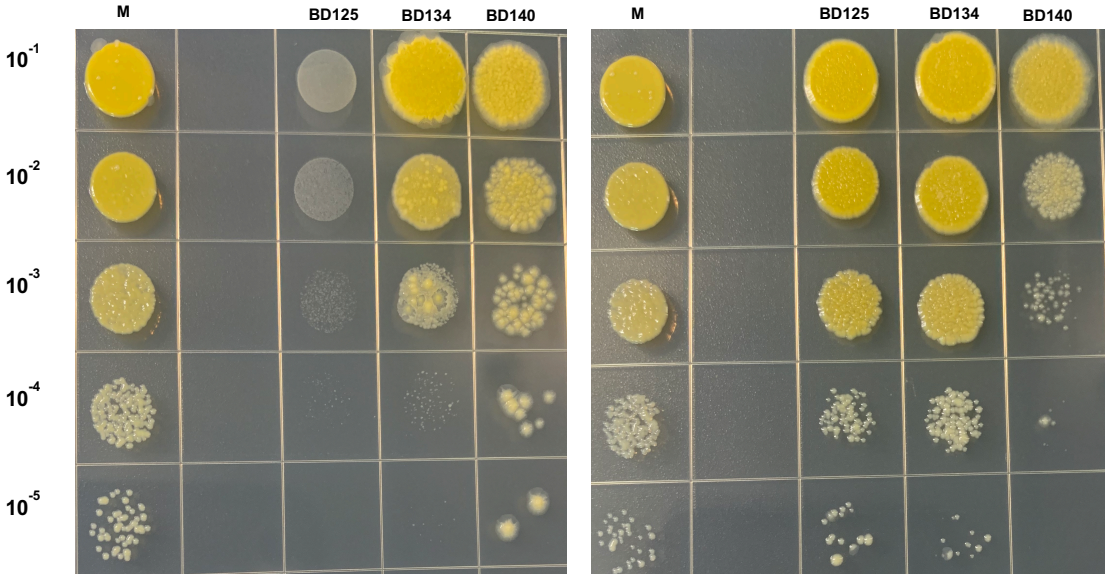

7H10 + TTM | 7H10 + TTM + $CuCl_2$

C

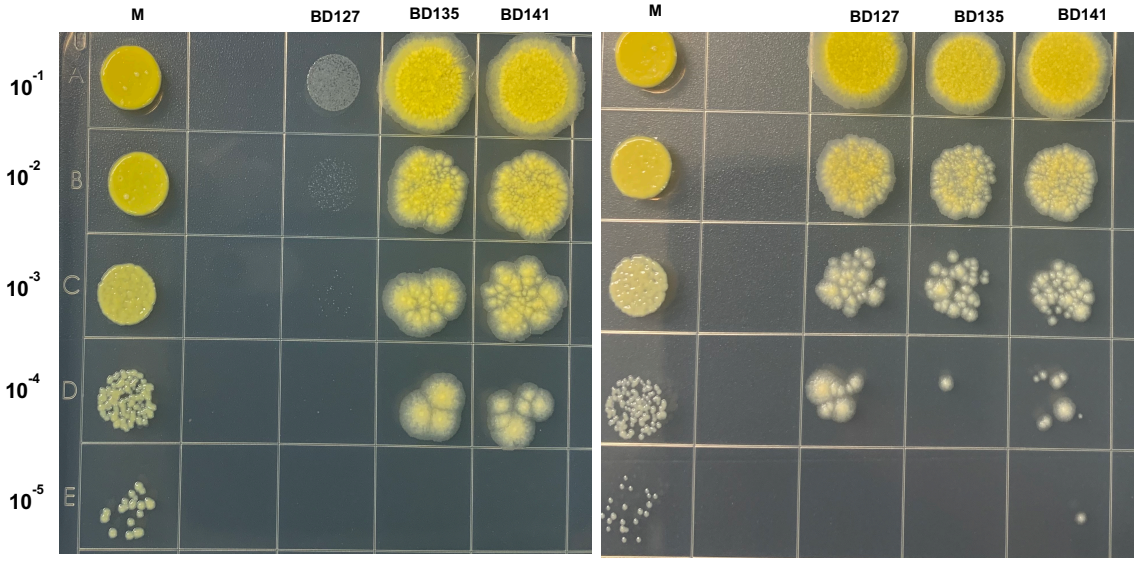

7H10 + TTM | 7H10 + TTM + $CuCl_2$

D

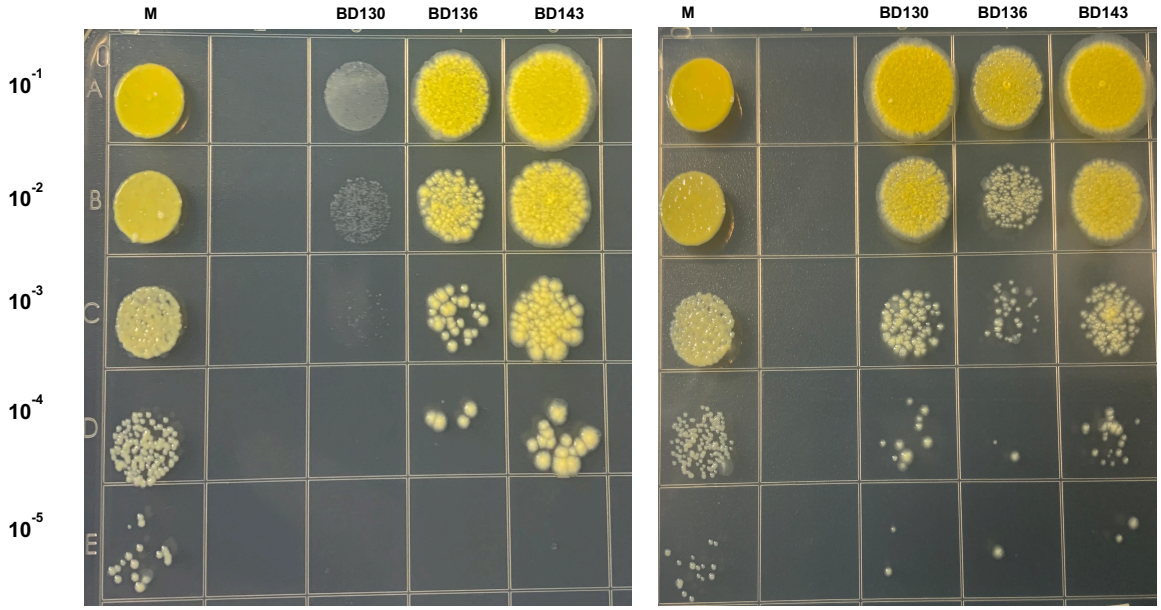

7H10 + TTM | 7H10 + TTM + $CuCl_2$

Fig. 4.6. ***M. marinum*** **NRPS operon genes are required for growth on copper-chelated solid medium.** Serial dilutions of strains *M. marinum* M (M), BD123 (*MMAR0260*$^{-}$), BD138 (*MMAR0260*$^{-}$/pP$_{myctetO}$*Rv0097-Rv0101*), BD139 (*MMAR02060*$^{-}$/pP$_{myctetO}$*Rv0097*), BD125 (*MMAR0259*$^{-}$), BD134 (*MMAR0259*$^{-}$/pP$_{myctetO}$*MMAR0259-MMAR0256*), BD140 (*MMAR0259*$^{-}$/pP$_{myctetO}$*Rv0097-Rv0101*), BD127 (*MMAR0258*$^{-}$), BD135 (*MMAR0258*$^{-}$/pP$_{myctetO}$*MMAR0259-MMAR0256*), BD141 (*MMAR0258*$^{-}$/pP$_{myctetO}$*Rv0097-Rv0101*), BD130 (*MMAR0256*$^{-}$), BD136 (*MMAR0256*$^{-}$/pP$_{myctetO}$*MMAR0259-MMAR0256*), and BD143 (*MMAR0256*$^{-}$/pP$_{myctetO}$*Rv0097-Rv0101*) were spotted onto 7H10tgADS agar with TTM (25 μM) +/- $CuCl_2$ (75 μM) as indicated and incubated 15 days at 30ºC.

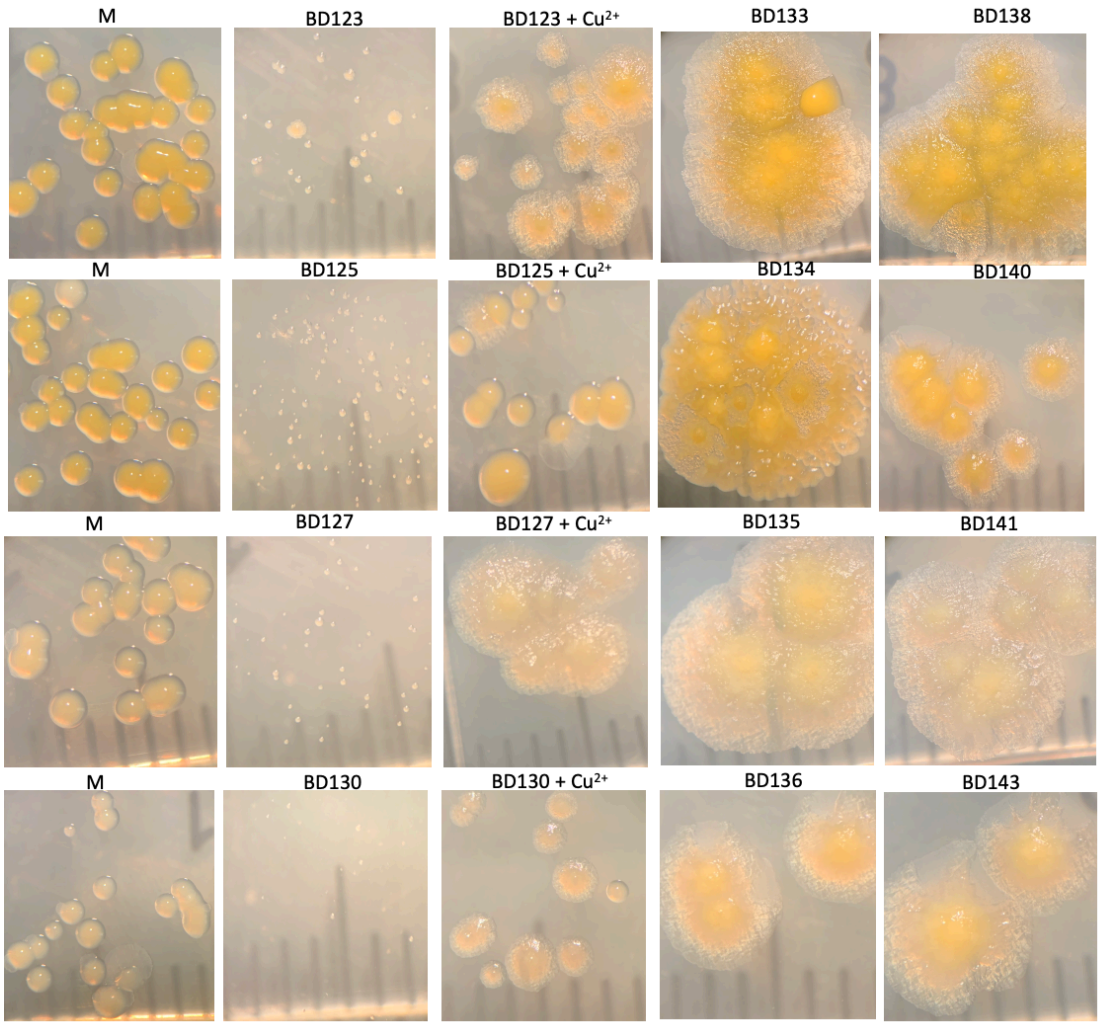

Fig. 4.7. Disruption of the *M. marinum* NRPS operon genes reduces colony size on copper-chelated medium. Shown are photographs of isolated colonies of strains *M. marinum* M, BD123 (*MMAR0260*$^{-}$), BD138 (*MMAR0260*$^{-}$/pP$_{myctetO}$*Rv0097-Rv0101*), BD139 (*MMAR0206*$^{-}$/pP$_{myctetO}$*Rv0097*], BD125 (*MMAR0259*$^{-}$), BD134 (*MMAR0259*$^{-}$/pP$_{myctetO}$*MMAR0259-MMAR0256*), BD140 (*MMAR0259*$^{-}$/pP$_{myctetO}$*Rv0097-Rv0101*], BD127 (*MMAR0258*$^{-}$), BD135 (*MMAR0258*$^{-}$/[pP$_{myctetO}$*MMAR0259-MMAR0256*]), BD141 (*MMAR0258*$^{-}$/[pP$_{myctetO}$*Rv0097-Rv0101*]), BD130 (*MMAR0256*$^{-}$), BD136 (*MMAR0256*$^{-}$/pP$_{myctetO}$*MMAR0259-MMAR0256*), and BD143 (*MMAR0256*$^{-}$/pP$_{myctetO}$*Rv0097-Rv0101*) after 21 day incubation at 30º on 7H10tgADS

agar containing TTM (25 μM) and the indicated mutant strains cultured similarly but with 75 μM $CuCl_2$ (Cu^{2+}) supplementation. Plates were photographed on a mm-scale transparent rule on a dissecting microscope (magnification = 10X).

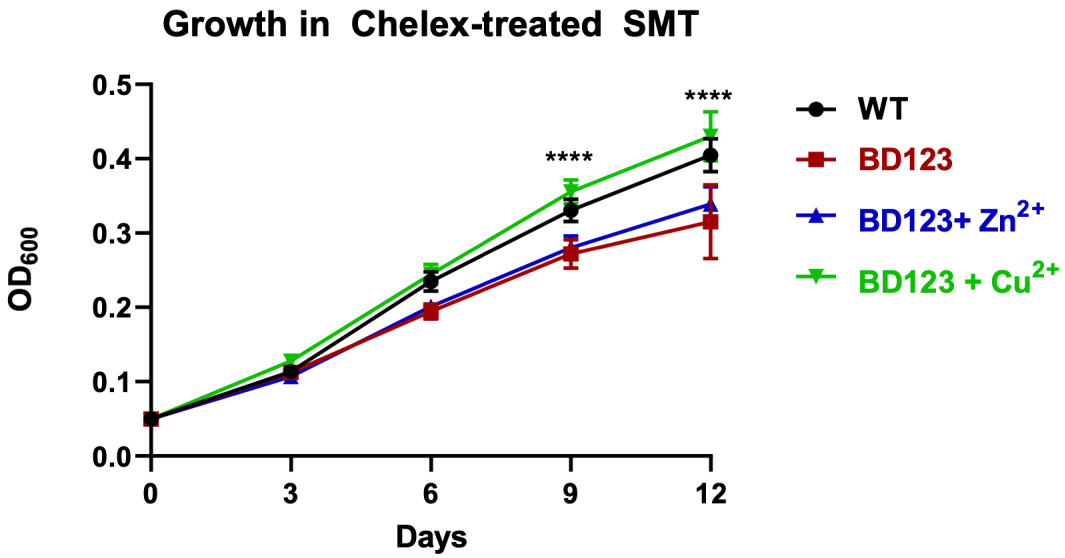

Fig. 4.8. Cu^{2+} restores growth of a *MMAR0260* mutant in Chelex-treated SMT. *M. marinum* BD123 (*MMAR0260⁻*) was cultured stationary at 30ºC in Chelex-treated SMT medium alone or supplemented with 25 µM $ZnSO_4$ (Zn^{2+}) or 25 µM $CuSO_4$ (Cu^{2+}) or both metals and compared with parent strain M (WT) cultured without metal supplementation. Cell densities shown (OD_{600}) are the mean +/- standard error from four independent cultures in triplicate. Significant differences in growth of WT or BD123 in SMT versus SMT + Cu^{2+} are indicated (****p<0.0001). No significant differences were obtained between BD123 grown in SMT versus SMT + Zn^{2+}.

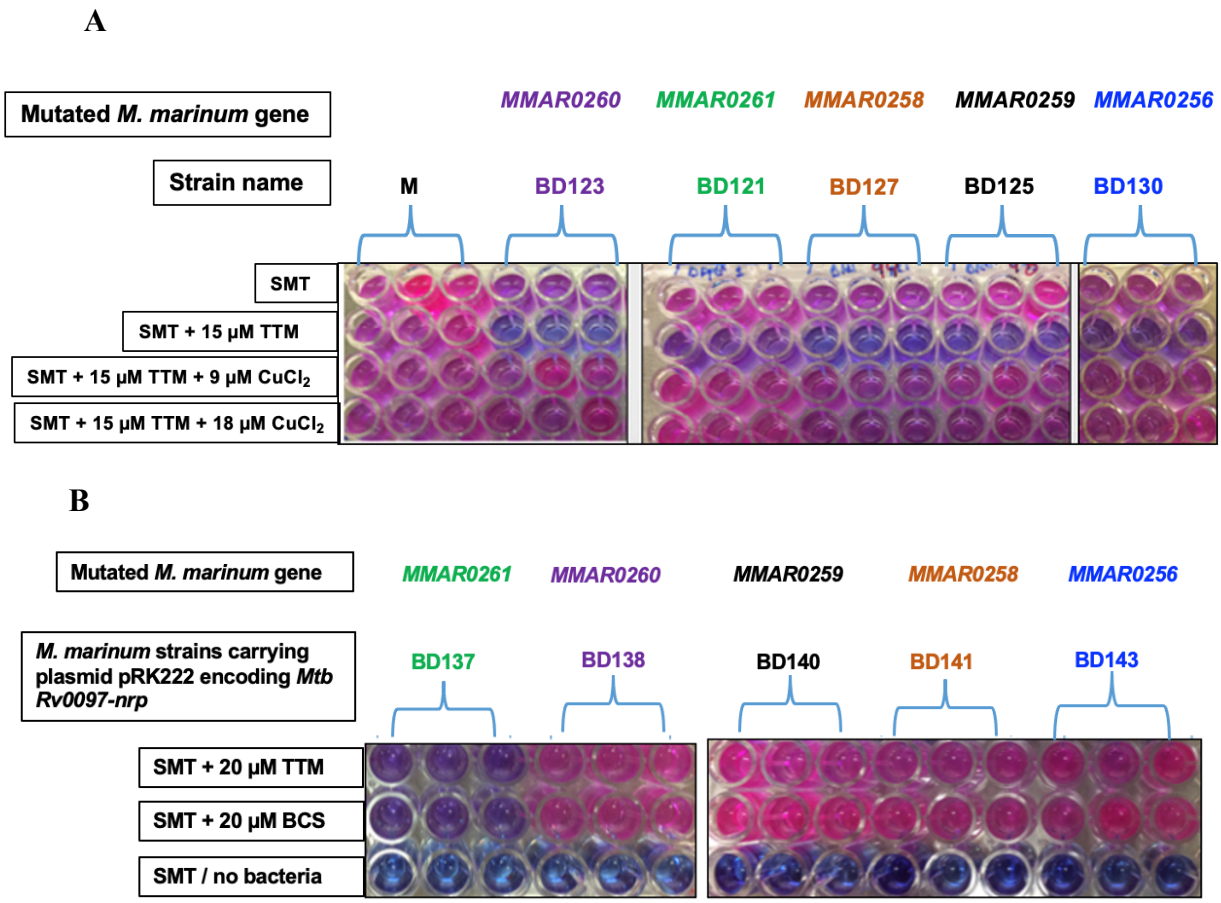

Fig. 4.9. Genes in the *M. marinum* NRPS operon are required for growth in copper (II)-chelated medium. A) *M. marinum* M and mutant strains (described in figures 4.6 and 4.7) were cultured in SMT in the presence or absence of copper (II) chelator TTM and copper chloride where indicated. After 4-day incubation at 30°C, alamarBlue reagent was added and cells incubated an additional 24 hours for color development. B) Growth of *M. marinum* mutants carrying *M. tuberculosis* genes, *Rv0097-Rv0101,* under control of a tetracycline-inducible promoter. Strains were cultured in SMT with 20 µM TTM or copper(I) chelator BCS and 50 ng/ml anhydrotetracycline and alamarBlue assays performed as described for panel A. Wells with medium lacking bacteria or growth remain blue. The experiment was performed three times in triplicate.

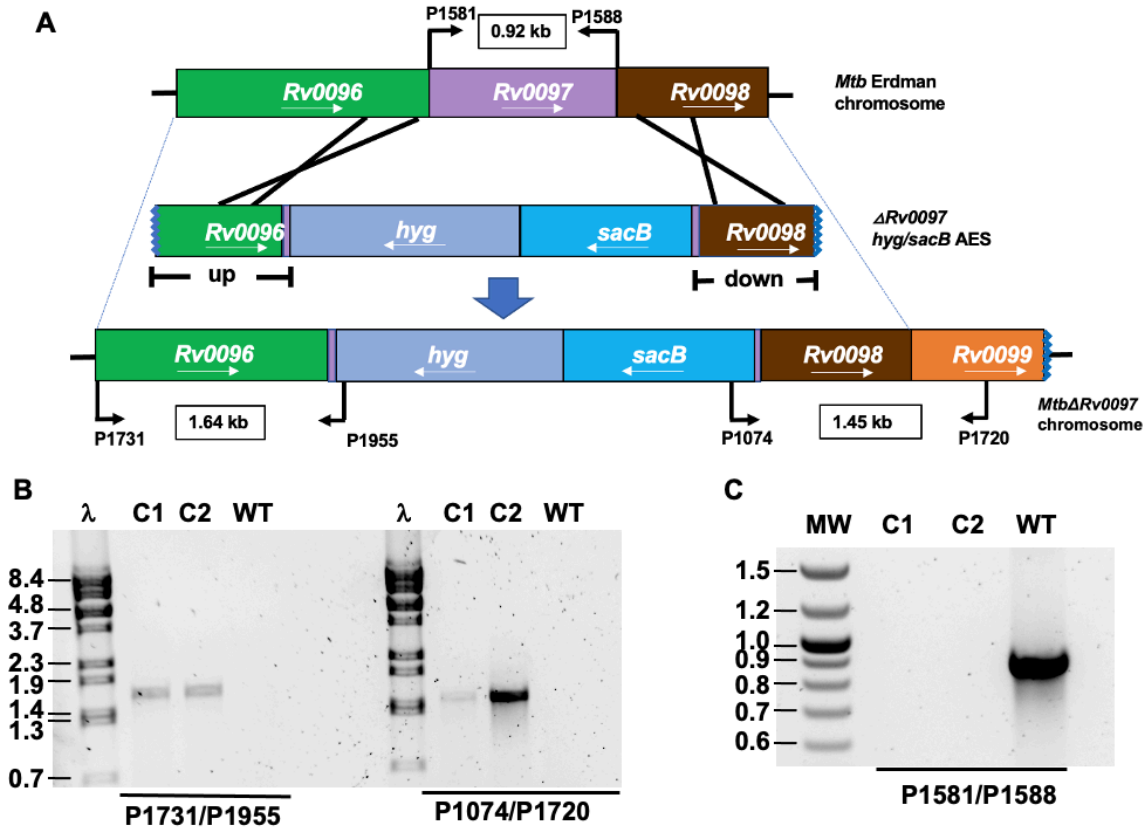

Fig 4.10. Confirmation of *M. tuberculosis ΔRv0097* mutants. A) Overview of *M. tuberculosis Rv0097* deletion. An allelic exchange substrate (AES) consisting of ~1 kb genomic regions upstream (up) and downstream (down) of *Rv0097* along with the first and last few codons of *Rv0097* cloned to flank a *hyg-sacB* cassette was used to replace *Rv0097* in *M. tuberculosis* strain Erdman by recombineering. The locations of primers (bent arrows) and expected PCR product sizes for the *Rv0097* mutant are shown. B) PCR screening of *ΔRv0097* candidates (C1 & 2) for the *Rv0096—hyg* and the *sacB—Rv0098* junctions with the indicated primer pair are shown. The expected amplicon sizes for the deletion mutant are 1.64 kb with primer pair P1731/P1955 and 1.45 kb with primers P1074/P1720. No bands are expected for parent Erdman (WT). Sizes (in kb) of the indicated bands of lambda/*Bst*EII DNA standards (λ) are indicated. C) PCR screening of

ΔRv0097 candidates for the loss of *Rv0097* using primer pair P1581/P1588 which amplify the 0.92 kb *Rv0097*gene in parent strain Erdman (WT). Sizes (in kb) of NEB 100 bp ladder DNA standards (MW) are indicated.

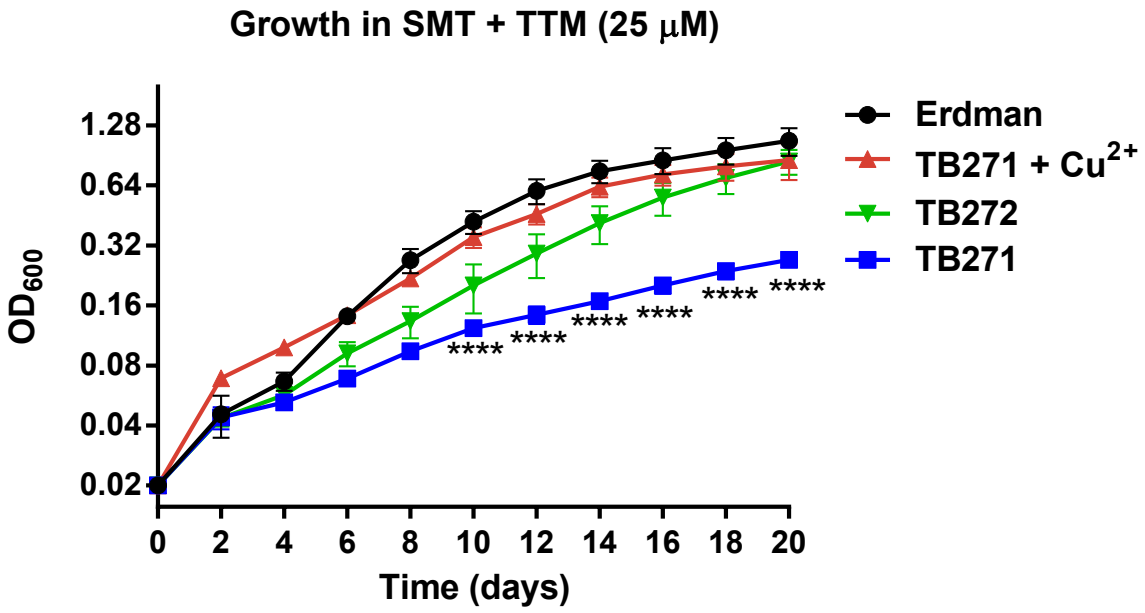

Fig. 4.11. ***Rv0097* is required growth in copper-restricted medium.** *M. tuberculosis* strains Erdman, TB271 (*ΔRv0097*/empty vector), and TB272 (*ΔRv0097*/$pP_{myctetO}$*Rv0097-Rv0101*) were cultured in SMT + TTM (25 μM) and TB271 in the same medium supplemented with 50 μM $CuCl_2$. The optical densities (OD_{600}) shown are the mean with standard error of two independent experiments in triplicate. Significant growth differences for TB271 relative to the other strains and to TB271 grown in the presence of $CuCl_2$ are indicated (****p<0.0001).

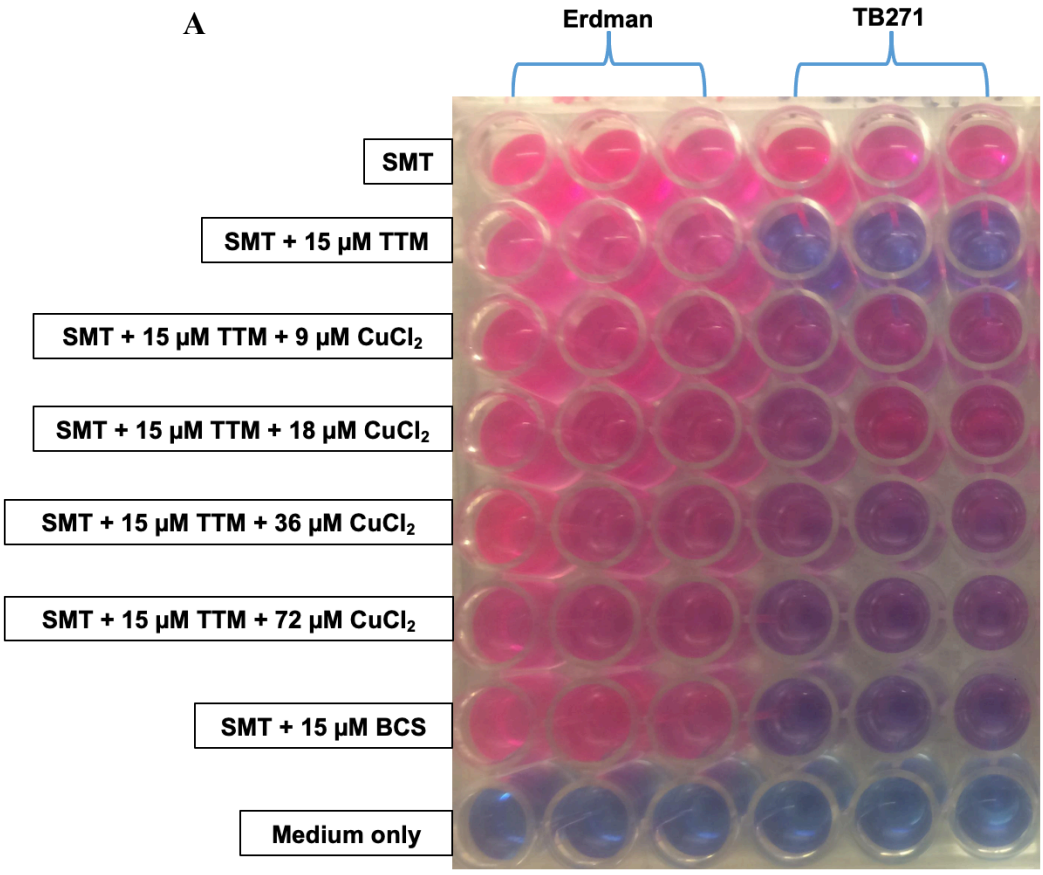
A
Erdman
TB271
SMT
SMT + 15 µM TTM
SMT + 15 µM TTM + 9 µM $CuCl_2$
SMT + 15 µM TTM + 18 µM $CuCl_2$
SMT + 15 µM TTM + 36 µM $CuCl_2$
SMT + 15 µM TTM + 72 µM $CuCl_2$
SMT + 15 µM BCS
Medium only

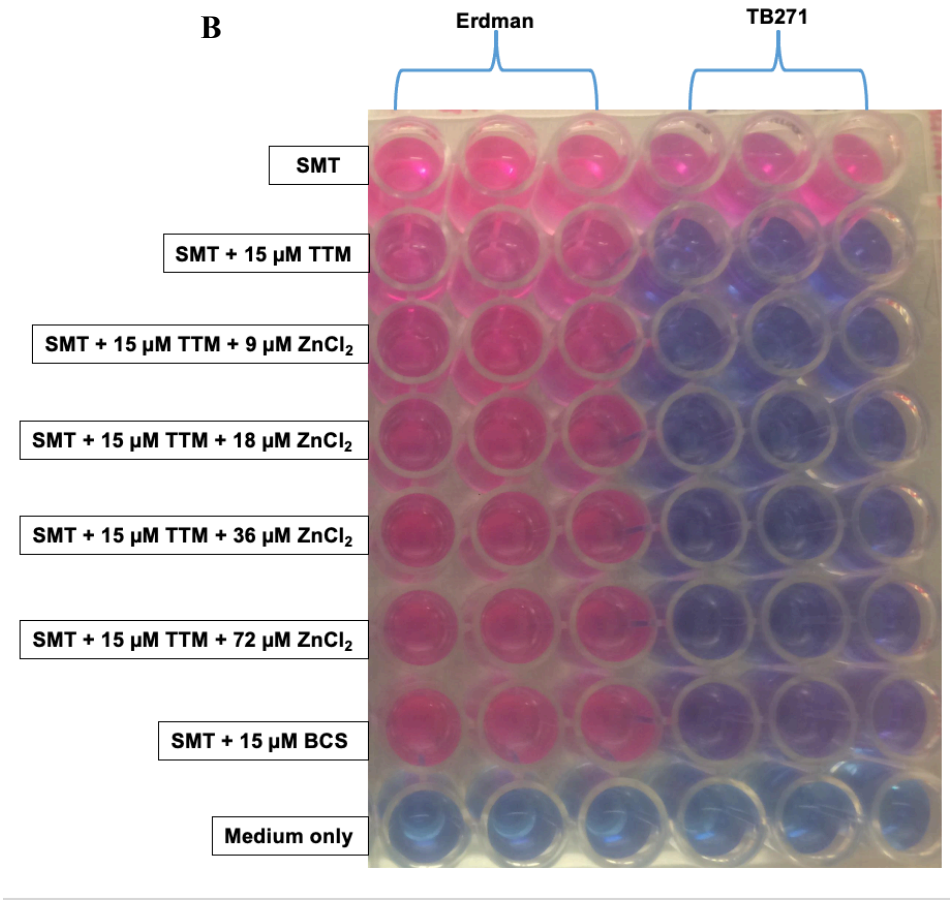
B
Erdman
TB271
SMT
SMT + 15 µM TTM
SMT + 15 µM TTM + 9 µM $ZnCl_2$
SMT + 15 µM TTM + 18 µM $ZnCl_2$
SMT + 15 µM TTM + 36 µM $ZnCl_2$
SMT + 15 µM TTM + 72 µM $ZnCl_2$
SMT + 15 µM BCS
Medium only

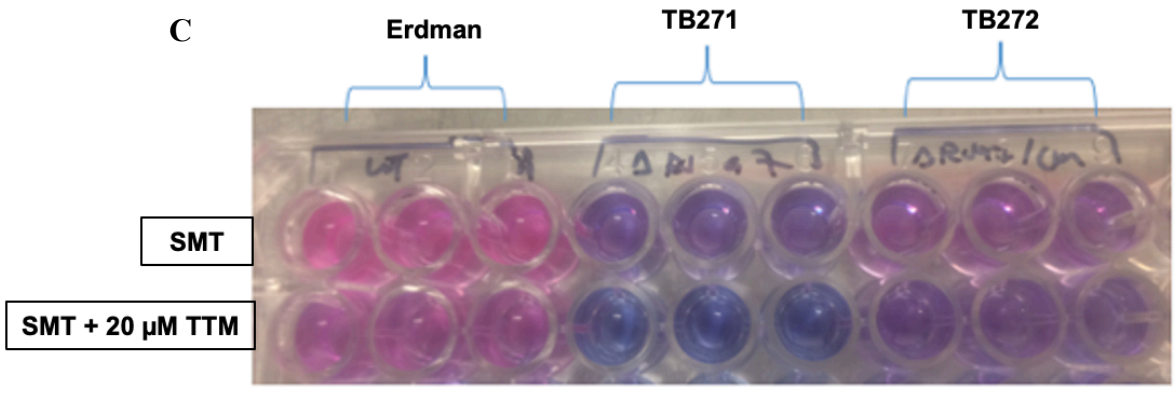
C
Erdman
TB271
TB272
SMT
SMT + 20 µM TTM

Fig. 4.12. Impaired growth of an *Rv0097* mutant in copper-restricted medium. Static microplate SMT cultures of *M. tuberculosis* strains were monitored for growth by alamarBlue assay. In medium without bacteria or bacterial growth, the alamarBlue indicator dye color is blue. Bacterial metabolic activity reduces the dye to yield a pink color. Strain Erdman was compared to TB271 (*ΔRv0097/*empty vector) for growth in SMT +/- 15 or 20 μM TTM +/- the indicated concentration of copper chloride or +/- 15 μM BCS (A-B). Zinc chloride was tested in TB271cultures to assess the possibility of zinc chelation by TTM (B). Strain Erdman was compared to TB271 and TB272 (*ΔRv0097/*pAH15) for growth in SMT +/- 20 μM TTM (C). After incubation for 8 days, alamarBlue was added to each well and cells color development examined after 24-hour incubation. The experiment was conducted five times in in triplicate with similar results.

A

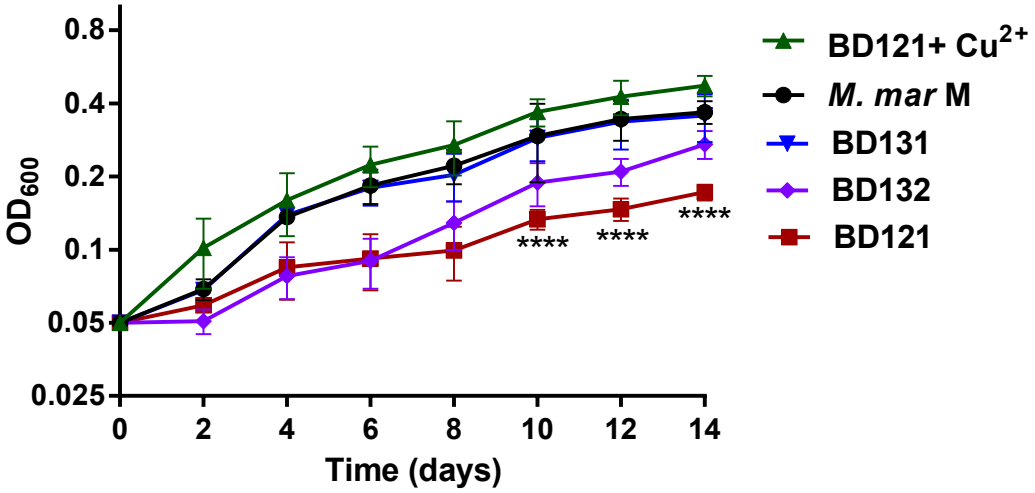
0.8
0.4
0.2
0.1
0.05
0.025
OD600
0
2
4
6
8
10
12
14
Time (days)
****
****
****
BD121+ Cu2+
M. mar M
BD131
BD132
BD121

B

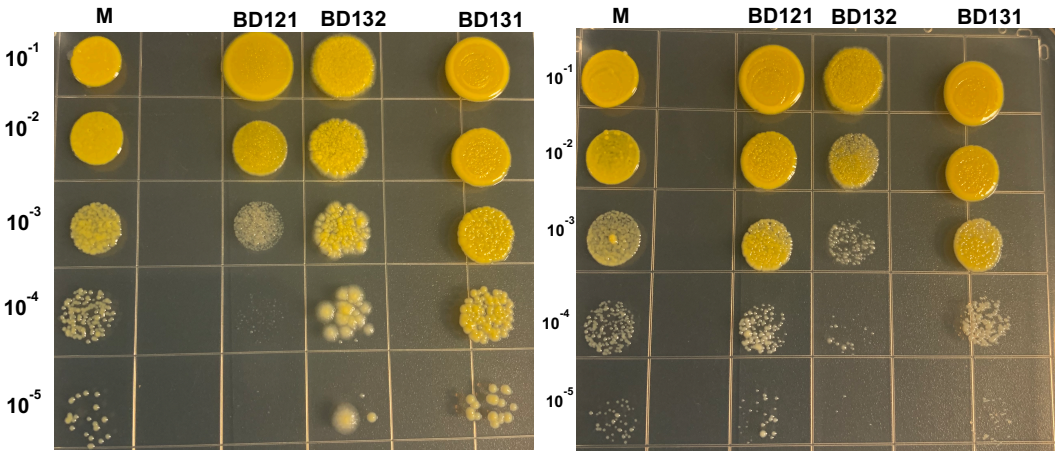
7H10ADSgt + TTM
7H10ADSgt + TTM
M
BD121
BD132
BD131
M
BD121
BD132
BD131
10-1
10-2
10-3
10-4
10-5

C

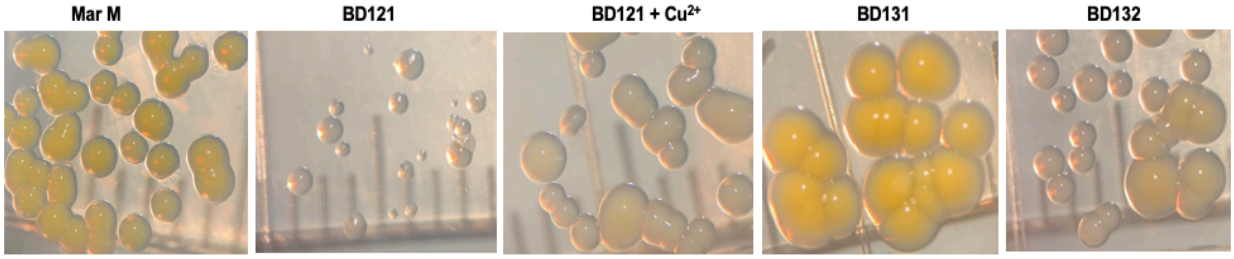

Fig. 4.13. ***PPE1* is required growth in copper-restricted medium.** A) Growth comparison (OD_{600}) of strains *M. marinum* M, BD121 (*MMAR0261*$^{-}$), BD131 (BD121/$pP_{myctetO}$*MMAR0261*), and BD132 (BD121/$pP_{myctetO}$*Rv0096*) cultured in SMT + TTM (20 µM) without or with 20 µM $CuCl_2$ (Cu^{2+}). The data shown are the mean with standard error of two independent experiments in triplicate. Significant growth differences for BD121 relative to all other strains and BD121 grown with $CuCl_2$ are indicated (****p<0.0001). B) The same strains were passaged twice in SMT to OD_{600} = 1, then serially diluted and spotted onto 7H10tgADS agar containing TTM (25 µM) without or with $CuCl_2$ (75 µM). After incubation for 15 days, plates were examined. (C) On day 21, the same plates were placed on a transparent mm-scale ruler and examined on a dissecting microscope to visualize individual colonies (magnification = 10X).

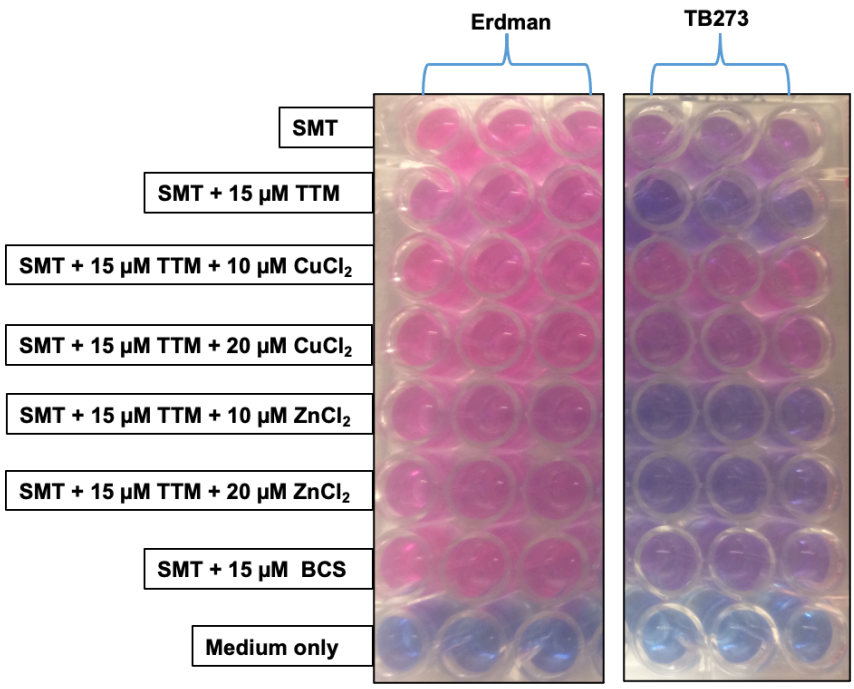

Fig. 4.14. Impaired growth of an *Rv0096* mutant in copper-restricted medium. Growth of strains *M. tuberculosis* Erdman and TB273 (*ΔRv0096*) was compared in SMT medium containing or lacking the indicated copper chelator or metal salt by alamarBlue assay. The experiment was conducted at least three times in triplicate.

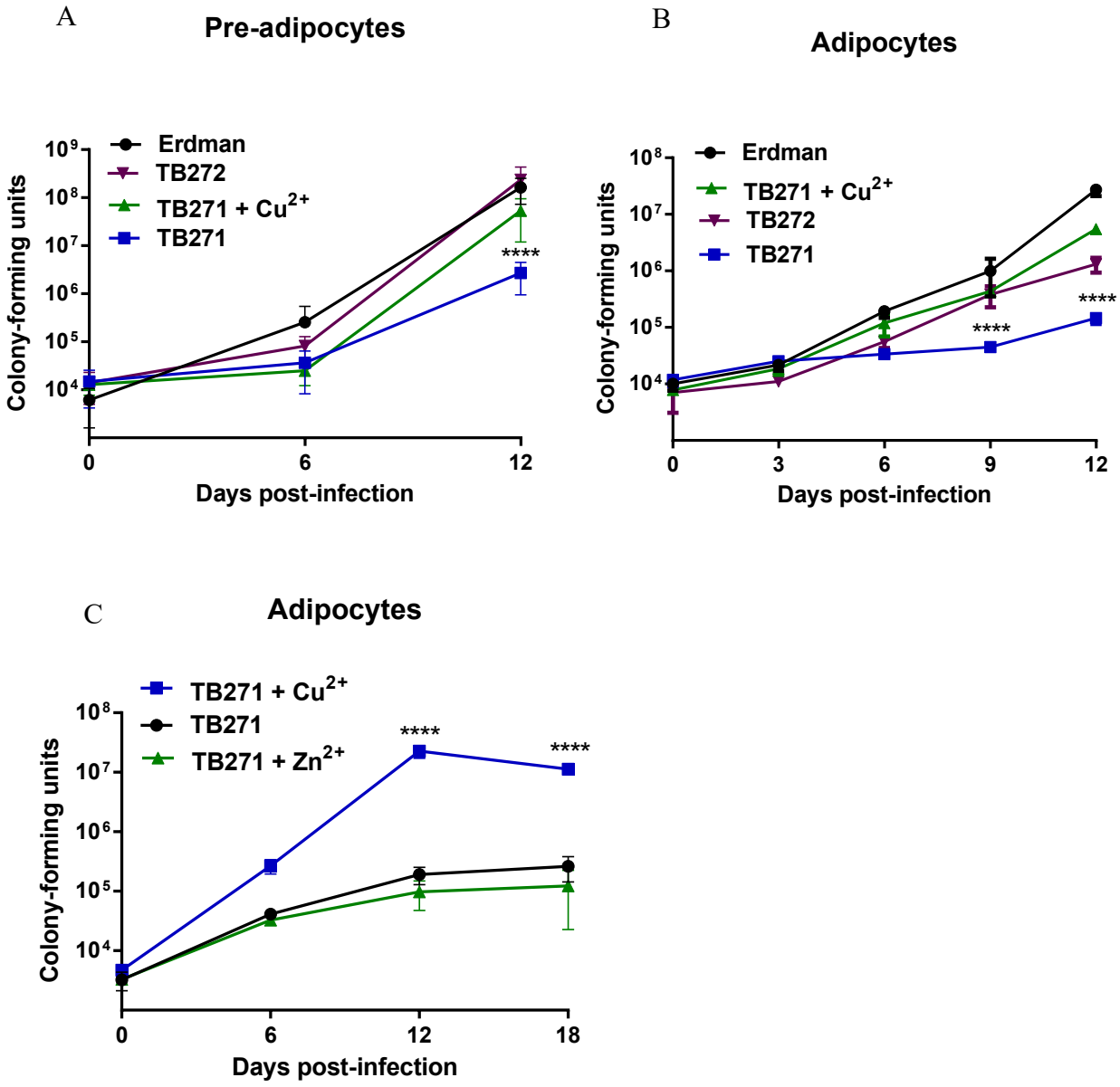

Fig. 4.15. *Rv0097* facilitates *M. tuberculosis* replication in 3T3-L1 cells. Pre-adipocytes (A) and adipocytes (B, C) derived from cell line 3T3-L1 were infected with *M. tuberculosis* strains Erdman, TB271 (*ΔRv0097*/empty vector), or TB272 (*ΔRv0097/* $pP_{myctetO}$*Rv0097-Rv0101*) at MOI = 1 for 24 hours at 37ºC in basal medium (BM) without or with $CuCl_2$ (60 µM) or $ZnSO_4$ (60 µM).

Cells were then incubated for 2 hours with fresh BM containing amikacin (200 µg /mL), and the medium was replaced with BM without drug. At the indicated time points, cells were lysed with triton X-100, and plated on 7H10tgADS agar for CFU enumeration. Data shown indicate the mean with standard error of three (A) or two (B, C) independent experiments with three biological replicates. Significant CFU differences of the indicated strain relative to other strains or conditions are indicated (****$p<0.0001$).

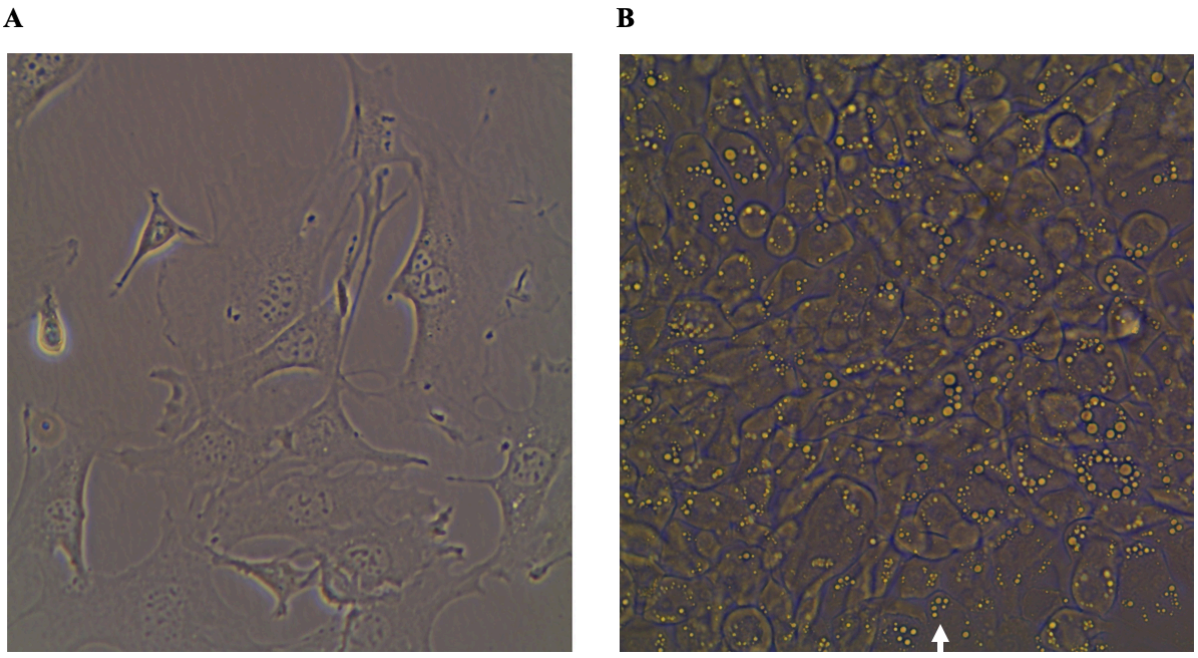

Fig. 4.16. Differentiation of 3T3-L1 pre-adipocytes to adipocytes. 3T3-L1 cells (A) were grown to confluency in DMEM-BCS and differentiated with IBMX + dexamethasone + insulin mix in DMEM-FBS for two days, then the medium was replaced with insulin-containing medium for another two days. Cells were fed DMEM-FBS every three days. Spherical lipid droplets (arrow) were visible seven days after differentiation (B). Shown are light microscopy images (40X magnification).

A

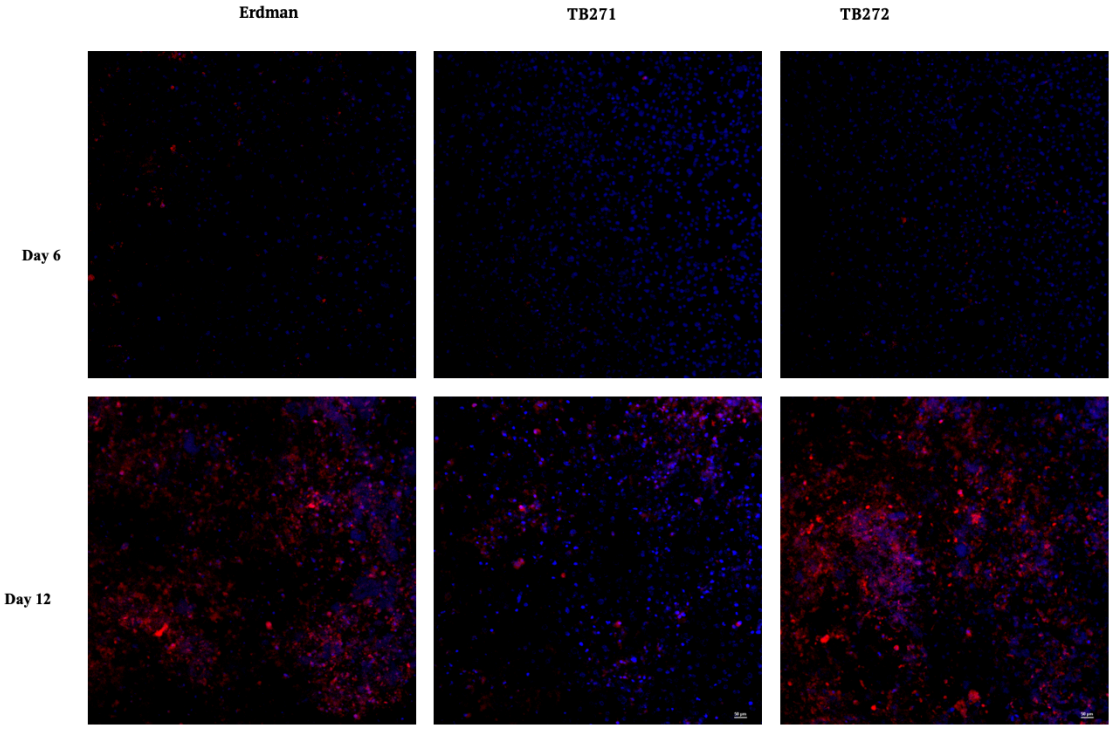
Erdman
TB271
TB272
Day 6
Day 12

B

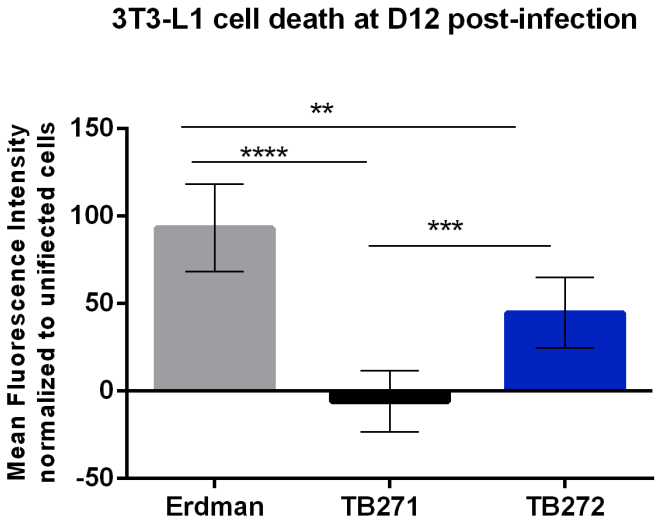
3T3-L1 cell death at D12 post-infection
Mean Fluorescence Intensity normalized to unifiected cells
150
100
50
0
-50
**
****
***
Erdman
TB271
TB272

Fig. 4.17. *M. tuberculosis ΔRv0097* is defective at killing 3T3-L1 pre-adipocytes. A) Pre-adipocyte 3T3-L1 pre-adipocytes were infected with *M. tuberculosis* Erdman, TB271 (*ΔRv0097*/empty vector), or TB272 (*ΔRv0097*/ $pP_{myctetO}$*Rv0097-Rv0101*) at MOI = 1. At day 6 (upper panels) and day 12 (lower panels) post-infection, cells were stained with Zombie Red (stains dead cells red) and nuclear stain DAPI (blue) and visualized by fluorescence microscopy (40X magnification, scale bar = 5 μm). B) Mean fluorescence intensity of Zombie Red was quantified relative to the uninfected cells at day 12 post-infection.

Uninfected – Day 1

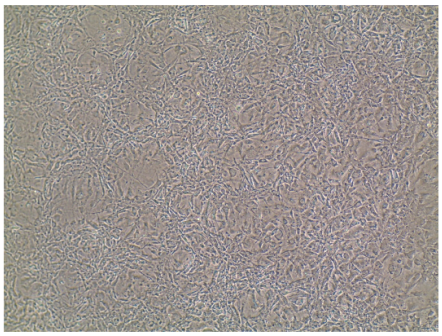

Erdman – Day 1

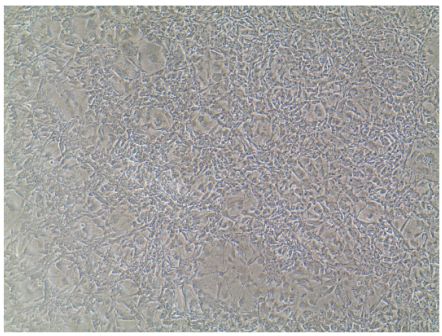

TB271 – Day 1

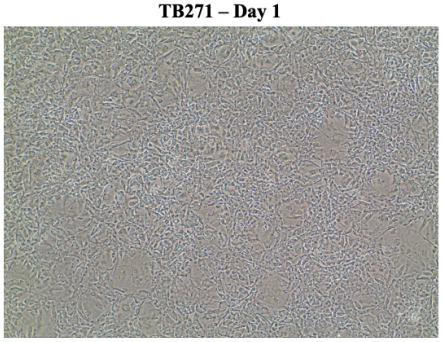

TB272 – Day 1

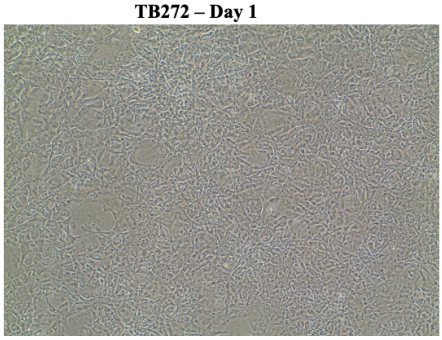

Erdman - Day 12 pi

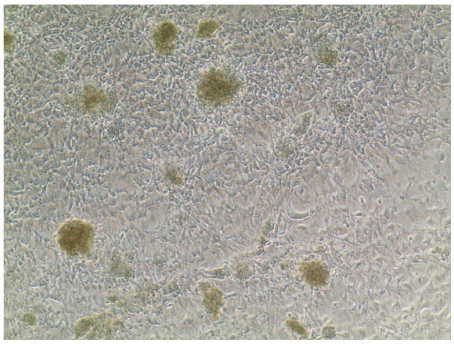

TB271 - Day 12 pi

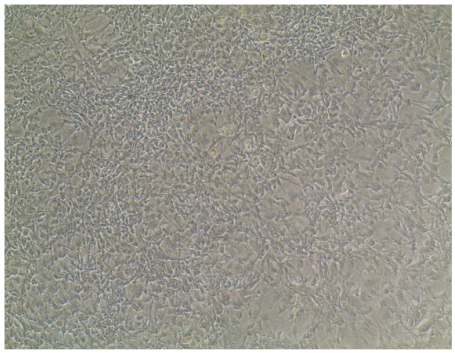

TB271+$CuCl_2$ 0.05 mM - Day 12 pi

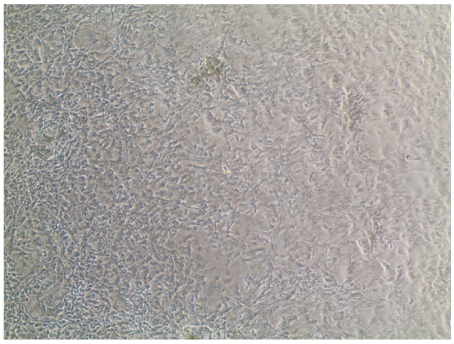

TB272 - Day 12 pi

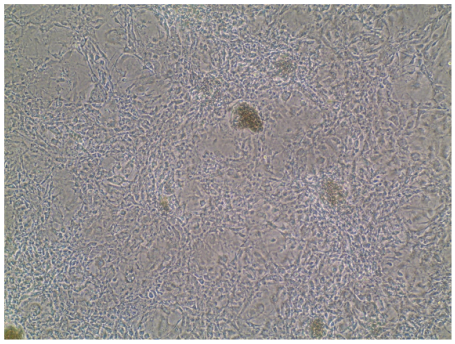

Erdman – Day 15 pi

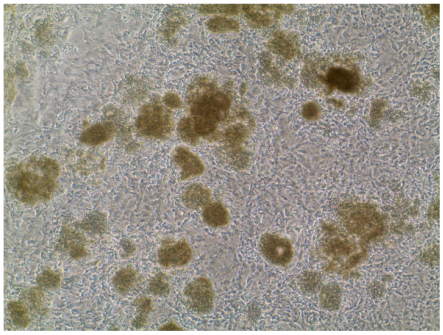

TB271 – Day 15 pi

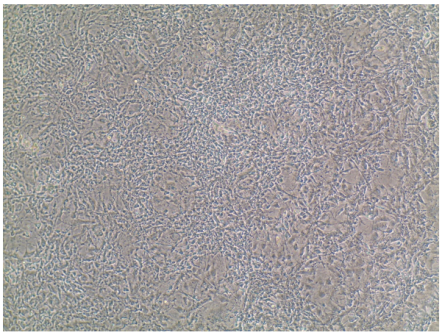

TB271+$CuCl_2$ 0.05 mM - Day 15 pi

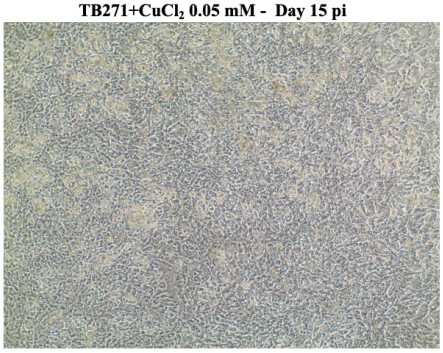

TB272 – Day 15 pi

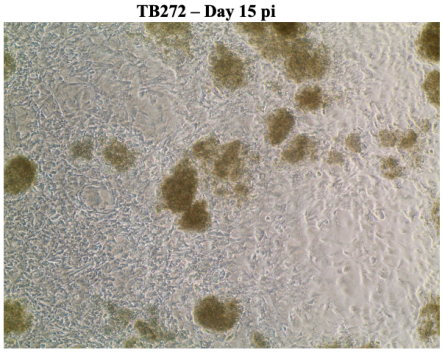

Erdman – Day 18 pi

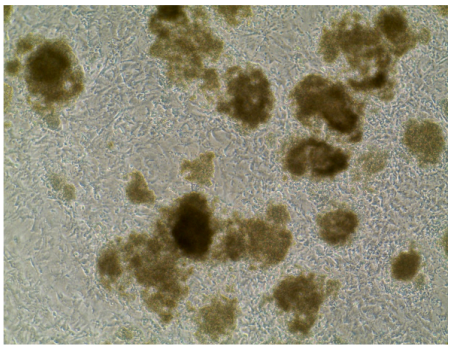

TB271 - Day 18 pi

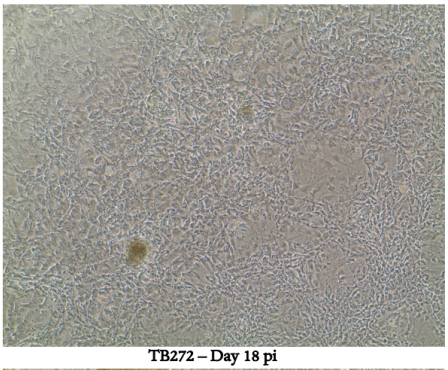

TB271+$CuCl_2$ 0.05 mM – Day 18 pi

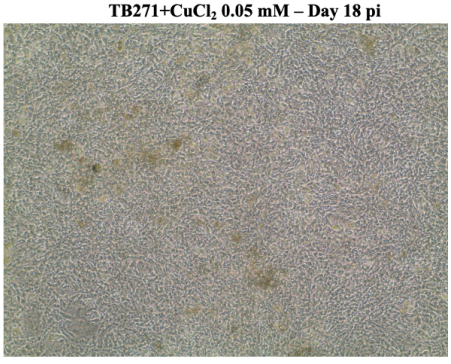

TB272 – Day 18 pi

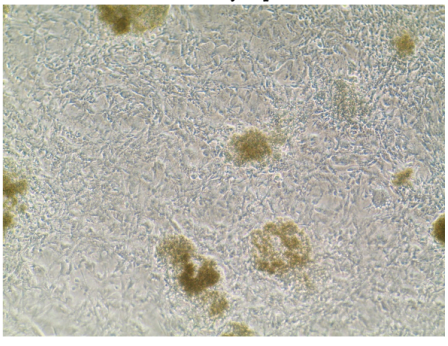

Erdman – Day 21 pi

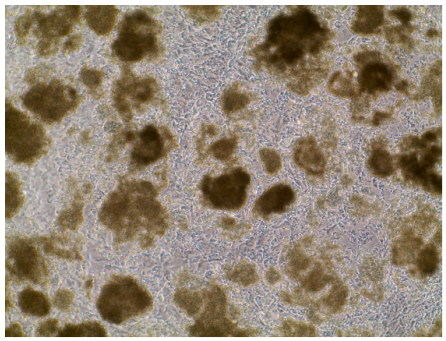

TB271 – Day 21 pi

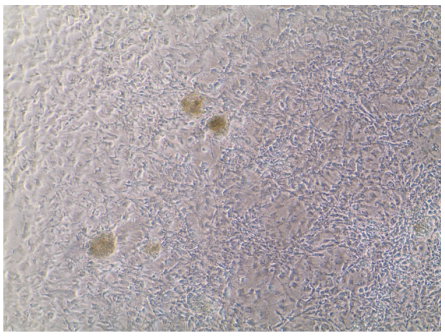

TB271+$CuCl_2$ 0.05 mM – Day 21 pi

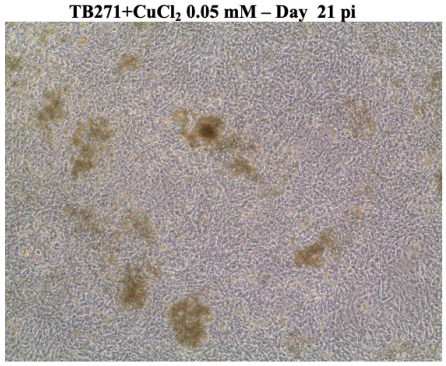

TB272 - Day 21 pi

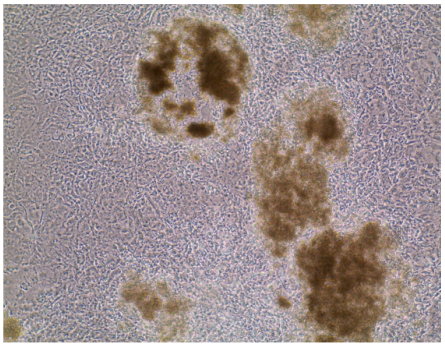

Erdman – Day 24 pi

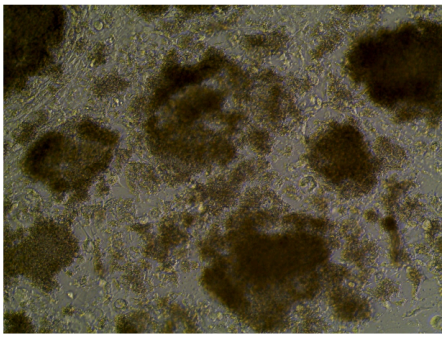

TB271 – Day 24 pi

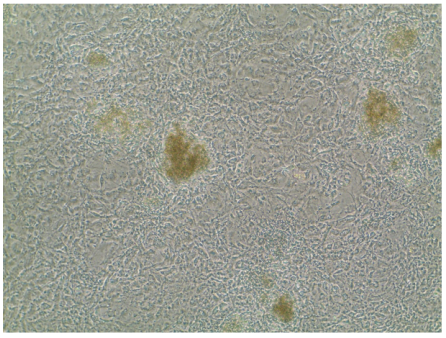

TB271+$CuCl_2$ 0.05 mM – Day 24 pi

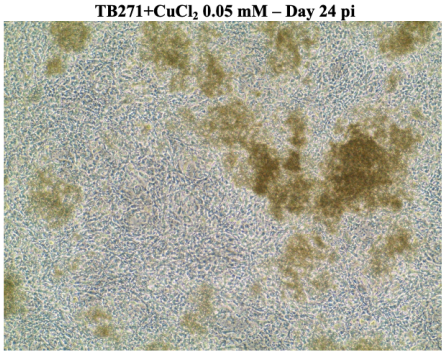

TB272 – Day 24 pi

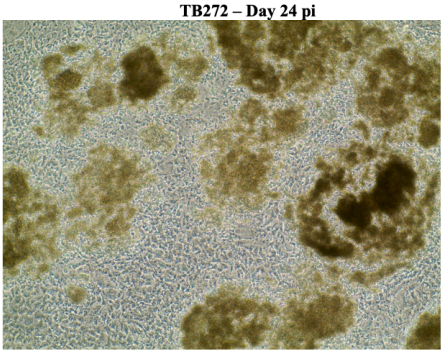

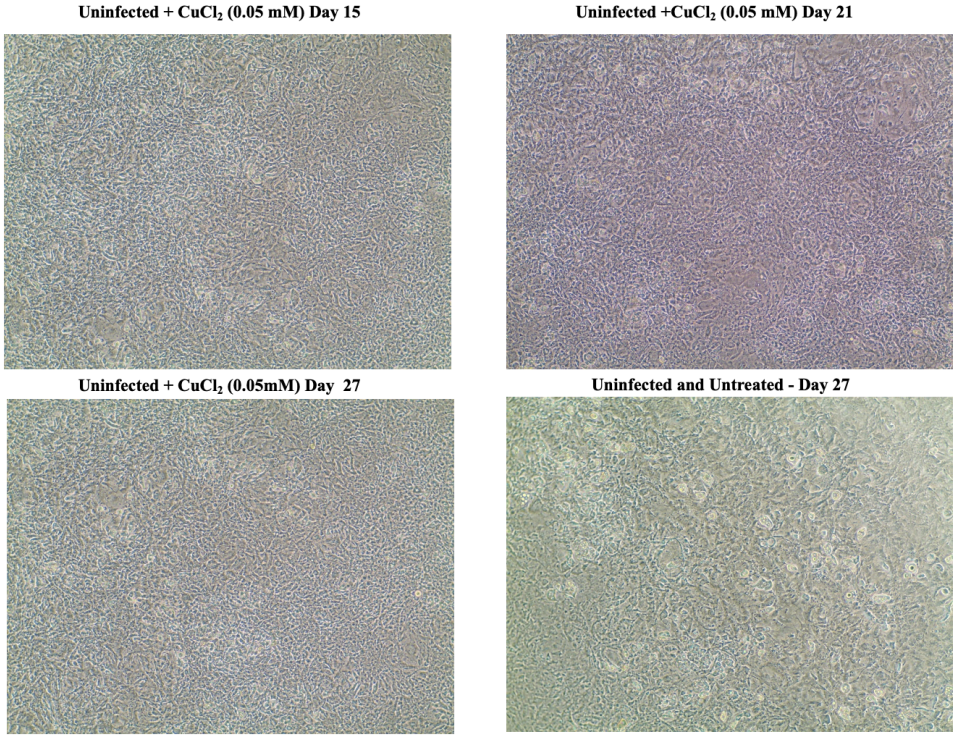

Fig. 4.18. Examination of 3T3-L1 pre-adipocyte infections over a 24-day infection period. 3T3-L1 pre-adipocyte cells were infected with *M. tuberculosis* strain Erdman, TB271 (*ΔRv0097*/empty vector) or TB272 (*ΔRv0097*/pP$_{myctetO}$*Rv0097-Rv0101*) at MOI = 1. Cells were cultured in basal medium alone or supplemented with 0.05 mM $CuCl_2$ where indicated. Infected cells were examined by light microscopy (10X magnification) over a 24-day period.

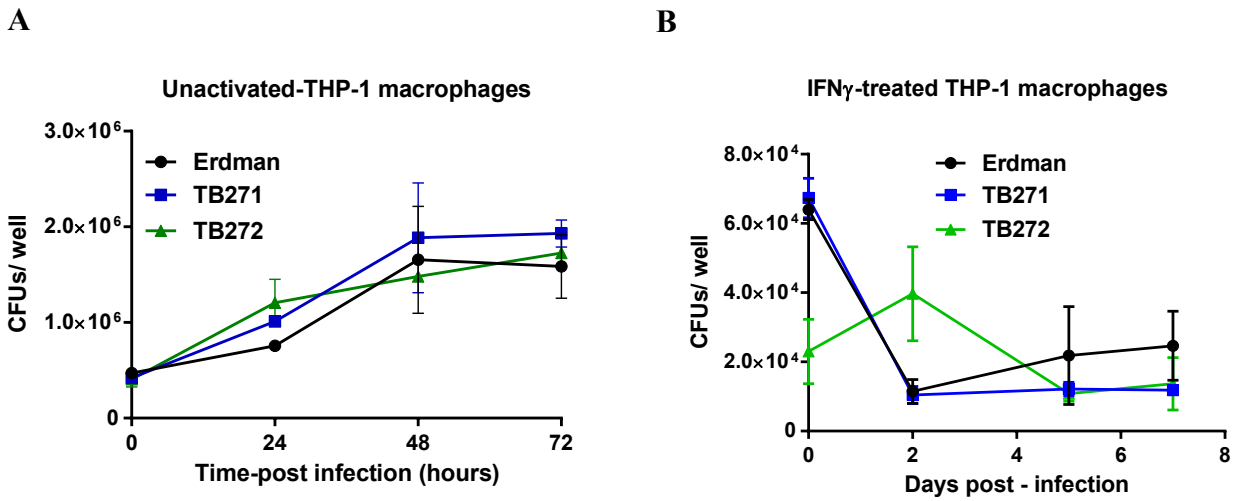

Fig. 4.19. Loss of *Rv0097* does not impacts replication in THP-1 macrophages. THP-1 cells were infected with *M. tuberculosis* Erdman, TB271(Δ*Rv0097*/empty vector) or TB272 (Δ*Rv0097*/pP$_{myctetO}$*Rv0097-Rv0101*) after differentiation into macrophages with PMA (A) and activation with IFN-γ (B) at an MOI of 10 (A) or 1 (B). At the indicated time points, cells were lysed with 0.1% Triton-X100 and plated on 7H10ADSgt to enumerate CFUs.

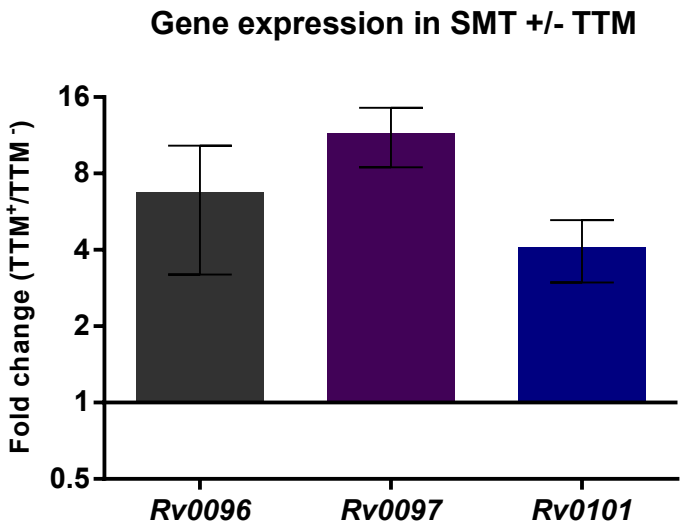

Fig. 4.20. Quantitative RT-PCR analysis of *Rv0096, Rv0097*, and *Rv0101* expression in strain Erdman cultured in SMT +/- TTM (20 µM). *M. tuberculosis* strain Erdman was cultured to OD_{600} = 0.35 in SMT prior to splitting into SMT cultures containing or lacking TTM (20 µM). Transcription of *Rv0096*, *Rv0097*, and *Rv0101* was examined after cultures reached OD_{600} = 0.45. The fold-change expression for each gene in the presence versus absence of TTM was normalized to housekeeping gene *sigA*. Data shown is the mean with standard error of two independent experiments with three biological replicates.

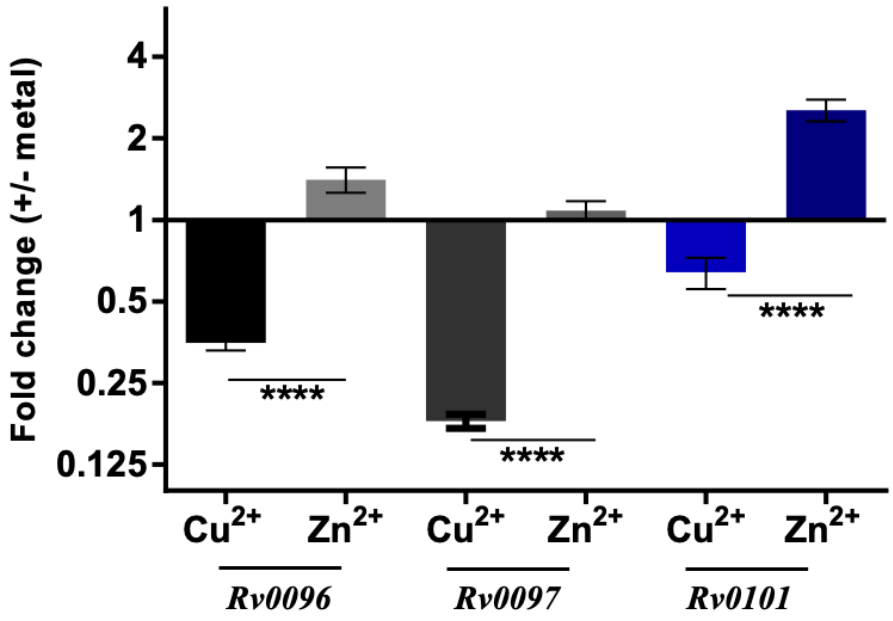

Fig. 4.21. Quantitative RT-PCR analysis of *Rv0096, Rv0097*, and *Rv0101* transcription in 3T3-L1 adipocytes infected with *M. tuberculosis* Erdman. Adipocytes derived from 3T3L1 cells were infected with *M. tuberculosis* Erdman at MOI = 1 and cultured in basal medium containing or lacking $CuCl_2$ (100 µM) or $ZnSO_4$ (100 µM) for 10 days prior to transcriptional analysis. Fold-change expression of the indicated genes in the absence relative to the presence of $CuCl_2$ after normalization to *sigA* are shown. Statistical differences in expression in the presence of Cu^{2+} versus Zn^{2+} was evaluated with Student's t-test (****p<0.0001).

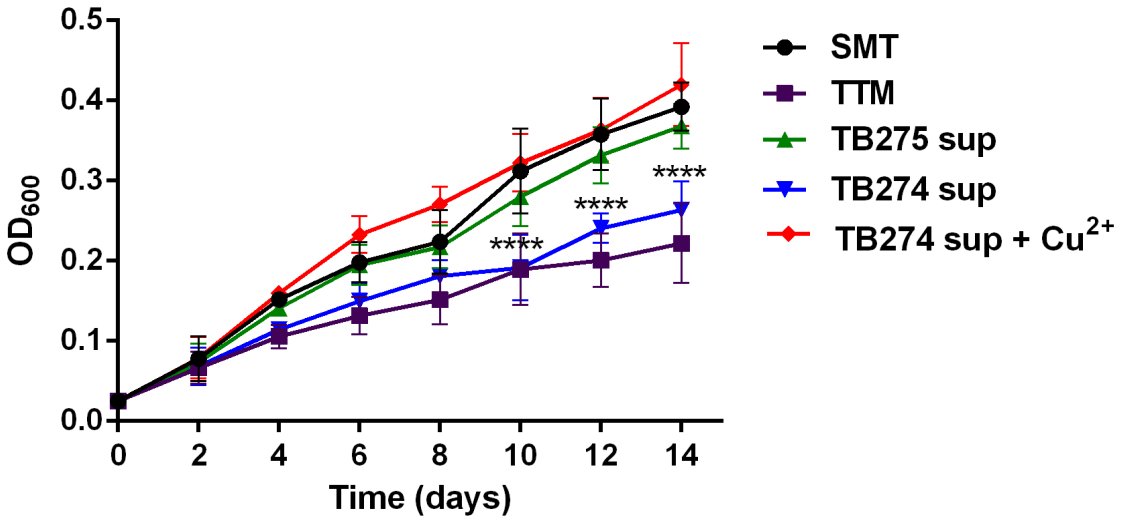

Fig. 4.22. Culture supernatant from *M. tuberculosis* Δ*Rv0096* with plasmid-encoding *Rv0097-R0101* enhances growth of *M. marinum* BD144 (*MMAR0260*⁻/p*MMAR0260*) in copper-restricted medium. Strain BD144 (*MMAR0260*⁻:/p*MMAR0260*) was grown in SMT or SMT + 25 µM TTM or supplemented with culture supernatant from TB275 (Δ*Rv0096*/pP$_{myctetO}$*Rv0097-Rv0101*) or TB274 (*ΔRv0096*/empty vector) grown in SMT + 25µM TTM, or supernatant from TB274 similarly grown but also containing 25 µM $CuCl_2$. Cell densities (OD_{600}) indicate the mean +/- standard error from two independent experiments in triplicate. Significant lack of growth stimulation by the TB274 supernatant grown in the absence of copper relative to growth afforded by TB274 supernatant with copper or by TB275 supernatant or in SMT without TTM is indicated (****$p<0.0001$).

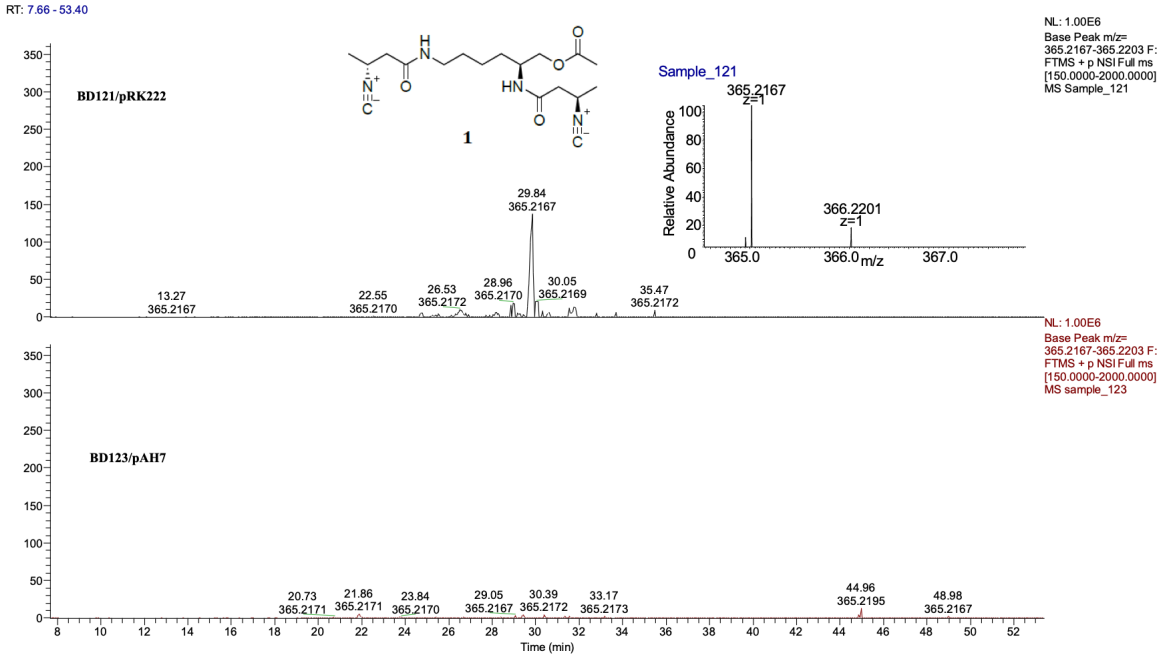

Fig. 4.23. High-resolution electrospray ionization mass spectrometry detection of an isonitrile signature. High-resolution electrospray ionization mass spectrometry comparison of extracted supernatants from *M. marinum* BD137 (*MMAR0261*$^{-}$/pP$_{\text{myctetO}}$*Rv0097-Rv0101*) and BD139 (*MMAR0260*$^{-}$/pP$_{\text{myctetO}}$*Rv0097*) cultured in SMT + 50 μM TTM. The 365.2167 Dalton peak detected only from BD137 corresponds to the mass of isonitrile molecule 1 (shown) identified from expression of *Streptomyces coeruleorubidus* NRPS genes *scoA-E* in *E. coli*.[10]

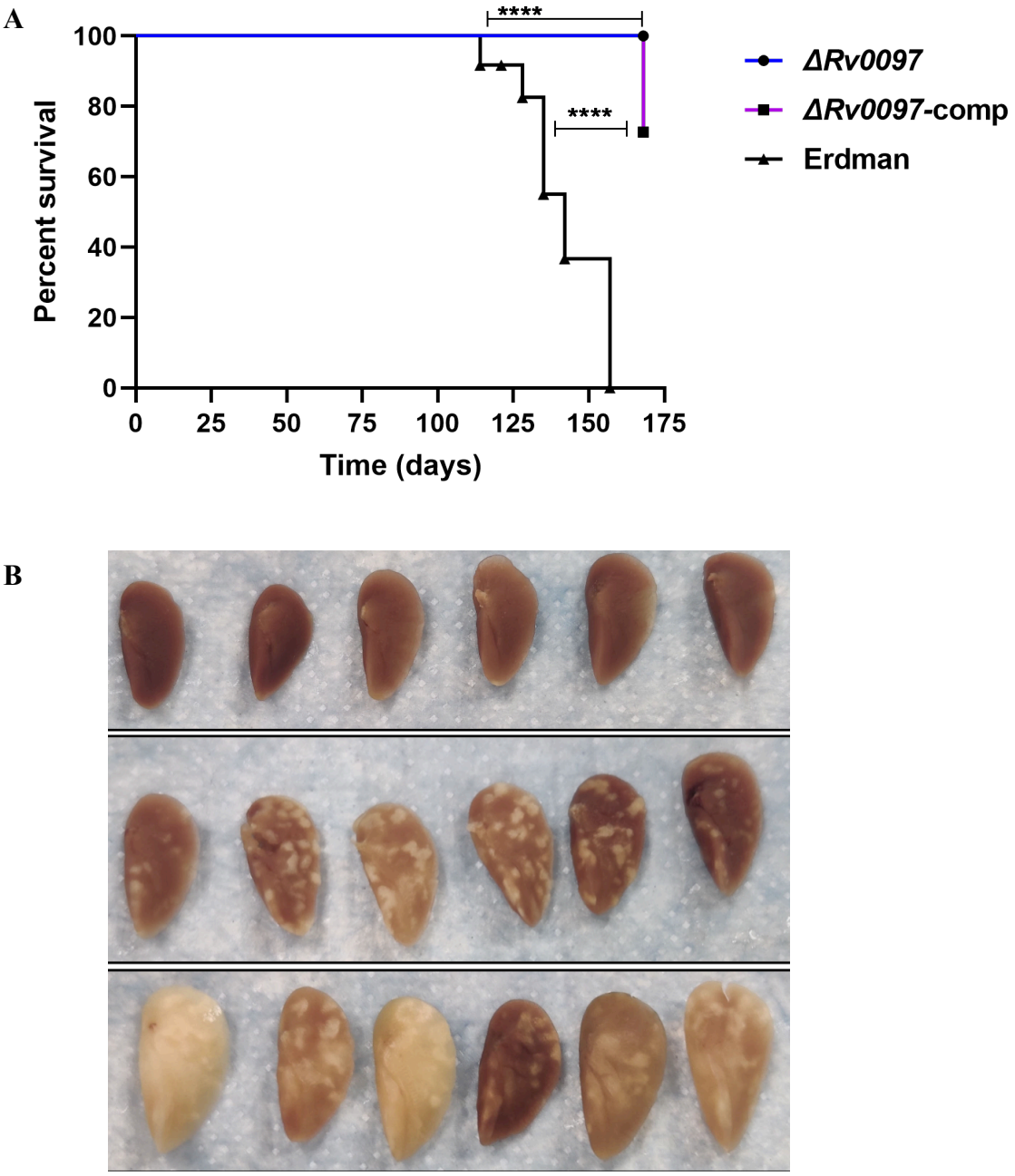

Fig. 4.24. Loss of *Rv0097* attenuates *M. tuberculosis* virulence in DBA/2 mice. A) Kaplan-Meier curves indicate relative survival of DBA/2 mice intravenously-infected with the *M.*

tuberculosis Erdman, *Rv0097* mutant (*ΔRv0097*), or *ΔRv0097*/$P_{myctetO}$*Rv0097-Rv0101* (*ΔRv0097*-comp) (A). The Mantel-Cox log-rank test was used to assess significant differences between groups (***$p<0.001$, ****$p<0.0001$). B) Gross lung pathology was examined after each animal was euthanized after reaching a humane endpoint score or at the end of the study. White foci indicate granulomas.

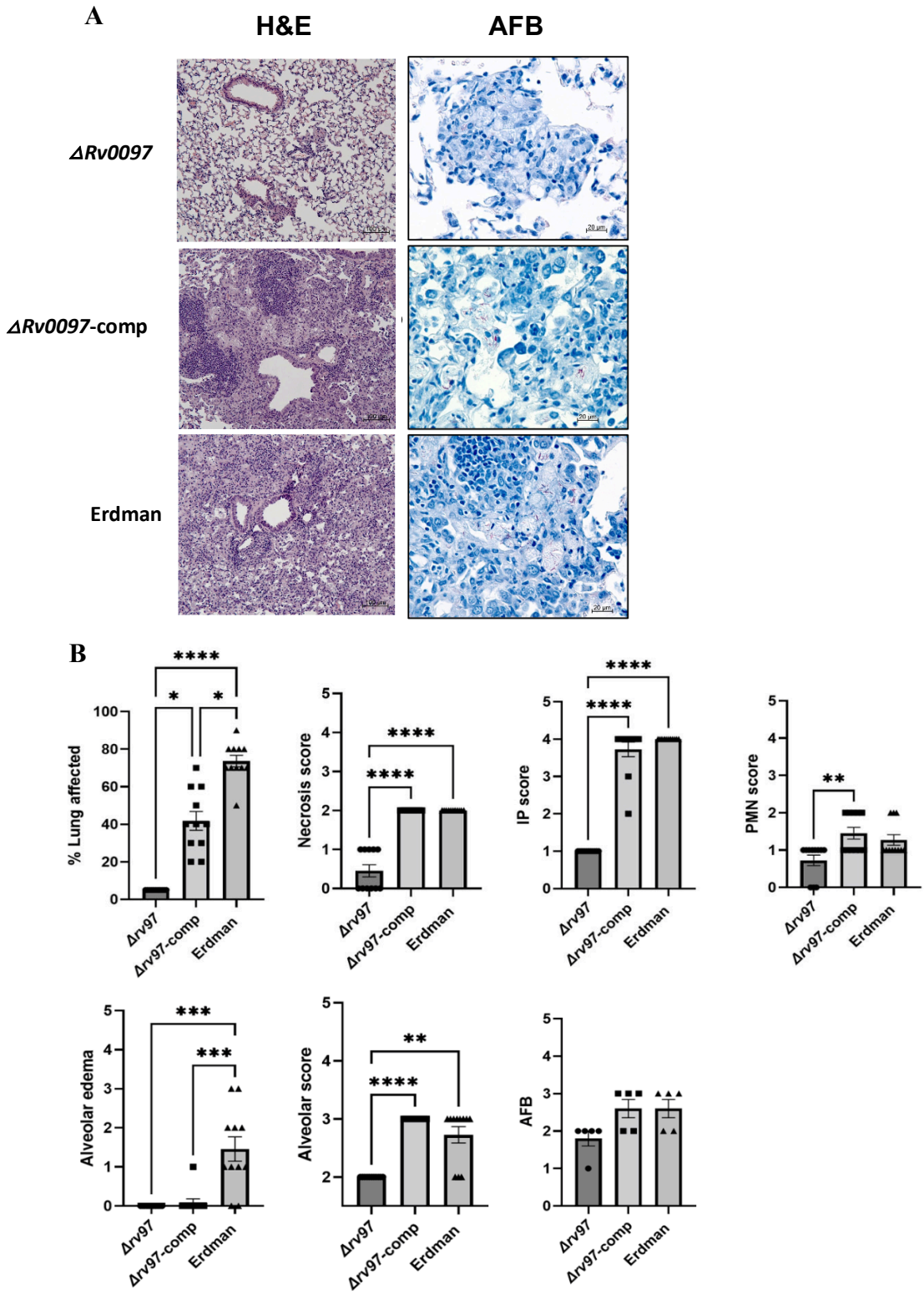
A
H&E
AFB
ΔRv0097
ΔRv0097-comp
Erdman
B
% Lung affected
Necrosis score
IP score
PMN score
Alveolar edema
Alveolar score
AFB
Δrv97
Δrv97-comp
Erdman

Fig. 4.25. Loss of *Rv0097* decreases *M. tuberculosis* lung pathology in DBA/2 mice. A) Histopathological (H&E) and acid-fast bacilli (AFB) stained lung images from mice infected with the indicated strains: Erdman, Δ*Rv0097* (Δ*rv97*), and Δ*Rv0097*/p$P_{myctetO}$*Rv0097-Rv0101* (Δ*rv97*-comp). B) Quantitation of histopathological assessments. Significant differences between groups for the indicated measures are shown (*p<0.05, **p<0.01, ***p<0.001, ****p<0.0001).

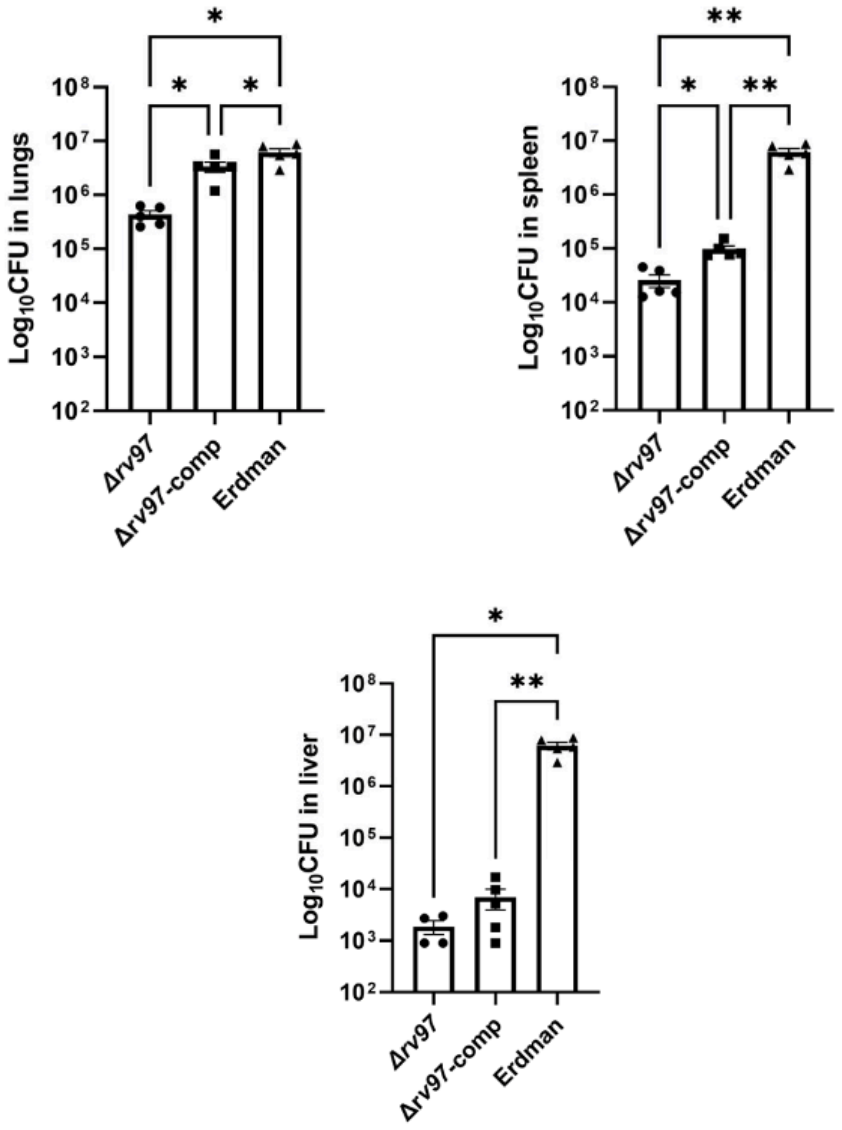

Fig. 4.26. Loss of *Rv0097* decreases *M. tuberculosis* replication and dissemination in DBA/2 mice. Plotted are colony forming units obtained from the lung, spleen, and liver of mice at moribund endpoint or on day 175 post-infection with the indicated strain: Erdman, Δ*Rv0097* (Δ*rv97*), and Δ*Rv0097*/$P_{myctetO}$*Rv0097-Rv0101* (Δ*rv97*-comp). Significance between groups was assessed by ANOVA and Tukey's test for pairwise comparisons (*p<0.05, **p<0.01).

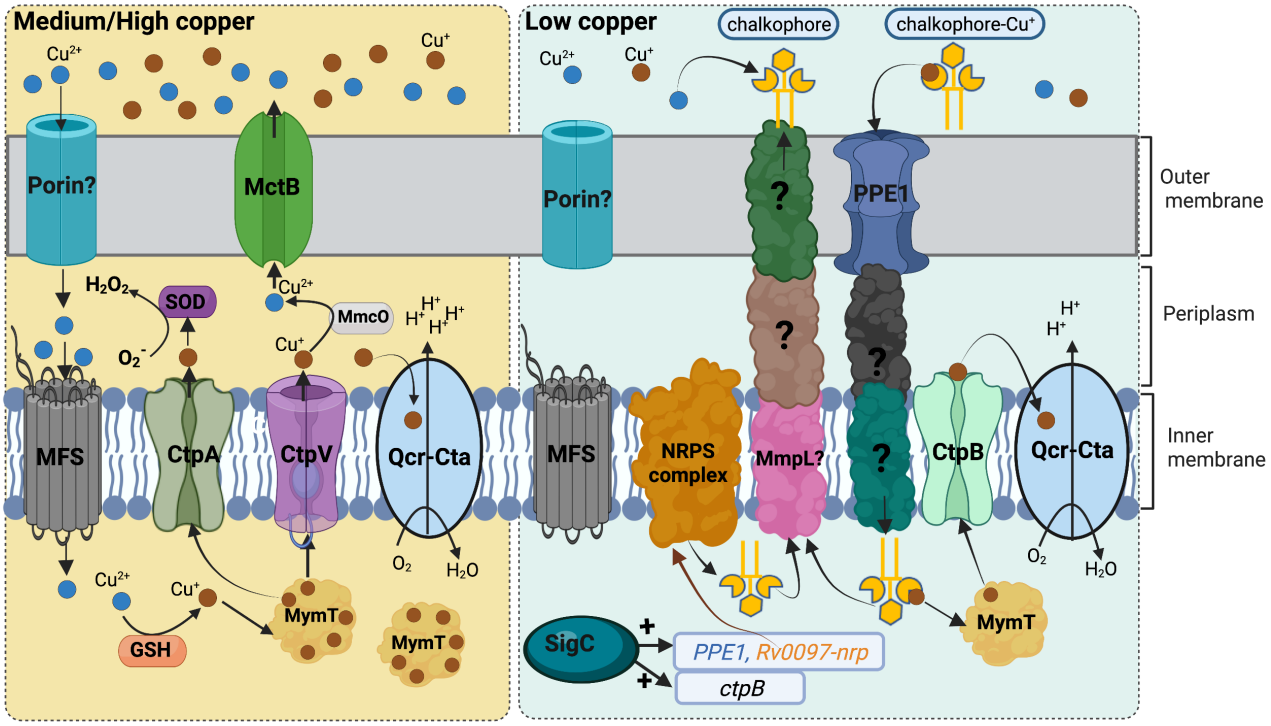

Fig. 4.27. Model for chalkophore function in copper scavenging by *M. tuberculosis*. In a moderate or high copper environment, copper is taken up by *M. tuberculosis* via an unknown mechanism that may involve outer membrane (OM) porin-like proteins and Major Facilitator Superfamily (MFS) importers in the cytoplasmic (inner) membrane (IM). Cytoplasmic glutathione (GSH) and other reductases reduce the Cu (II) to Cu(I). MymT proteins bind up to 6 Cu (I) ions to minimize highly-reactive free Cu (I) ions. As cytoplasmic copper levels increase, CtpV begins to pump Cu (I) to the periplasm where some is oxidized to less reactive Cu (II) which can be exported via MctB. If oxidative stress is sensed, CtpA pumps Cu (I) to the periplasm to metallate Cu-Zn superoxide dismutase (SOD). The Qcr-Cta respiration complexes are metallated by diffusion of periplasmic Cu (I). In contrast, in low-copper niches, insufficient copper ions enter the cytoplasm leading to SigC-directed transcription of the NRPS operon and *ctpB* genes. PPE1 localizes to the

OM, while Rv0097-Nrp proteins form a cytoplasmic membrane NRPS complex that synthesizes chalkophores that are exported via an uncharacterized route which may include an IM-localized MmpL family exporter. Upon chalkophore binding, Cu (II) may be reduced to Cu (I). PPE1 may function to import of Cu (I)-chalkophore complexes to the cytoplasm where the metal can be stored on MymT and transferred to CtpB to pump Cu (I) to the periplasm for directed metallation of Qcr-Cta complexes needed for aerobic respiration and energy generation. The chalkophores may then be re-exported to capture more copper.

Materials and methods

Strains and growth conditions

Plasmids were constructed in *Escherichia coli* strain TAM1 cultured in Luria-Bertani media with appropriate antibiotic selection. *Mycobacterium tuberculosis* and *Mycobacterium marinum* strains were routinely cultured at 37°C and 32°C, respectively, in Middlebrook 7H9 broth or 7H10 agar supplemented with 10% albumin-dextrose-saline (ADS), 0.5% glycerol, and 0.05% Tween 80 (7H9tgADS and 7H10tgADS, respectively) with appropriate antibiotic selection for plasmid maintenance [134]. When required, antibiotics were added at the following concentrations: hygromycin (50 μg/mL), kanamycin (50 μg/mL), gentamicin (50 μg/mL) for *E. coli* TAM1 cells; and for *Mtb* and *M. marinum* strains, hygromycin (50 μg/mL), kanamycin (20 μg/mL), and gentamicin (15 μg/mL) were used. When examining metal-associated growth phenotypes, mycobacteria were cultured in Sauton medium with cell dispersant 0.05% tyloxapol (SMT)[8] and supplemented with copper (II) chelator tetrathiomolybdate (TTM) at 15, 20, or 25 μM or copper (I) chelator bathocuproine sulfate (BCS) at 15 or 20 μM, as indicated.

To facilitate the generation of a *Rv0097* deletion in *M. tuberculosis*, three plasmids were created. The counter-selectable gene *sacB* with its native promoter was obtained from *Bacillus subtilis* genomic DNA by PCR with primers P1928 and P1929 and inserted into the *Sph*I site upstream of the hygromycin-resistance gene (*hyg*) in plasmid pYUB854 [135] to form plasmid pAH4. Plasmid pAH4 was digested with *Xho*I, ends blunted with T4 DNA polymerase, then digested with *Spe*I and ligated with a DNA fragment encoding a ~1000 bp region upstream of the *Rv0097* gene obtained by PCR of *M. tuberculosis* genomic DNA with primers P1583 and P1522 and digested with *Stu*I and *Spe*I to yield plasmid pAH5. A ~950-bp region encoding the last 9 codons of *Rv0097* and 927-bp downstream was obtained by PCR with primers P1585 and P1586

and inserted into the blunted *Age*I site of pAH5 to yield plasmid pAH6 encoding the downstream *Rv0097* region in the same orientation as the upstream *Rv0097* region. For the plasmids generated, the inserted regions were confirmed to be free of PCR-generated mutations by DNA sequencing. Plasmid pAH6 was digested with *Spe*I and *Nsi*I to obtain the *ΔRv0097::hyg-sacB* allelic-exchange substrate (*ΔRv97* AES) used for homologous replacement of the *Rv0097* gene in *M. tuberculosis* strain Erdman expressing mycobacteriophage Che9c recombineering proteins GP60 and GP61 from plasmid pJV53 using mycobacterial recombineering methodology [116]. Hygromycin-resistant transformants were screened by PCR for *ΔRv0097* junctions. Plasmids, strains, and primers used in this study are provided (Tables 4.1-4.3).

Plasmid pAH15 was constructed for complementation of the *ΔRv0097* mutant due to potential polar effects by the deletion replacement. Since *Rv0097* is the second in a six gene operon that is co-regulated,[8]*Rv0097* and the genes *Rv0098-Rv0101* downstream in the operon were placed under the control of an anhydrous tetracycline (aTc)-inducible promoter $P_{myctetO}$. To do this, plasmid pSR173 [117] encoding *M. tuberculosis sigC* downstream of $P_{myctetO}$, was first modified by insertion of the *E. coli lacZ* promoter plus operator region (obtained by annealing primers P1638 and P1639) into the blunted *Sph*I site upstream of the *tetR(B)* gene to increase production of repressor protein to reduce leaky expression in *E. coli* of genes cloned downstream of $P_{myctetO}$. Resulting plasmid pOSN20 was modified by insertion of a multiple-cloning site (made by annealing primers P2258 and P2259) into the blunted *Spe*I site to yield plasmid pRK218. The *Rv0097-Rv0100* and *Rv0101* coding regions were PCR amplified from *M. tuberculosis* genomic DNA with primer pairs P2260 + P2255 and P2256 + P2257, respectively. The *Rv0097-Rv0100* PCR product digested with *Spe*I and *Eco*RI was ligated with the *Rv0101* PCR product digested with *Eco*RI and *Nsi*I and with plasmid pRK218 digested with *Spe*I and *Nsi*I in a three-way ligation

to produce plasmid pRK222. The blunted *Sap*I-*Nhe*I hygromycin-resistance/*oriE* region of plasmid pRK222 was replaced with the blunted *Hpa*I-*Ahd*I gentamycin-resistance/*oriE* region from plasmid pOSN50 (plasmid pMV306 [136] with the *Spe*I-*Nhe*I kanamycin-resistance gene replaced by the gentamycin-resistance gene obtained from plasmid pJQ200 [137] by PCR with primers P2250 and P2251) yielding plasmid pAH15 used for complementation of *ΔRv0097* with *Rv0097-Rv0101* after selecting for gentamycin-resistant transformants and PCR screening for plasmid-encoded operon regions with primer pairs P1718 + P1271 and P1473 + P1763.

A set of *M. marinum* mutants with transposon Tn5370 -mediated insertions in the genomic region homologous to *M. tuberculosis Rv0096-Rv0101* were among a transposon mutant library constructed by Alibaud et al. and kindly provided by the Ramakrishnan lab (University of Cambridge) [115]. Each mutant has an insertion consisting of a hygromycin-resistance gene flanked by resolvase sites (RES) for the gamma-delta phage site-specific recombinase. Mutants were unmarked using plasmid pRK266 encoding the gamma-delta site specific recombinase TnpR. The unmarked mutants were confirmed by PCR for loss of *hyg* (Table 4.3). To complement *M. marinum* BD121 (*MMAR0261*) mutant, the integrative plasmid pAH31 that encodes *MMAR0261* was constructed by amplifying *MMAR0261* and its native promoter with primers P2370 and P2371, digest with *Hind*III and inserted into pOSN50 digested with *Hind*III. The *M. marinum* mutants: BD125, BD127, and BD130, were complemented with the plasmid pAH25 which encodes *MMAR0256-MMAR0259* genes was constructed by amplifying the coding regions of those genes using primers P2425 and P2262, digest with the restriction enzymes, *Spe*I and *Nsi*I, and ligate it in pAH25. The *M. marinum* BD123, however, was complemented using the plasmids pAH25 (described above) and pAH28, which was generated by amplifying *MMAR0260* with primers P2426 and P2427, digested with *Hind*III and inserted into plasmid pOSN50 digested with

*Hind*III. The electrocompetent *M. marinum* BD121, BD123, BD125, BD127, and BD130 were electroporated with the forementioned plasmids using Gene Pulser Xcell (Bio-Rad, CA, USA). Transformants were plated onto 7H10tgADS + 50 μg/mL hygromycin (for plasmid pAH25) 15 μg/mL gentamicin for plasmids pAH28, pAH29 and pAH31). The complemented strains were confirmed by PCR (Table 4.3). Additionally, the heterologous complementation studies of *M. marinum* strains BD123, BD125, BD127 and BD130 with *M. tuberculosis* genes *Rv0097-Rv0101* used plasmid pRK222 which encodes *Rv0097-Rv0101* under the control of aTc- inducible promoter $P_{myctetO}$. Heterologous complementation of *M. marinum* BD121 used plasmid pAH31, which encodes *Rv0096* and its native promoter amplified using primers P1603 and P1604, digested with *Hin*dIII and ligated into pOSN50 digested with *Hin*dIII.

In vitro growth curves

The *M. tuberculosis* strains were inoculated into Sauton medium alone or supplemented with 0.05% Tyloxapol (SMT) and 25 μM TTM to OD_{600} = 0.05 and incubated at 37°C with slow shaking (70 rpm). 50 μM $CuCl_2$ was added to one group of *MtbΔRv0097*/empty vector. Growth was monitored by measuring the OD_{600} every two days for three weeks. For the growth curves of *M. marinum* strains, they were grown in SMT and 15 or 20 μM TTM with or without 15 μM $CuCl_2$ to OD_{600} = 0.05 in 96- well plates and incubated stationary at 30°C. Growth was monitored every two days by measuring the absorption at 600 nm for 14 to 16 days. For the growth curves of *M. marinum* strains M and BD123 in Chelex-treated Sauton medium, glassware used was treated with 0.01% EDTA for 16 hours, rinsed with 0.1N HCl, followed by rinsing several times with double-deionized (MilliQ) water and autoclaved for 90 minutes. To each liter of Sauton medium prepared in this glassware, 10 g Chelex-100 resin (Sigma) was added and the medium was incubated

overnight, prior to filtration and addition of tyloxapol to 0.05%. Strains *M. marinum* M and BD123 were passaged three times in SMT before inoculation into Chelex-treated SMT in 96-well plates. Strain BD123 was also cultured in the same medium supplemented with 25 μM $CuSO_4$ and/or 25 μM $ZnSO_4$. Plates were incubated stationary at 30°C but mixed immediately prior to measuring absorbances at $OD6_{00}$.

Alamar Blue Assays

Strains of *M. tuberculosis* were inoculated to OD_{600} = 0.05 into 96-well dishes containing SMT alone or with 15 μM TTM or with 15 μM TTM plus 9 - 72 μM $CuCl_2$ and incubated at 37°C. Strains of *M. marinum* were cultured similarly except that $CuCl_2$ was added at 9 – 18 μM and plates incubated at 30°C. On day 8, 20 μL alamarBlue reagent (ThermoFisher Scientific) and 20 μL 10% Tween-80 was added to each well. After an additional 16-18 hours incubation, plates were examined to determine whether sufficient metabolic activity (an indicator of growth) had occurred to reduce the indicator dye color from blue to pink.

Chalkophore activity screening

For assessing the presence of chalkophore activity in culture supernatants, TB275 strain (*MtbΔPPE1* expressing *Mtb Rv0097-Rv0101* genes) and *MtbΔPPE1*/Ev (TB274) strain (used as a negative control which does not make chalkophores) cultured in SMT at 37°C to OD_{600}= 0.35 at which point 50 μM TTM and 128 ng/mL anhydrous tetracycline (aTC) were added. After 72-hour incubation at 37°C/shaking, culture supernatants were filter-sterilized and 100 μL applied to microplate wells containing 100 μL of OD_{600} = 0.05 *M. marinum* BD144 *(MMAR0260*–

::MMAR0260) passaged at least twice in SMT. Plates were incubated at 37°C and cell densities (OD_{600}) monitored to assess for enhanced growth indicative of chalkophore activity.

Detection of the chalkophore signature

To screen for unique chemical profiles in mycobacterial culture supernatants, *M. marinum* BD121 expressing *Mtb Rv0097-nrp* and *M. marinum* BD123 expressing *Mtb Rv0097* were grown in SMT and incubated stationary at 30 ºC to OD_{600}=0.45. Next, TTM was added to 100 μM and cultures incubated for 48 hours at 30ºC prior to harvesting the cells. Both culture supernatant and pellet were extracted with equal volumes of chloroform and methanol. The culture supernatant organic phase was dried and resuspended in 70% methanol and analyzed by LC-MS/MS.

Culture and infection of cells lines

3T3-L1 fibroblast cells (ATCC® CL-173) were cultured in DMEM basal medium supplemented with 10% heat-inactivated bovine calf serum (DMEM-BCS) at 37ºC and 5% CO_2 and replaced every three days with fresh-pre-warmed medium. Differentiation of pre-adipocytes to adipocytes was started two days after confluency by stimulation of cells with 0.5 mM 3-isobutyl-1-methylxanthine (IBMX), 0.25 μM dexamethasone, 2 μM rosiglitazone, and 1 μg/ml insulin in DMEM plus 10% heat-inactivated fetal bovine serum (DMEM-FBS)[138]. Two days later, medium was replaced with DMEM-FBS with 1 μg/mL insulin [138]. Lipid droplets are visible inside the cells eight days after differentiation. Adipocytes were maintained in DMEM-FBS that was replaced with fresh-pre-warmed medium twice a week. Cells of the monocytic human cell line THP-1 were cultured in RPMI+10%FBS and differentiated into macrophages with 32.5 ng/mL phorbol 12-myristate 13-acetate (PMA) for 24 hours prior to replacing medium with RPMI+FBS

without PMA [139]. Pre-adipocytes and adipocytes were infected at MOI = 1 with the indicated *M. tuberculosis* strains for 24 hours, while macrophages were infected at MOI = 5 for 2 hours. Infected cells were washed with PBS and medium replaced with pre-warmed amikacin (200 μg/mL)-containing DMEM-BCS, DMEM-FBS, and RPMI-10% FBS medium, respectively, for pre-adipocytes, adipocytes, and macrophages. At the indicated time-points, cells were lysed with triton X-100 (0.1% for pre-adipocytes and macrophages, and 1% for adipocytes). Cell lysates were serially diluted in phosphate-buffered saline (PBS) + 0.05% tween 80 and plated onto 7H10ADStg. After 3 to 4 weeks incubation at 37°C, colony counts were obtained.

RNA isolation and quantitative RT-PCR

For RNA isolation from in vitro cultures*, M. tuberculosis* strain Erdman was passaged three times in SMT then replicate cultures were grown in SMT at OD_{600} = 0.05. At OD_{600} = 0.35 TTM was added to 20 μM to the half of the cultures. At OD_{600} = 0.45, bacteria were harvested by centrifugation (3,500 x *g*, 5 min) and the pellets stored at -80^{0}C. RNA was isolated as described previously [8]. For RNA isolation from the *M. tuberculosis*-infected 3T3-L1 adipocytes, host cells infected at MOI = 1 in T-150 flasks and maintained in DMEM + 10% FBS, DMEM + 10% FBS + $CuCl_2$ (100 μM) or DMEM + 10% FBS + $ZnSO_4$ (100 μM). Old media were replaced with fresh pre-warmed DMEM media with the indicated supplements every 3 days. Infected cells were harvested after 10 days of incubation at 37°C, 5% CO_2. Cells were lysed by suspension in 4 M guanidine isothiocyanate and bacteria harvested by centrifugation (4,600 x *g*, 45 min). Bacterial RNA was isolated from the pellets using the method previously indicated for bacterial cultures. For cDNA synthesis, 0.5 μg RNA was used with 200 ng random hexamers and Superscript III Reverse Transcriptase (Invitrogen) according to the manufacturer instructions. Quantitative PCR

was performed using SYBR Green PCR Master Mix (Applied Biosystems), gene-specific primers, and prepared cDNA on a BioRad iCyler. For ΔΔCt analysis, gene expression was normalized to the *M. tuberculosis* housekeeping gene *sigA*[140].

Microscopic visualization of infected cell lines

At the indicted times following infection of 3T3-L1 pre-adipocytes with MOI = 1 of the indicted *M. tuberculosis* strains, cells were incubated with Zombie Red stain (1:3000 in PBS) for 30 minutes, washed with PBS, fixed with 4% paraformaldehyde overnight at room temperature, stained with DAPI, and visualized with a confocal microscopy (Nikon Eclipse Ti) (five images were taken from each of two infected wells). Zombie Red penetrates and stains dead cells. DAPI stains DNA. Unstained infected cells were monitored for up to 24 days under a bright field microscope (EVOS XI Core) with a magnification of 20x. At each time-point, at least three images were taken from each well infected with the indicated strains in parallel with the uninfected wells.

Murine infection study

Female DBA/2J mice, 6-8 weeks of age. were purchased from Jackson Laboratories and injected intravenously with 1-2 x 10^5 CFU *M. tuberculosis* strain Erdman, *ΔRv0097*, or *ΔRv0097*-comp. Animals were euthanized when show signs of morbidity or at the termination of the study (175 days). Necropsy, gross pathology, histopathology, and bacterial loads in the indicated organs were performed as described previously [97].

Statistical analysis

Statistically-significant difference between groups in growth curves and transcriptional analysis was calculated using ANOVA with pair-wise comparisons. For the mouse survival study, significant-difference was estimated using the log-rank (Mantel-Cox) test for the Kaplan-Meier curves.

Table 4.1. Plasmids used in this study		
Plasmid	**Relevant characteristics**	**Source**
pAH4	Plasmid pYUB854 with *Bacillus subtilis sacB* inserted into the *Sph*I site. [*oriE*, *hyg*, *sacB*]	This study
pAH5	Plasmid pAH4 with ~ 1 kb *Rv0097* upstream-flanking region inserted into the *Xho*I/*Spe*I region. [*oriE,* upstream-*Rv0097, hyg, sacB*]	This study
pAH6	Plasmid pAH5 with ~ 1 kb *Rv0097* downstream-flanking region inserted into the *Age*I site for use in generating an *Rv0097* knockout in *Mtb* by recombineering. [*oriE*, upstream-*Rv0097*, *hyg*, *sacB*, downstream-*Rv0097*]	This study
pAH7	*Mtb Rv0097* inserted into *Pac*I-*Nsi*I region from pSR173. [*OriE, OriM, hyg,* P_{tb21}:tetR(B)	This study
pAH15	*Sap*I-*Ahd*I $P_{myctetO}$*:Rv0097-Rv0101* region from pRK222 inserted into the *Hpa*I-*Ahd*I sites of plasmid pOSN50. [*oriE, oriM*, *gen,* P_{lacZO}, P_{tb21}*:tetR(B),* $P_{myctetO}$:*Rv0097-nrp*]	This study
pAH25	Plasmid pRK218 after replacement of the *Spe*I-*Nsi*I *sigC* region with *Mmar0259-Mmar0256*. [*oriE, oriM*, *hyg,* P_{lacZO}, P_{tb21}*:tetR(B)*, $P_{myctetO}$*:Mmar0259-Mmar0256*]	This study
pAH28	Plasmid pOSN50 with *Mmar0260* and upstream promoter region inserted into the *HindIII* site. [*oriE,* L5 *att/int, gen*, *Mmar0260*]	This study
pAH29	Plasmid pOSN50 with *Mmar0261* and upstream promoter region inserted into the *HindIII* site. [*oriE*, L5 *att/int*, *gen*, *Mmar0261*]	This study
pAH31	Plasmid pOSN50 with *Rv0096* and upstream promoter region inserted into the *HindIII* site. [*oriE*, L5 *att/int*, *gen*, *Rv0096*]	This study
pGH542	Source of gd resolvase gene *tnpR* inserted into plasmid pRK266.	Van Kessel and Hatfull [141]
pJQ200	Source of gentamicin-resistance gene (*gen*) inserted into plasmid pOSN50.	Quandt, et al. [137]
pJV53	Plasmid encoding acetamide-inducible expression of mycobacteriophage *Che9c* recombineering proteins gp60 and gp60. [*oriE, oriM, kan*, P_{ace}:*gp60, gp61*]	Van Kessel and Hatfull [116]
pMV306	*M. tuberculosis* genome-integrating plasmid. [*oriE*, L5 *att/int, kan*]	Kong and Kunimoto [142]
pOSN50	Plasmid pMV306 with *kan* replaced with *gen* from plasmid pJQ200. [*oriE*, L5 *att/int, gen*]	Shey-Njila, et al. [96]

Table 4.1. (continued)		
Plasmid	**Relevant characteristics**	**Source**
pRK218	This plasmid was used as a vector to generate pRK222. *Mtb sigC* was excised using *Sph*I and *Nsi*I restriction enzymes. [*oriE, oriM, hygR, tetR, ptb21, PlacZO, PmyctetO*]	This study
pRK222	Plasmid pRK218 with *Mtb Rv0097-Rv0101* inserted into the *Sph*I/*Nsi*I region downstream of promoter $P_{myctetO}$. [*oriE*, *oriM*, *hyg*, P_{lacZO} P_{tb21}:tetR(B), $P_{myctetO}$:*Rv0097-Rv0101*]	This study
pRK225	used to generated pRK266. Mtb bacteriophage *che9 c gp60* and *gp61* genes were replaced with *tnpR*.	Shey-Njila [96]
pRK266	Plasmid pRK225 with *tnpR* from plasmid pGH542 inserted into the *Sph*I-*Not*I region downstream of tetracycline-inducible promoter P*myctetO*. [*oriE*, *oriM*, *kan*, P_{lacZO} P_{tb21}:*tetR(B)*, $P_{myctetO}$:*tnpR*]	This study
pSR173	[*oriE, oriM, hyg,* P_{lacZO} P_{tb21}:tetR(B), $P_{myctetO}$:*sigC*]	Grosse-Siestrup et al. [8]
pYUB854	Vector used to create plasmid pAH4. [*oriE*, *hyg*]	Braunstein, et al. [134]

Table 4.2. Strains used in this study		
Strain	**Relevant characteristics**	**Source/Reference**
M. tuberculosis strains		
Erdman	Virulent *Mycobacterium tuberculosis* laboratory strain	CDC/ATCC 35801
TB270	Erdman *ΔRv0097::hyg-sacB*	this study
TB271	Erdman *ΔRv0097::hyg-sacB*/pOSN50	this study
TB272	Erdman *ΔRv0097::hyg-sacB*/pAH15	this study
TB273	Erdman *ΔRv0096::hyg-sacB*	this study
TB274	Erdman *ΔRv0096/*pOSN50	this study
TB275	Erdman *ΔRv0096/*pAH15	this study
M. marinum strains		
M. marinum M	*M. marinum* strain Aronson	ATCC BAA-535
Tn7481	*M. marinum* M with *Tn5370* transposon-mediated insertion in *Mmar0261*, Hyg^R	115
Tn15431	*M. marinum* M with *Tn5370* transposon-mediated insertion in *Mmar0260*, Hyg^R	115
Tn18187	*M. marinum* M with *Tn5370* transposon-mediated insertion in *MMAR0259*, Hyg^R	115
Tn5623	*M. marinum* M with *Tn5370* transposon-mediated insertion in *Mmar0258*, Hyg^R	115
Tn7649	*M. marinum* M with *Tn5370* transposon-mediated insertion in *Mmar0256*, Hyg^R	115
BD121	Hyg^S Tn7481 after transformation with pRK266	this study
BD123	Hyg^S Tn15431 after transformation with pRK266	this study
BD125	Hyg^S Tn18187 after transformation with pRK266	this study
BD127	Hyg^S Tn5623 after transformation with pRK266	this study
BD130	Hyg^S Tn7649 after transformation with pRK266	this study
BD131	BD121::pAH31	this study
BD132	BD121::pAH29	this study
BD133	BD123::pAH28/pAH25	this study
BD134	BD125/pAH25	this study
BD135	BD127/pAH25	this study

Table 4.2. Strains used in this study (continued)		
Strain	**Relevant characteristics**	**Source/Reference**
BD136	BD130/pAH25	this study
BD137	BD121/pRK222	this study
BD138	BD123/pRK222	this study
BD139	BD123/pAH7	this study
BD140	BD125/pRK222	this study
BD141	BD127/pRK222	this study
BD143	BD130/pRK222	this study
BD144	BD123::pAH28	this study
BD145	BD121/pAH25	this study

Table 4.3. Primers used in this study		
Primer	**Sequence (5′ → 3′)**	**Use**
P1074	GGGACTAGTATGGTGAGCAAGGGC GAG	Used with P1720 to screen for the downstream-*Rv0097/sacB* junction in Δ*Rv0097* candidates
P1196	AGTGAGCTCTACGCCATCCC	Used with P2283 to screen for plasmid pRK225 in *M. marinum* transformants
P1249	AAACAGATCGGCAAGGTAGC	Used with P1250 for qRT-PCR of *M. tuberculosis sigA*
P1250	CTGGATCAGGTCGAGAAACG	Used with P1249 for qRT-PCR of *M. tuberculosis sigA*
P1271	AGCTCTAGAAATATTGGATCGTCGG CAC	Used with P1718 to screen for pAH15 (the complement plasmid for *Mtb⊿Rv0097)*
P1285	GGTGGTCTGCAGTCACCGCCGCGGC	Used with P2280 to screen for deletion of *hyg* in Tn15431 and Tn19009 following transformation with pRK266
P1473	CTCACATGTTCTTTCCTGCGTTATCC C	Used with P1763 to screen for pAH15 (the complement plasmid for *Mtb⊿Rv0097)*
P1522	ATCGAGAAGCTTTCATGCCGCGTAT CCCGGCGTC	Used with P2261 to screen for deletion of hyg in Tn7481 transformed with pRK266
P1583	GGACTAGTCTGATCGCCACCAACTT CTTCG	Used with P1584 to PCR a 1091 bp region upstream of *Rv0097*
P1584	GCCTTTGACCTTAAGCGTCATCGG	used with P1583 to amplify a 1091 region upstream of Rv0097
P1585	CTCAAGACGCCGGGATACGC	Used with P1586 to PCR a 985 bp region downstream of *Rv0097*
P1586	CCAATGCATGCCATCTTGCTCCCTG GTG	Used with P1585 to PCR a 985 bp region downstream of Rv0097
P1603	GTGAAGCTTCAGATCCTACGAGTTG ATACGGGAAGG	Used with P1604 to amplify 143 bp upstream to 39 bp downstream of *Rv0096* for insertion into pOSN50 to create pAH29
P1604	GTGAAGCTTGCCTTTGACCTTAAGC GTCATCGG	Used with P1603 to amplify 143 bp upstream to 39 bp downstream of *Rv0096* for insertion into pOSN50 to create pAH29

Table 4.3. Primers used in this study (continued)		
Primer	**Sequence (5′ → 3′)**	**Use**
P1631	GGTTATCAAGTGAGAAATCACCATG AGTGACG	Used with P2202 to screen for pAH25 (the complement plasmid for *M. marinum* BD125, BD127, and BD130 mutants)
P1638	CACGTGAGCGCAACGCAATTAATGT GGTTAGCTCACTCATTAGGCACCCC AGGCTTTACAC	Used with P2202 to screen for pAH25 (the complement plasmid for *M. marinum* BD125, BD127, and BD130 mutants)
P1639	GGTAACTCCACACAACATACGAGCC GGAAGCATAAAGTGTAAAGCCTGG GTGCCTAATGAG	Annealed with P1638 to create the *lacZ* promoter-operator as a *Pml*I-*Hpa*I fragment to insert into the blunted *Sph*I site upstream of *tetR(B)* in pSR173
P1718	AGTCGATATGCCAGAACGCGCC	used with P1271 to screen for pAH15 (the complement plasmid for *Mtb⊿Rv0097).* It also used with P2282 to screen for the loss of *hyg* in the unmarked *M. marinum MMAR_Tn29977* mutant.
P1720	GCTGGCTGCATCCAAGGAATGC	Used with P1074 to screen for the downstream-*Rv0097/sacB* junction in Erdman*⊿Rv0097* candidates
P1731	GGAATTCCATATGGCTATACCACCG GAGGTGCAC	Used with P1955 to screen for the upstream-*Rv0097/hyg* junction
P1763	GCTTTACTAAGTCATCGCGATGGAG C	Used with P1473 to PCR screen for pAH15 (the complement plasmid for *Mtb⊿Rv0097)*
P1874	GGACTAGTCCAGAGTGCTCGAGCCC TACTCC	Used with P1976 to screen for *hyg* deletion in Tn23984, Tn18187, Tn5623, and Tn21692 mutants transformed with pRK266
P1900	TCGAGGATCCTGCCGCGTATCCCGG CGTC	Used with P1985 to screen for deletion of *Rv0097*
P1928	GATGACCGGTCCTTTTTAACCC TCACATATACCTG	Used with P1929 to PCR s*acB* with native promoter from *Bacillus subtilis*
P1929	GGGTCGGCATTTTCTTTTGCGTTT	Used with P1928 to PCR *sacB* with native promoter from *Bacillus subtilis*

Table 4.3. Primers used in this study (continued)		
Primer	**Sequence (5′ → 3′)**	**Use**
P1955	GTGTACTAGTCCCAGGTGGCTAAAA ATGTATCCTAAATCAGATATCGG	Used with P1731 to screen for the upstream-*Rv0097/hyg* junction in Erdman*ΔRv0097* candidates
P1976	TGACATGCATGCTCAATCCGTAGAC CTGTGC	Used with P1874 to screen for *hyg* deletion in Tn23984, Tn18187, Tn5623, and Tn21692 mutants transformed with pRK266
P1985	GAGGTTAATTAAGACGCTTAAGGTC AAAGGCGAGGGAC	Used with P1900 to screen for the deletion of *Rv0097*
P2202	GTTGTCGGCGTGCCGAATATCCC	Used with P1631 to screen for pAH25 (the complement plasmid for *M. mar* BD125, BD127, and BD130 mutants)
P2250	GTGTGCTAGCCCCGGGAATTAATTC TGCTCGCGCAG	Used with P2251 to PCR *gen* from pJQ200
P2251	GGACTAGTGGCCGCGGCGTTGTGAC	Used with P2250 to PCR *gen* from pJQ200
P2255	CCGAATTCTCCAGGACGCAAAGTTG CACGGG	Used with P2260 to PCR *MtbRv0097-Rv0100* genes from *Mtb*/Erdman to be inserted into pRK222, a plasmid encodes *Mtb Rv0097-nrp* genes.
P2256	CGTCCTGGAGAATTCGGGGGCAGAC	Used with P2257 to PCR *Mtb nrp* gene to be inserted into pRK222, a plasmid encodes *Mtb Rv0097-nrp* genes.
P2257	CCAATGCATCTACAGCAGTCCGAGC AGTTGTAGGTTGGTGACG	used with P2256 to PCR *Mtb nrp* gene to be inserted into pRK222, a plasmid encodes *Mtb Rv0097-nrp* genes.
P2258	CACTAGTGCGGCCGCTTAAT	Annealed with P2259 to yield a *Sph*I-*Spe*I-*Pac*I linker usedin pRK218
P2259	TAAGCGGCCGCACTAGTGCATG	Annealed with P2258 to form a *Sph*I-*Spe*I-*Pac*I linker used in pRK218
P2260	GCACTAGTCTTAATCGTCAGGAGGT CGACTGATGACGCTTAAGGTCAAAG GCGAGGGAC	Used with P2255 to PCR *MtbRv0097-Rv0100* genes from *Mtb*/Erdman to be inserted into pRK222, a plasmid encodes *Mtb Rv0097-nrp* genes.

Table 4.3. Primers used in this study (continued)		
Primer	**Sequence (5′ → 3′)**	**Use**
P2261	GCACTAGTCTTAATCGTCAGGAGGTCGACTGATGACGCTCAACGTGAAAGGCGAGGG	Used with P1522 to screen for *hyg* deletion in Tn7481 after transformation with pRK266
P2262	GTGAAGCTTGTTGCTGCCCGCCACCTG	Used with P2425 to PCR *M. marinum MMAR0259* - *MMAR0256* genes to generate pAH25, a complement plasmid for *M. mar*BD125, BD127, and BD130 mutants.
P2280	CACATGCATGTCATTGCGCAGGGCGATGG	Used with P1285 to screen for *hyg* deletion in Tn15431 and Tn19009 after transformation with pRK266
P2282	GATGACCGGTTGCTGCCCGCCACCTG	Used with P1718 to screen for *hyg* deletion in Tn29977 after transformation of pRK266
P2283	GCTCTAGAGGAGGAGACAAAGATCTCCGGGTG	used with P1196 to screen for pRK222
P2313	GATAGCATGCTCTAAGGAAATACTTACATATGCGACTTTTTGGTTACGC	Used with P2314 to PCR *tnpR* from pGH542
P2314	TGCAGTTAGTTGCTTTCATTTATTACT TTA TAT ACT GTT GAA CGA GC	Used with P2313 to PCR *tnpR* from pGH542
P2370	GTGAAGCTTGATGACGGGCGTCAATGACTGG	Used with P2371 to PCR *Mmar0261* with upstream promoter region inserted into pOSN50 to create pAH31
P2371	GTGAAGCTTGCTACAGGAGGAGTCGGATGCG	Used with P2370 to PCR Mmar0261 with upstream promoter region inserted into pOSN50 to create pAH31
P2403	TCGTTGATCGCCTCAAACC	Used with P2404 for qRT-PCR of *Rv0101*
P2404	TCACCCAAATTCAGCTGTCC	Used with P2403 for qRT-PCR of *Rv0101*
P2407	TCCTTGCCCTTGTTGCC	Used with P2408 for qRT-PCR of *Rv0096*
P2408	CAAGGTGGGAGTGAAGAACG	Used with P2407 for qRT-PCR of *Rv0096*
P2411	CCACCAAGATCGAGGACAAG	Used with P2412 for qRT-PCR of *Rv0097*
P2412	CCTGGTAGTGCTGAGTATGTATG	Used with P2411 for qRT-PCR of *Rv0097*

Table 4.3. Primers used in this study (continued)		
Primer	**Sequence (5′ → 3′)**	**Use**
P2425	GCACTAGTGAGGAAAGACCCGGCAT GAGCACCACCGATTTGAC	Used with P2262 to PCR *M. marinum MMAR0259* - *MMAR0256* genes to generate pAH25, a complement plasmid for *M. mar* BD125, BD127, and BD130 mutants.
P2426	GTGAAGCTTGTTGC TGC CCG CCA CCT G	Used with P2427 to PCR *Mmar0260* inserted into pOSN50 to generate pAH28
P2427	GTGAAGCTTTCATGCCGGGTAGCCC GGCGTC	Used with P2426 to PCR *Mmar0260* inserted into pOSN50 to generate pAH28

CHAPTER 5

CONCLUSION REMARKS AND FUTURE DIRECTIONS

Despite the global endeavor to end tuberculosis, *M. tuberculosis* is now second to COVID-19 as a leading cause of death in humans from a single infectious agent [1]. As a successful pathogen, *M. tuberculosis* must maintain internal metal homeostasis and overcome host nutritional immunity. Host cells orchestrate mechanisms to safely store and transport essential trace metals, but also deploy toxic amounts in specific environments to intoxicate invading microbes. Copper is an essential trace mineral required for single electron-transfer reactions by cuproenzymes in bacteria and host cells, but the high reactivity of copper ions can lead to production of reactive oxygen radicals and displacement of iron-sulfur complex from the active sites of some enzymes. Thus, intricate copper-acquisition and homeostatic control mechanisms are crucial for viability in all living organisms.

Copper-binding chalkophores have been identified in pathogenic and non- pathogenic bacteria. The necessity to produce chalkophores depends on the environments in which the bacteria reside. The essentiality of copper combined with a copper-limited environment have likely directed the evolution of bacterial species that have developed mechanisms to efficiently scavenge this metal from copper-poor niches. Chalkophore named methanobactins have been identified in methanotrophic bacteria [143]. In other bacteria, however, siderophores, which bind iron and copper, are used to protect pathogens from toxic levels of copper in the environment and acquire zinc, such as yersiniabactin (Ybt) [59][144]. Copper is not only involved in cuproenzymes but also

in maintaining cell morphology of some bacteria, such as *Streptomyces* [145], which may increase demand for this metal and why evolution of a system to produce diisonitrile natural products may have evolved in some species [71]. Interestingly, the nonribosomal peptide synthase gene cluster that produces the diisonitrile products is conserved in several streptomycetes and pathogenic mycobacteria, but absent in non-pathogenic species [91][10][71].

In the third chapter of this thesis, we demonstrated that CtpB, a cytoplasmic membrane P-type ATPase, is upregulated in copper-deficient medium and important in *M. tuberculosis* replication in a copper-restricted murine adipocyte cell line. Additionally, loss of *ctpB* results in hypervirulence in DBA/2J mice. The fourth chapter of this dissertation revealed a copper scavenging mechanism conserved in *M. tuberculosis* and *M. marinum*. The NRPS operons in both species was found to be required for growth *in vitro* and *in vivo*, but only when the bacteria encounter copper deficiency. The data confirmed that NRPS operon genes are required for generating chalkophores; how these secondary metabolites are exported remains to be elucidated.

Chapter 4 demonstrated that *PPE1* is required growth in low-copper conditions but not for export of chalkophore as chalkophore activity is detected in the supernatant of a PPE1-null strain. Given that PPE family proteins are surface-located, PPE1 may function in import of chalkophore-associated copper. Whether this is the case and whether chalkophore-copper complexes or copper alone enters through this mechanism remains to be determined. Also unresolved is whether they are deposited in the periplasm or are fully imported to the cytoplasm. One way to answer this question might be to isolate chalkophores from a *M. marinum MMAR0261*/*PPE1* mutant, incubate with Cu-64 to produce copper-chalkophore adducts, and then determine if only the Cu-64 or the Cu-64/chalkophore adducts enter a strain that is wildtype for *PPE1*, but has a mutation in one of the downstream genes required for chalkophore synthesis.

After infecting a mammalian host, *M. tuberculosis* bacilli encounter both low and high-copper niches. Studies with Cu-64 added to copper-deficient medium could be used to test the hypothesis that a CtpB null strain accumulates more cytoplasmic copper than wild type because the NRPS operon will continue to be expressed until redox stress is eased in the cytoplasm only after sufficient copper (I) is exported to the periplasm by an CtpB-independent to increase periplasmic levels to enable respiration complexes to obtain copper by diffusion.

How copper ions are transferred to CtpB is also an open question. If chalkophore-copper complexes only enter the periplasm, the complexes directly dock to a periplasmic pocket in CtpB to deliver the metal if CtpB acts as a copper importer. Alternatively, if the complexes are imported to the cytoplasm, then interactions may occur with a cytoplasmic portion of CtpB if this protein delivers copper to the periplasm. It may be possible to test this hypothesis by measuring ATPase activity of CtpB-enriched mycobacterial membranes upon incubation with chalkophore-copper complexes. If chalkophore-copper complexes bind CtpB, an increase in ATPase activity should occur since Cu^{+} was the only cation reported to increase ATPase activity in CtpB-enriched membranes engineered in *Mycobacterium smegmatis* [106].

The *Rv0096-Rv0101* operon functions in response to different stress stimuli. Our studies support the NRPS genes functioning to produce isonitrile products that function in copper scavenging and *Rv0096/PPE1* functioning for copper import. The study by Mehdiratta and colleagues reported the need for the same NRPS genes in responding to zinc limitation [11]. The NRPS is also upregulated in response to nitric oxide (NO) and expression may be required for protection against copper toxicity [95]. In that study, induction of NRPS genes in response to NO required *rip1*, which encodes protease Rip1, and deletion of *rip1* greatly reduced *M. tuberculosis* resistance to copper toxicity [95]. Nitric oxide-induced transcription of *Rv0097-Rv0101* is also

negatively controlled by response regulator PdtaR which binds to the *PPE1*-5′ transcript [95]. Thus, there are many levels of regulation of NRPS operon genes that warrant further investigation.

Understanding mechanisms of copper acquisition can aid in developing drugs or vaccine that target components of these systems. Due to their small size (543-1216 Daltons), chalkophores are not immunogenic [71][70][146]. However, they might serve as vaccine targets if conjugated to immunogenic peptides to train immune responses to target the pathogen or pathogen-infected host cells. Blocking copper-uptake mechanisms has the potential to starve *M. tuberculosis* of copper and impair the ability of the pathogen to replicate or emerge from a quiescent stated in adipose tissues or granulomas. A recent study described a vaccine that targets siderophores in salmonella in which siderophore Ent was conjugated with immunogenic carrier protein cholera toxin subunit B (CTB); results showed that the CTB-Ent conjugate led to anti-siderophore antibodies in the gut mucosa and decreased the salmonella burden in the intestinal tract of the infected mice [146]. A similar drug conjugate approach could be taken to generate anti-*M. tuberculosis* chalkophore antibodies. Another theoretical approach to target copper-uptake in this pathogen is to test whether chalkophore-antibiotic complexes can traverse the outer membrane through. PPE1 can be also a potential drug target, which might be blocked by an inhibitor to obstruct the transport of chalkophores-copper complexes or receipt of copper from the complexes. Thus, understanding the mechanism by which *M. tuberculosis* and related pathogens acquire essential trace metals from their hosts has great potential in targeted design of novel drugs and vaccines to increase the arsenal to deploy in the battle against tuberculosis and other pathogenic mycobacteria.

REFERENCES

1. World Health Organization. *Global Tuberculosis Report*; 2021
2. Fine, P.E. Variation in Protection by BCG : Implications of and for Heterologous Immunity. *Lancet* **1995**, *346*, 1339–1345, doi:doi.org/10.1016/S0140-6736(95)92348-9.
3. Samanovic, M.I.; Ding, C.; Thiele, D.J.; Darwin, K.H. Copper in Microbial Pathogenesis: Meddling with the Metal. *Cell Host Microbe* **2012**, *11*, 106–115, doi:10.1016/j.chom.2012.01.009.
4. Cook, G., Hards, K., Vilcheze, C., Hartman T., and Berney, M. Energetics of Respiration and Oxidative Phosphorylation in Mycobacteria. *Microbiol Spectr* **2014**, *2*, MGM2-0015–2013, doi:10.1128/microbiolspec.MGM2-0015-2013.f1.
5. Palmer, L.D.; Skaar, E.P. Transition Metals and Virulence in Bacteria. *Annu. Rev. Genet* **2016**, *50*, 67–91, doi:10.1146/annurev-genet-120215-035146.
6. Piddington, D.L.; Fang, F.C.; Laessig, T.; Cooper, M.; Orme, I.M.; Buchmeier, N. a; Cooper, A.M. Cu , Zn Superoxide Dismutase of Mycobacterium Tuberculosis Contributes to Survival in Activated Macrophages That Are Generating an Oxidative Burst. *Infect. Immun.* **2001**, *69*, 4980–4987, doi:10.1128/IAI.69.8.4980.
7. Speer, A.; Rowland, J.L.; Haeili, M.; Niederweis, M.; Wolschendorf, F. Porins Increase Copper Susceptibility of Mycobacterium Tuberculosis. *J. Bacteriol.* **2013**, *195*, 5133–5140, doi:10.1128/JB.00763-13.
8. Grosse-Siestrup, B.T.; Gupta, T.; Helms, S.; Tucker, S.L.; Voskuil, M.I.; Quinn, F.D.; Karls, R.K. A Role for Mycobacterium Tuberculosis Sigma Factor c in Copper Nutritional

Immunity. *Int. J. Mol. Sci.* **2021**, *22*, 1–18, doi:10.3390/ijms22042118.

9. Hotter, G.S.; Wards, B.J.; Mouat, P.; Besra, G.S.; Gomes, J.; Singh, M.; Bassett, S.; Kawakami, P.; Wheeler, P.R.; de Lisle, G.W.; et al. Transposon Mutagenesis of Mb0100 at the Ppe1-Nrp Locus in Mycobacterium Bovis Disrupts Phthiocerol Dimycocerosate (PDIM) and Glycosylphenol-PDIM Biosynthesis, Producing an Avirulent Strain with Vaccine Properties at Least Equal to Those of M. Bovis BCG. *J Bacteriol* **2005**, *187*, 2267–2277, doi:10.1128/JB.187.7.2267-2277.2005.

10. Harris, N.C.; Sato, M.; Herman, N.A.; Twigg, F.; Cai, W.; Liu, J.; Zhu, X. Biosynthesis of Isonitrile Lipopeptides by Conserved Nonribosomal Peptide Synthetase Gene Clusters in Actinobacteria. *Proc. Nat. Acad. Sci. U. S. A.* **2017**, *114*, doi:10.1073/pnas.1705016114.

11. Mehdiratta, K.; Singh, S.; Sharma, S.; Bhosale, R.S.; Choudhury, R.; Masal, D.P.; Manocha, A.; Dhamale, B.D.; Khan, N.; Asokachandran, V.; et al. Kupyaphores Are Zinc Homeostatic Metallophores Required for Colonization of Mycobacterium Tuberculosis. *Proc. Natl. Acad. Sci. U. S. A.* **2022**, *119*, doi:10.1073/pnas.2110293119.

12. Koch, R. Die Aetiologie Der Tuberculose (Nach Einem in Der Physiologischen Gesellschaft Zu Berlin Am 24. März Gehaltenem Vortrage). *Berliner klin Wochenschr* **1882**, *19*, 221–230, doi:10.1016/S0174-3031(82)80099-1.

13. Frothingham, R.; Hills, H.G.; Wilson, K.H. Extensive DNA Sequence Conservation throughout the Mycobacterium Tuberculosis Complex. *J Clin Microbiol* **1994**, *32*, 1639–1643, doi:10.1128/jcm.32.7.1639-1643.1994.

14. Niemann, S.; Kubica, T.; Bange, F.C.; Adjei, O.; Browne, E.N.; Chinbuah, M. a; Diel, R.; Gyapong, J.; Horstmann, R.D.; Meyer, C.G.; et al. The Species Mycobacterium Africanum in the Light of New Molecular Markers The Species Mycobacterium

Africanum in the Light of New Molecular Markers. *J. Clin. Microbiol.* **2004**, *42*, 3958–3962, doi:10.1128/JCM.42.9.3958.

15. Pai, M.; Behr, M.A.; Dowdy, D.; Dheda, K.; Divangahi, M.; Boehme, C.C.; Ginsberg, A.; Swaminathan, S.; Spigelman, M.; Getahun, H.; et al. Tuberculosis. *Nat. Rev. Dis. Prim.* **2016**, *2*, 16076, doi:10.1038/nrdp.2016.76.
16. Russell, D.G. Mycobacterium Tuberculosis and the Intimate Discourse of a Chronic Infection. *Immunol. Rev.* **2012**, *240*, 252–268, doi:10.1111/j.1600-065X.2010.00984.x.
17. Houben, D.; Demangel, C.; van Ingen, J.; Perez, J.; Baldeón, L.; Abdallah, A.M.; Caleechurn, L.; Bottai, D.; van Zon, M.; de Punder, K.; et al. ESX-1-Mediated Translocation to the Cytosol Controls Virulence of Mycobacteria. *Cell. Microbiol.* **2012**, *14*, 1287–1298, doi:10.1111/j.1462-5822.2012.01799.x.
18. Wolf, A.J.; Desvignes, L.; Linas, B.; Banaiee, N.; Tamura, T.; Takatsu, K.; Ernst, J.D. Initiation of the Adaptive Immune Response to Mycobacterium Tuberculosis Depends on Antigen Production in the Local Lymph Node, Not the Lungs. *J. Exp. Med.* **2008**, *205*, 105–115, doi:10.1084/jem.20071367.
19. Peters, W.; Ernst, J.D. Mechanisms of Cell Recruitment in the Immune Response to Mycobacterium Tuberculosis. *Microbes Infect.* **2003**, *5*, 151–158, doi:10.1016/S1286-4579(02)00082-5.
20. Brennan, P.J. Structure , Function , and Biogenesis of the Cell Wall of Mycobacterium Tuberculosis. *Tuberculosis* **2003**, *9792*, 91–97, doi:10.1016/S1472-9792(02)00089-6.
21. Rossi, E. De; Riccardi, G. Role of Mycobacterial Efflux Transporters in Drug Resistance : An Unresolved Question. *FEMS Microbiol. Rev.* **2006**, *30*, 36–52, doi:10.1111/j.1574-6976.2005.00002.x.

22. Zhang, Y.; Yew, W.W. Mechanisms of Drug Resistance in Mycobacterium Tuberculosis. *int j Tuberc Lung Dis* **2009**, *13*, 1320–1330.

23. Skaar, M.I.H. and E.P. Nutritional Immunity: Transition Metals at the Pathogen-Host Interface. *Nat Rev Microbiol* **2012**, *100*, 130–134, doi:10.1016/j.pestbp.2011.02.012.Investigations.

24. Andreini, C., Bertini, I., Cavallaro, G., Holliday, G. L., and Thornton, J.M. Metal Ions in Biological Catalysis : From Enzyme Databases to General Principles. *J Biol Inorg Chem* **2008**, *13*, 1205–1218, doi:10.1007/s00775-008-0404-5.

25. Andrews, S.C.; Robinson, A.K.; Rodr, F. Bacterial Iron Homeostasis. *FEMS Microbiol. Lett.* **2003**, *27*, 215–237, doi:10.1016/S0168-6445(03)00055-X.

26. Cassat, J.E.; Skaar, E.P. Iron in Infection and Immunity. *Cell Host Microbe* **2013**, *13*, 509–519, doi:10.1016/j.chom.2013.04.010.

27. Jabado, B.N.; Jankowski, A.; Dougaparsad, S.; Picard, V.; Grinstein, S.; Gros, P. Natural Resistance to Intracellular Infections : Natural Resistance – Associated Macrophage Protein 1 (NRAMP1) Functions as a PH-Dependent Manganese Transporter at the Phagosomal Membrane. *J. Exp. Med.* **2000**, *192*, 1237–1247, doi:10.1084/jem.192.9.1237.

28. Kuhn, Donald E., Baker, Beth D., Lafuse, William P., and Zwilling, B.S. Differential Iron Transport into Phagosomes Isolated from the RAW264.7 Macrophage Cell Lines Transfected with Nramp1Gly169 or Nramp1Asp169. *J. Leukoc. Biol.* **1999**, *66*, 113–119, doi:10.1002/jlb.66.1.113.

29. Tong, Y.; Guo, M. Bacterial Heme-Transport Proteins and Their Heme-Coordination Modes. *Arch. Biochem. Biophys.* **2009**, *481*, 1–15, doi:10.1016/j.abb.2008.10.013.

30. Snow, G.A. Isolation and Structure of Mycobactin T, a Growth Factor from

Mycobacterium Tuberculosis. *Biochem. J.* **1965**, *97*, 166–175, doi:10.1042/bj0970166.

31. Gobin, J.; Moore, C.H.; Reeve, J.R.; Wong, D.K.; Gibson, B.W.; Horwitz, M.A. Iron Acquisition by Mycobacterium Tuberculosis: Isolation and Characterization of a Family of Iron-Binding Exochelins. *Proc. Natl. Acad. Sci.* **1995**, *92*, 5189–5193, doi:10.1073/pnas.92.11.5189.
32. Lane, S.J.; Marshall, P.S.; Upton, R.J.; Ratledge, C.; Ewing, M. Novel Extracellular Mycobactins, the Carboxymycobactin from Mycobacterium Avium. *Tetrahedron Lett.* **1995**, *36*, 4129–4132, doi:10.1128/CMR.14.3.489.
33. Gobin, J.; Horwitz, M.A. Exochelins of Mycobacterium Tuberculosis Remove Iron from Human Iron-Binding Proteins and Donate Iron to Mycobactins in the M. Tuberculosis Cell Wall. *J. Exp. Med.* **1996**, *183*, 1527–1532, doi:10.1084/jem.183.4.1527.
34. Wells, R.M.; Jones, C.M.; Xi, Z.; Speer, A.; Danilchanka, O.; Doornbos, K.S.; Sun, P.; Wu, F.; Tian, C.; Niederweis, M. Discovery of a Siderophore Export System Essential for Virulence of Mycobacterium Tuberculosis. *PLoS Pathog* **2013**, *9*, e1003120, doi:10.1371/journal.ppat.1003120.
35. Sandhu, P.; Akhter, Y. Siderophore Transport by MmpL5-MmpS5 Protein Complex in Mycobacterium Tuberculosis. *J. Inorg. Biochem.* **2017**, *170*, 75–84, doi:10.1016/j.jinorgbio.2017.02.013.
36. Ratledge, C.; Ewing, M. The Occurrence of Carboxymycobactin , the Siderophore of Pathogenic Mycobacteria , as a Second Extracellular Siderophore in Mycobacterium Srnegrna t i S. *Microbiology* **1996**, *142*, 2207–2212, doi:10.1099/13500872-142-8-2207.
37. Rodriguez, G.M.; Smith, I. Identification of an ABC Transporter Required for Iron Acquisition and Virulence in Mycobacterium Tuberculosis Identification of an ABC

Transporter Required for Iron Acquisition and Virulence in Mycobacterium Tuberculosis. *J. Bacteriol.* **2006**, *188*, 424–430, doi:10.1128/JB.188.2.424.

38. Ryndak, M.B.; Wang, S.; Smith, I.; Rodriguez, G.M. The Mycobacterium Tuberculosis High-Affinity Iron Importer, IrtA, Contains an FAD-Binding Domain. *J. Bacteriol.* **2010**, *192*, 861–869, doi:10.1128/JB.00223-09.

39. Jones, C.M.; Niederweis, M. Mycobacterium Tuberculosis Can Utilize Heme as an Iron Source. *J. Bacteriol.* **2011**, *193*, 1767–1770, doi:10.1128/JB.01312-10.

40. Tullius, M. V; Harmston, C.A.; Owens, C.P.; Chim, N.; Morse, R.P.; Mcmath, L.M.; Iniguez, A.; Kimmey, J.M.; Sawaya, M.R.; Whitelegge, J.P.; et al. Discovery and Characterization of a Unique Mycobacterial Heme Acquisition System. *Proc Natl Acad Sci U S A* **2011**, *108*, 5051–5056, doi:10.1073/pnas.1009516108.

41. Pandey, R.; Rodriguez, G.M. A Ferritin Mutant of Mycobacterium Tuberculosis Is Highly Susceptible to Killing by Antibiotics and Is Unable To Establish a Chronic Infection in Mice. *Infect. Immun.* **2012**, *80*, 3650–3659, doi:10.1128/IAI.00229-12.

42. Waldron, K.J.; Robinson, N.J. How Do Bacterial Cells Ensure That Metalloproteins Get the Correct Metal ? *Nat. Rev. Microbiol.* **2009**, *6*, 25–35, doi:10.1038/nrmicro2057.

43. Rodriguez, G.M.; Neyrolles, O. Metallobiology of Tuberculosis. *Microbiol Spectr* **2014**, *2*, MGM2-0012–2013, doi:10.1128/microbiolspec.MGM2-0012-2013.

44. Botella, H.; Peyron, P.; Levillain, F.; Poincloux, R.; Poquet, Y.; Brandli, I.; Wang, C.; Tailleux, L.; Tilleul, S.; Charrire, G.M.; et al. Mycobacterial P 1-Type ATPases Mediate Resistance to Zinc Poisoning in Human Macrophages. *Cell Host Microbe* **2011**, *10*, 248–259, doi:10.1016/j.chom.2011.08.006.

45. Padilla-Benavides, T.; Long, J.E.; Raimunda, D.; Sassetti, C.M.; Argüello, J.M. A Novel

P1B-Type Mn2+-Transporting ATPase Is Required for Secreted Protein Metallation in Mycobacteria. *J. Biol. Chem.* **2013**, *288*, 11334–11347, doi:10.1074/jbc.M112.448175.

46. Hanna, N.; Koliwer-Brandl, H.; Lefrançois, L.H.; Kalinina, V.; Cardenal-Muñoz, E.; Appiah, J.; Leuba, F.; Gueho, A.; Hilbi, H.; Soldati, T.; et al. Zn2+ Intoxication of Mycobacterium Marinum during Dictyostelium Discoideum Infection Is Counteracted by Induction of the Pathogen Zn2+ Exporter Ctpc. *MBio* **2021**, *12*, 1–15, doi:10.1128/mBio.01313-20.

47. Maciąg, A.; Dainese, E.; Rodriguez, G.M.; Milano, A.; Provvedi, R.; Pasca, M.R.; Smith, I.; Palù, G.; Riccardi, G.; Manganelli, R. Global Analysis of the Mycobacterium Tuberculosis Zur (FurB) Regulon. *J. Bacteriol.* **2007**, *189*, 730–740, doi:10.1128/JB.01190-06.

48. Argüello, J.M.; Raimunda, D.; Padilla-Benavides, T. Mechanisms of Copper Homeostasis in Bacteria. *Front. Cell. Infect. Microbiol.* **2013**, *3*, 73, doi:10.3389/fcimb.2013.00073.

49. Andrei, A.; Öztürk, Y.; Khalfaoui-Hassani, B.; Rauch, J.; Marckmann, D.; Trasnea, P.I.; Daldal, F.; Koch, H.G. Cu Homeostasis in Bacteria: The Ins and Outs. *Membranes (Basel).* **2020**, *10*, 1–45, doi:10.3390/membranes10090242.

50. Osman, D.; Cavet, J.S. Copper Homeostasis in Bacteria. *Adv. Appl. Microbiol.* **2008**, *65*, 217–247, doi:10.1016/S0065-2164(08)00608-4.

51. Macomber, L.; Imlay, J.A. The Iron-Sulfur Clusters of Dehydratases Are Primary Intracellular Targets of Copper Toxicity. *Proc. Natl. Acad. Sci. U. S. A.* **2009**, *106*, 8344–8349, doi:10.1073/pnas.0812808106.

52. Solioz, M.; Stoyanov, J. V. Copper Homeostasis in Enterococcus Hirae. *FEMS Microbiol. Rev.* **2003**, *27*, 183–195, doi:10.1016/S0168-6445(03)00053-6.

53. Odermatt Alex, Suter Heinrich, Krapfs Reto, S.M. Primary Structure of Two P-Type ATPases Involved in Copper Homeostasis in Enterococcus Hirue. *Biochemistry* **1993**, *17*, 12775–12779.

54. Samanovic, M.I.; Ding, C.; Thiele, D.J.; Darwin, K.H. Review Copper in Microbial Pathogenesis : Meddling with the Metal. *Cell Host Microbe* **2012**, *11*, 106–115, doi:10.1016/j.chom.2012.01.009.

55. Cobine, P.; Wickramasinghe, W.A.; Harrison, M.D.; Weber, T.; Solioz, M.; Dameron, C.T. The Enterococcus Hirae Copper Chaperone CopZ Delivers Copper(I) to the CopY Repressor. *FEBS Lett.* **1999**, *445*, 27–30, doi:10.1016/S0014-5793(99)00091-5.

56. Outten, F.W.; Outten, C.E.; Hale, J.; O'Halloran, T. V. Transcriptional Activation of an Escherichia Coli Copper Efflux Regulon by the Chromosomal MerR Homologue, CueR. *J. Biol. Chem.* **2000**, *275*, 31024–31029, doi:10.1074/jbc.M006508200.

57. Outten, F.W.; Huffman, D.L.; Hale, J.A.; O'Halloran, T. V. The Independent Cue and Cus Systems Confer Copper Tolerance during Aerobic and Anaerobic Growth in Escherichia Coli. *J. Biol. Chem.* **2001**, *276*, 30670–30677, doi:10.1074/jbc.M104122200.

58. Rensing, C.; Fan, B.; Sharma, R.; Mitra, B.; Rosen, B.P. CopA : An Escherichia Coli Cu (I) -Translocating P-Type ATPase. *Proc Natl Acad Sci U S A* **2000**, *97*, 652–656, doi:10.1073/pnas.97.2.652.

59. Chaturvedi, K.S.; Hung, C.S.; Crowley, J.R.; Stapleton, A.E.; Henderson, J.P. The Siderophore Yersiniabactin Binds Copper to Protect Pathogens during Infection. *Nat. Chem. Biol.* **2012**, *8*, 731–736, doi:10.1038/nchembio.1020.

60. Wagner, D.; Maser, J.; Lai, B.; Cai, Z.; Barry, C.E.; Höner zu Bentrup, K.; Russell, D.G.; Bermudez, L.E. Elemental Analysis of Mycobacterium Avium -, Mycobacterium

Tuberculosis -, and Mycobacterium Smegmatis -Containing Phagosomes Indicates Pathogen-Induced Microenvironments within the Host Cell's Endosomal System . *J. Immunol.* **2005**, *174*, 1491–1500, doi:10.4049/jimmunol.174.3.1491.

61. Liu, T.; Ramesh, A.; Ma, Z.; Ward, S.K.; Zhang, L.; George, G.N.; Talaat, A.M.; Sacchettini, J.C.; Giedroc, D.P. CsoR Is a Novel Mycobacterium Tuberculosis Copper-Sensing Transcriptional Regulator. *Nat Chem Biol* **2007**, *3*, 60–68, doi:10.1038/nchembio844.

62. Ward, S.K.; Abomoelak, B.; Hoye, E.A.; Steinberg, H.; Talaat, A.M. CtpV: A Putative Copper Exporter Required for Full Virulence of Mycobacterium Tuberculosis. *Mol Microbiol* **2010**, *77*, 1096–1110, doi:10.1111/j.1365-2958.2010.07273.x.

63. Ward, S.K.; Hoye, E.A.; Talaat, A.M. The Global Responses of Mycobacterium Tuberculosis to Physiological Levels of Copper. *J Bacteriol* **2008**, *190*, 2939–2946, doi:10.1128/JB.01847-07.

64. Festa, R.A.; Jones, M.B.; Butler-Wu, S.; Sinsimer, D.; Gerads, R.; Bishai, W.R.; Peterson, S.N.; Darwin, K.H. A Novel Copper-Responsive Regulon in Mycobacterium Tuberculosis. *Mol Microbiol* **2011**, *79*, 133–148, doi:10.1111/j.1365-2958.2010.07431.x.

65. Gold, B.; Deng, H.; Bryk, R.; Vargas, D.; Eliezer, D.; Roberts, J.; Jiang, X.; Nathan, C. Identification of a Copper-Binding Metallothionein in Pathogenic Mycobacteria. *Nat Chem Biol* **2008**, *4*, 609–616, doi:10.1038/nchembio.109.

66. Wolschendorf, F.; Ackart, D.; Shrestha, T.B.; Hascall-Dove, L.; Nolan, S.; Lamichhane, G.; Wang, Y.; Bossmann, S.H.; Basaraba, R.J.; Niederweis, M. Copper Resistance Is Essential for Virulence of *Mycobacterium Tuberculosis*. *Proc. Nat. Acad. Sci. U. S. A.* **2011**, *108*, 1621–1626, doi:10.1073/pnas.1009261108.

67. Rowland, J.L.; Niederweis, M. A Multicopper Oxidase Is Required for Copper Resistance in Mycobacterium Tuberculosis. *J. Bacteriol.* **2013**, *195*, 3724–3733, doi:10.1128/JB.00546-13.

68. Hanson, R.S.; Hanson, T.E.; Hanson, R.S. Methanotrophic Bacteria. *Microbiol. Rev.* **1996**, *60*, 439–471, doi:10.1128/mr.60.2.439-471.1996.

69. Balasubramanian, R.; Rosenzweig, A.C. Copper Methanobactin: A Molecule Whose Time Has Come. *Curr. Opin. Chem. Biol.* **2008**, *12*, 245–249, doi:10.1016/j.cbpa.2008.01.043.

70. Kim, H.J.; Graham, D.W.; Dispirito, A.A.; Alterman, M.A.; Galeva, N.; Larive, C.K.; Asunskis, D.; Sherwood, P.M.A. Methanobactin , a Copper-Acquisition Compound from Methane-Oxidizing Bacteria. *Science.* **2004**, *305*, 16–19, doi:10.1126/science.1098322.

71. Wang, L.; Zhu, M.; Zhang, Q.; Zhang, X.; Yang, P.; Liu, Z.; Deng, Y.; Zhu, Y.; Huang, X.; Han, L.; et al. Diisonitrile Natural Product SF2768 Functions As a Chalkophore That Mediates Copper Acquisition in Streptomyces Thioluteus. *ACS Chem. Biol.* **2017**, *12*, 3067–3075, doi:10.1021/acschembio.7b00897.

72. S. T. Cole, R. Brosch, J. Parkhill, T. Garnier, C. Churcher, D. Harris, S. V. Gordon, K. Eiglmeier, S. Gas, C.E.B.I.; F. Tekaia, K. Badcock, D. Basham, D. Brown, T. Chillingworth, R. Connor, R. Davies, K. Devlin, T. Feltwell, S.G.; N. Hamlin, S. Holroyd, T. Hornsby, K. Jagels, A. Krogh, J. McLean, S. Moule, L. Murphy, K. Oliver, J. Osborne, M. A. Quail, M.-A. Rajandream, J. Rogers, S. Rutter, K. Seeger, J. Skelton, R. Squares, S. Squares, J. E. Sulston, K. Taylor, S.W.& B.G.B. Deciphering the Biology of Mycobacterium Tuberculosis from the Complete Genome Sequence. *Nature* **1998**, *394*, 651–653, doi:10.1038/29241.

73. Sampson, S.L. Mycobacterial PE/PPE Proteins at the Host-Pathogen Interface. *Clin Dev*

Immunol **2011**, *2011*, 497203, doi:10.1155/2011/497203.

74. Sampson, S.L.; Lukey, P.; Warren, R.M.; van Helden, P.D.; Richardson, M.; Everett, M.J. Expression, Characterization and Subcellular Localization of the Mycobacterium Tuberculosis PPE Gene Rv1917c. *Tuberculosis (Edinb).* **2001**, *81*, 305–317, doi:10.1054/tube.2001.0304.

75. Kruh, N.A.; Troudt, J.; Izzo, A.; Prenni, J.; Dobos, K.M. Portrait of a Pathogen : The Mycobacterium Tuberculosis Proteome In Vivo. *PLoS One* **2010**, *5*, doi:10.1371/journal.pone.0013938.

76. Cascioferro, A.; Delogu, G.; Colone, M.; Sali, M.; Stringaro, A.; Arancia, G.; Fadda, G.; Palù, G.; Manganelli, R. PE Is a Functional Domain Responsible for Protein Translocation and Localization on Mycobacterial Cell Wall. *Mol. Microbiol.* **2007**, *66*, 1536–1547, doi:10.1111/j.1365-2958.2007.06023.x.

77. Abdallah, A.M.; Verboom, T.; Hannes, F.; Safi, M.; Strong, M.; Eisenberg, D.; Musters, R.J.P.; Vandenbroucke-Grauls, C.M.J.E.; Appelmelk, B.J.; Luirink, J.; et al. A Specific Secretion System Mediates PPE41 Transport in Pathogenic Mycobacteria. *Mol. Microbiol.* **2006**, *62*, 667–679, doi:10.1111/j.1365-2958.2006.05409.x.

78. Abdallah, A.M.; Verboom, T.; Weerdenburg, E.M.; Gey Van Pittius, N.C.; Mahasha, P.W.; Jiménez, C.; Parra, M.; Cadieux, N.; Brennan, M.J.; Appelmelk, B.J.; et al. PPE and PE-PGRS Proteins of Mycobacterium Marinum Are Transported via the Type VII Secretion System ESX-5. *Mol. Microbiol.* **2009**, *73*, 329–340, doi:10.1111/j.1365-2958.2009.06783.x.

79. Lamichhane, G.; Zignol, M.; Blades, N.J.; Geiman, D.E.; Dougherty, A.; Grosset, J.; Broman, K.W.; Bishai, W.R. A Postgenomic Method for Predicting Essential Genes at

Subsaturation Levels of Mutagenesis: Application to Mycobacterium Tuberculosis. *Proc. Natl. Acad. Sci. U. S. A.* **2003**, *100*, 7213–7218, doi:10.1073/pnas.1231432100.

80. Rengarajan, J.; Bloom, B.R.; Rubin, E.J. Genome-Wide Requirements for Mycobacterium Tuberculosis Adaptation and Survival in Macrophages. *Proc. Natl. Acad. Sci. U. S. A.* **2005**, *102*, 8327–8332, doi:10.1073/pnas.0503272102.

81. Mycobrowser Available online: https://mycobrowser.epfl.ch/genes/Rv0097 (accessed on 5 July 2018).

82. Kerns, P.W.; Ackhart, D.F.; Basaraba, R.J.; Leid, J.G.; Shirtliff, M.E. Mycobacterium Tuberculosis Pellicles Express Unique Proteins Recognized by the Host Humoral Response. *Pathog Dis* **2014**, *70*, 347–358, doi:10.1111/2049-632X.12142.

83. Talaat, A.M.; Lyons, R.; Howard, S.T.; Johnston, S.A. The Temporal Expression Profile of Mycobacterium Tuberculosis Infection in Mice. *Proc. Natl. Acad. Sci.* **2004**, *101*, 4602–4607, doi:10.1073/pnas.0306023101.

84. Rosenkrands, I.; King, A.; Weldingh, K.; Moniatte, M.; Moertz, E.; Andersen, P. Towards the Proteome of Mycobacterium Tuberculosis. *Electrophoresis* **2000**, *21*, 3740–3756, doi:10.1002/1522-2683(200011)21:17<3740::AID-ELPS3740>3.0.CO;2-3.

85. Wang, F.; Langley, R.; Gulten, G.; Wang, L.; Sacchettini, J.C. Identification of a Type III Thioesterase Reveals the Function of an Operon Crucial for Mtb Virulence. *Chem Biol* **2007**, *14*, 543–551, doi:10.1016/j.chembiol.2007.04.005.

86. Liu, Z.; Ioerger, T.R.; Wang, F.; Sacchettini, J.C. Structures of Mycobacterium Tuberculosis FadD10 Protein Reveal a New Type of Adenylate-Forming Enzyme. *J Biol Chem* **2013**, *288*, 18473–18483, doi:10.1074/jbc.M113.466912.

87. Mycobrowser Available online: https://mycobrowser.epfl.ch/genes/Rv0101 (accessed on 5

July 2018).

88. Mawuenyega, K.G.; Forst, C. V.; Dobos, K.M.; Belisle, J.T.; Chen, J.; Bradbury, E.M.; Bradbury, A.R.M.; Chen, X. Mycobacterium Tuberculosis Functional Network Analysis by Global Subcellular Protein Profiling. *Mol. Biol. Cell* **2005**, *16*, 396–404, doi:10.1091/mbc.E04-04-0329.

89. Sassetti, C.M.; Boyd, D.H.; Rubin, E.J. Genes Required for Mycobacterial Growth Defined by High Density Mutagenesis. *Mol Microbiol* **2003**, *48*, 77—84, doi:10.1046/j.1365-2958.2003.03425.x.

90. Sassetti, C.M.; Rubin, E.J. Genetic Requirements for Mycobacterial Survival during Infection. *Proc. Natl. Acad. Sci. U. S. A.* **2003**, *100*, 12989–12994, doi:10.1073/pnas.2134250100.

91. Bhatt K, Machado H, Osório NS, Sousa J, Cardoso F, Magalhães C, Chen B, Chen M, Kim J, Singh A, Ferreira CM, Castro AG, Torrado E, Jacobs WR Jr, Bhatt A, S.M.A.N.P.S.G.D.V. in M. tuberculosis. mSphere. 2018 O. 31;3(5):e00352-18. doi: 10. 1128/mSphere. 0035.-18. P. 30381350; P.P. A Nonribosomal Peptide Synthase Gene Driving Virulence in Mycobacterium Tuberculosis. *mSphere* **2018**, *3*, 1–14, doi:10.1128/mSphere.00352-18.

92. Chhabra, A.; Haque, a. S.; Pal, R.K.; Goyal, A.; Rai, R.; Joshi, S.; Panjikar, S.; Pasha, S.; Sankaranarayanan, R.; Gokhale, R.S. Nonprocessive [2 + 2]e- off-Loading Reductase Domains from Mycobacterial Nonribosomal Peptide Synthetases. *Proc. Natl. Acad. Sci.* **2012**, *109*, 5681–5686, doi:10.1073/pnas.1118680109.

93. Parish, T.; Smith, D.A.; Roberts, G.; Betts, J.; Stoker, N.G. The SenX3-RegX3 Two-Component Regulatory System of Mycobacterium Tuberculosis Is Required for

Virulence. *Microbiology* **2003**, *149*, 1423–1435, doi:10.1099/mic.0.26245-0.

94. Raman, S.; Puyang, X.; Cheng, T.; Young, C.; Moody, D.B.; Husson, R.N.; Raman, S.; Puyang, X.; Cheng, T.; Young, D.C.; et al. Mycobacterium Tuberculosis SigM Positively Regulates Esx Secreted Protein and Nonribosomal Peptide Synthetase Genes and Down Regulates Virulence-Associated Surface Lipid Synthesis Mycobacterium Tuberculosis SigM Positively Regulates Esx Secreted Protein A. *J Bacteriol* **2006**, *188*, doi:10.1128/JB.01212-06.

95. Buglino, J.A.; Sankhe, G.D.; Lazar, N.; Bean, J.M.; Glickman, M.S. Integrated Sensing of Host Stresses by Inhibition of a Cytoplasmic Two-Component System Controls m. Tuberculosis Acute Lung Infection. *Elife* **2021**, *10*, doi:10.7554/eLife.65351.

96. Shey-Njila, O. Examining the Role of Mycobacterium Tuberculosis CtpB in Copper Transport. *Ph.D. Diss. Univ. Georg.* **2019**, 347.

97. Shey-Njila, O.; Hikal, A.F.; Gupta, T.; Sakamoto, K.; Azami, H.Y.; Watford, W.T.; Quinn, F.D.; Karls, R.K. CtpB Facilitates Mycobacterium Tuberculosis Growth in Copper-Limited Niches. *Int. J. Mol. Sci.* **2022**, *23*, doi:doi.org/10.3390/ijms23105713.

98. Chène, P. ATPases as Drug Targets: Learning from Their Structure. *Nat. Rev. Drug Discov.* **2002**, *1*, 665–673, doi:10.1038/nrd894.

99. Novoa-Aponte, L.; Soto Ospina, C.Y. Mycobacterium Tuberculosis P-Type Atpases: Possible Targets for Drug or Vaccine Development. *Biomed Res. Int.* **2014**, *2014*, doi:10.1155/2014/296986.

100. Novoa-Aponte, L.; León-Torres, A.; Patiño-Ruiz, M.; Cuesta-Bernal, J.; Salazar, L.M.; Landsman, D.; Mariño-Ramírez, L.; Soto, C.Y. In Silico Identification and Characterization of the Ion Transport Specificity for P-Type ATPases in the

Mycobacterium Tuberculosis Complex. *BMC Struct. Biol.* **2012**, *12*, doi:10.1186/1472-6807-12-25.

101. Gupta, H.K.; Shrivastava, S.; Sharma, R. A Novel Calcium Uptake Transporter of Uncharacterized P-Type ATPase Family Supplies Calcium for Cell Surface Integrity in Mycobacterium Smegmatis. *MBio* **2017**, *8*, 1–14, doi:10.1128/mBio.01388-17.

102. López, M.; Quitian, L.V.; Calderón, M.N.; Soto, C.Y. The P-Type ATPase CtpG Preferentially Transports Cd2+ across the Mycobacterium Tuberculosis Plasma Membrane. *Arch. Microbiol.* **2018**, *200*, 483–492, doi:10.1007/s00203-017-1465-z.

103. Chen, L.; Li, X.; Xu, P.; He, Z.-G. A Novel Zinc Exporter CtpG Enhances Resistance to Zinc Toxicity and Survival in Mycobacterium Bovis. *Microbiol. Spectr.* **2022**, *10*, doi:10.1128/spectrum.01456-21.

104. Ward, S.K.; Abomoelak, B.; Hoye, E.A.; Steinberg, H.; Talaat, A.M. CtpV: A Putative Copper Exporter Required for Full Virulence of Mycobacterium Tuberculosis. *Mol. Microbiol.* **2010**, *77*, 1096–1110, doi:10.1111/j.1365-2958.2010.07273.x.

105. León-Torres, A.; Novoa-Aponte, L.; Soto, C.Y. CtpA, a Putative Mycobacterium Tuberculosis P-Type ATPase, Is Stimulated by Copper (I) in the Mycobacterial Plasma Membrane. *BioMetals* **2015**, *28*, 713–724, doi:10.1007/s10534-015-9860-x.

106. León-Torres, A.; Arango, E.; Castillo, E.; Soto, C.Y. CtpB Is a Plasma Membrane Copper (I) Transporting P-Type ATPase of Mycobacterium Tuberculosis. *Biol. Res.* **2020**, *53*, 1–13, doi:10.1186/s40659-020-00274-7.

107. Hennigar, S.R.; McClung, J.P. Nutritional Immunity: Starving Pathogens of Trace Minerals. *Am. J. Lifestyle Med.* **2016**, *10*, 170–173, doi:10.1177/1559827616629117.

108. Yang, L.; McRae, R.; Henary, M.M.; Patel, R.; Lai, B.; Vogt, S.; Fahrni, C.J. Imaging of

the Intracellular Topography of Copper with a Fluorescent Sensor and by Synchrotron X-Ray Fluorescence Microscopy. *Proc. Natl. Acad. Sci. U. S. A.* **2005**, *102*, 11179–11184, doi:10.1073/pnas.0406547102.

109. Agarwal, P.; Khan, S.R.; Verma, S.C.; Beg, M.; Singh, K.; Mitra, K.; Gaikwad, A.N.; Akhtar, M.S.; Krishnan, M.Y. Mycobacterium Tuberculosis Persistence in Various Adipose Depots of Infected Mice and the Effect of Anti-Tubercular Therapy. *Microbes Infect.* **2014**, *16*, 571–580, doi:10.1016/j.micinf.2014.04.006.

110. Neyrolles, O.; Hernández-Pando, R.; Pietri-Rouxel, F.; Fornès, P.; Tailleux, L.; Payán, J.A.B.; Pivert, E.; Bordat, Y.; Aguilar, D.; Prévost, M.C.; et al. Is Adipose Tissue a Place for Mycobacterium Tuberculosis Persistence? *PLoS One* **2006**, *1*, doi:10.1371/journal.pone.0000043.

111. Ayyappan, J.P.; Ganapathi, U.; Lizardo, K.; Vinnard, C.; Subbian, S.; Perlin, D.S.; Nagajyothi, J.F. Adipose Tissue Regulates Pulmonary Pathology during TB Infection Janeesh. *MBio* **2019**, *10*, 1–16.

112. Li, P.; Gu, Y.; Li, J.; Xie, L.; Li, X.; Xie, J. Mycobacterium Tuberculosis Major Facilitator Superfamily Transporters. *J. Membr. Biol.* **2017**, *250*, 573–585, doi:10.1007/s00232-017-9982-x.

113. Via, L.E.; Lin, P.L.; Ray, S.M.; Carrillo, J.; Allen, S.S.; Seok, Y.E.; Taylor, K.; Klein, E.; Manjunatha, U.; Gonzales, J.; et al. Tuberculous Granulomas Are Hypoxic in Guinea Pigs, Rabbits, and Nonhuman Primates. *Infect. Immun.* **2008**, *76*, 2333–2340, doi:10.1128/IAI.01515-07.

114. Murdoch, C.C.; Skaar, E.P. Nutritional Immunity: The Battle for Nutrient Metals at the Host–Pathogen Interface Caitlin. *Nat Rev Microbiol* **2022**, *0123456789*.

115. Alibaud, L.; Rombouts, Y.; Trivelli, X.; Burguière, A.; Cirillo, S.L.G.; Cirillo, J.D.; Dubremetz, J.F.; Guérardel, Y.; Lutfalla, G.; Kremer, L. A Mycobacterium Marinum TesA Mutant Defective for Major Cell Wall-Associated Lipids Is Highly Attenuated in Dictyostelium Discoideum and Zebrafish Embryos. *Mol. Microbiol.* **2011**, *80*, 919–934, doi:10.1111/j.1365-2958.2011.07618.x.

116. Kessel, J.C. Van; Hatfull, G.F. Recombineering in Mycobacterium Tuberculosis. *Nat. Methods* **2007**, *4*, doi:10.1038/NMETH996.

117. Rodrigue, S.; Brodeur, J.; Jacques, P.É.; Gervais, A.L.; Brzezinski, R.; Gaudreau, L. Identification of Mycobacterial ?? Factor Binding Sites by Chromatin Immunoprecipitation Assays. *J. Bacteriol.* **2007**, *189*, 1505–1513, doi:10.1128/JB.01371-06.

118. Ananya Nandy, Anupam Kumar Mondal, Rajesh Pandey, Prabhakar Arumugam, Stanzin Dawa, Neetika Jaisinghani, Vivek Rao, Debasis Dash, G.S. Adipocyte Model of Mycobacterium Tuberculosis Infection. *Infect. Immun.* **2018**, *86*, 1–18, doi:10.1128/IAI.00041-18.

119. Wagner, D.; Maser, J.; Lai, B.; Cai, Z.H.; Barry, C.E.; Bentrup, K.H.Z.; Russell, D.G.; Bermudez, L.E. Elemental Analysis of Mycobacterium Avium-, Mycobacterium Tuberculosis-, and Mycobacterium Smegmatis-Containing Phagosomes Indicates Pathogen-Induced Microenvironments within the Host Cell's Endosomal System. *J. Immunol.* **2005**, *174*, 1491–1500, doi:174/3/1491 [pii].

120. Schwarzer, D.; Finking, R.; Marahiel, M.A. Nonribosomal Peptides: From Genes to Products. *Nat. Prod. Rep.* **2003**, *20*, 275–287, doi:10.1039/b111145k.

121. Henderson, J.P.; Crowley, J.R.; Pinkner, J.S.; Walker, J.N.; Tsukayama, P.; Stamm, W.E.;

Hooton, T.M.; Hultgren, S.J. Quantitative Metabolomics Reveals an Epigenetic Blueprint for Iron Acquisition in Uropathogenic Escherichia Coli. *PLoS Pathog.* **2009**, *5*, doi:10.1371/journal.ppat.1000305.

122. Snow, G.A. Mycobactins: Iron -Chelating Growth Factors from Mycobacteria. *Bacteriol. Rev.* **1970**, *34*, 99–125.

123. Drew, D.; North, R.A.; Nagarathinam, K.; Tanabe, M. Structures and General Transport Mechanisms by the Major Facilitator Superfamily (MFS). *Chem. Rev.* **2021**, *121*, 5289–5335, doi:10.1021/acs.chemrev.0c00983.

124. Aliaga, M.E.; López-Alarcón, C.; Bridi, R.; Speisky, H. Redox-Implications Associated with the Formation of Complexes between Copper Ions and Reduced or Oxidized Glutathione. *J. Inorg. Biochem.* **2016**, *154*, 78–88, doi:10.1016/j.jinorgbio.2015.08.005.

125. Ward, S.K.; Hoye, E.A.; Talaat, A.M. The Global Responses of Mycobacterium Tuberculosis to Physiological Levels of Copper. *J. Bacteriol.* **2008**, *190*, 2939–2946, doi:10.1128/JB.01847-07.

126. Wolschendorf, F.; Ackart, D.; Shrestha, T.B.; Hascall-Dove, L.; Nolan, S.; Lamichhane, G.; Wang, Y.; Bossmann, S.H.; Basaraba, R.J.; Niederweis, M. Copper Resistance Is Essential for Virulence of Mycobacterium Tuberculosis. *Proc. Nat. Acad. Sci. U. S. A.* **2011**, *108*, 1621–1626, doi:10.1073/pnas.1009261108.

127. Liao, D.; Fan, Q.; Bao, L. The Role of Superoxide Dismutase in the Survival of Mycobacterium Tuberculosis in Macrophages. *Jpn. J. Infect. Dis.* **2013**, *66*, 480–488, doi:10.7883/yoken.66.480.

128. Melly, G.; Purdy, G.E. Mmpl Proteins in Physiology and Pathogenesis of m. Tuberculosis. *Microorganisms* **2019**, *7*, 1–16, doi:10.3390/microorganisms7030070.

129. Schimo, S.; Wittig, I.; Pos, K.M.; Ludwig, B. Cytochrome c Oxidase Biogenesis and Metallochaperone Interactions: Steps in the Assembly Pathway of a Bacterial Complex. *PLoS One* **2017**, *12*, 1–19, doi:10.1371/journal.pone.0170037.

130. Fernando Antunes, and E.C. The Mechanism of Cytochrome C Oxidase Inhibition by Nitric Oxide. *Front. Biosci.* **2007**, 975–985.

131. Zhu, M.; Wang, L.; Zhang, Q.; Ali, M.; Zhu, S.; Yu, P.; Gu, X.; Zhang, H.; Zhu, Y.; He, J. Tandem Hydration of Diisonitriles Triggered by Isonitrile Hydratase in Streptomyces Thioluteus. *Org. Lett.* **2018**, *20*, 3562–3565, doi:10.1021/acs.orglett.8b01341.

132. Hotter, G.S.; Wards, B.J.; Mouat, P.; Besra, G.S.; Gomes, J.; Singh, M.; Bassett, S.; Kawakami, P.; Wheeler, P.R.; De Lisle, G.W.; et al. Transposon Mutagenesis of Mb0100 at the Ppe1-Nrp Locus in Mycobacterium Bovis Disrupts Phthiocerol Dimycocerosate (PDIM) and Glycosylphenol-PDIM Biosynthesis, Producing an Avirulent Strain with Vaccine Properties at Least Equal to Those of M. Bovis BCG. *J. Bacteriol.* **2005**, *187*, 2267–2277, doi:10.1128/JB.187.7.2267-2277.2005.

133. Dhar, N.; McKinney, J.D. Mycobacterium Tuberculosis Persistence Mutants Identified by Screening in Isoniazid-Treated Mice. *Proc. Natl. Acad. Sci. U. S. A.* **2010**, *107*, 12275–12280, doi:10.1073/pnas.1003219107.

134. Braunstein, M.; Bardarov, S.S.; Jacobs, W.R. Genetic Methods for Deciphering Virulence Determinants of Mycobacterium Tuberculosis. *Methods Enzymol.* **2002**, *358*, 67–99, doi:10.1016/S0076-6879(02)58081-2.

135. Bardarov, S.; Bardarov, S.; Pavelka, M.S.; Sambandamurthy, V.; Larsen, M.; Tufariello, J.A.; Chan, J.; Hatfull, G.; Jacobs, W.R. Specialized Transduction: An Efficient Method for Generating Marked and Unmarked Targeted Gene Disruptions in Mycobacterium

Tuberculosis, M. Bovis BCG and M. Smegmatis. *Microbiology* **2002**, *148*, 3007–3017, doi:10.1099/00221287-148-10-3007.

136. Kong, D.; Kunimoto, D.Y. Secretion of Human Interleukin 2 by Recombinant Mycobacterium Bovis BCG. *Infect. Immun.* **1995**, *63*, 799–803.

137. Quandt, J.; Hynes, M.F. Versatile Suicide Vectors Which Allow Direct Selection for Gene Replacement in Gram-Negative Bacteria. *Gene* **1993**, *127*, 15–21, doi:10.1016/0378-1119(93)90611-6.

138. Zebisch, K.; Voigt, V.; Wabitsch, M.; Brandsch, M. Protocol for Effective Differentiation of 3T3-L1 Cells to Adipocytes. *Anal. Biochem.* **2012**, *425*, 88–90, doi:10.1016/j.ab.2012.03.005.

139. Abreu, R.; Quinn, F.; Giri, P.K. Role of the Hepcidin-Ferroportin Axis in Pathogen-Mediated Intracellular Iron Sequestration in Human Phagocytic Cells. *Blood Adv.* **2018**, *2*, 1089–1100, doi:10.1182/bloodadvances.2017015255.

140. Manganelli, R.; Dubnau, E.; Tyagi, S.; Kramer, F.R.; Smith, I. Differential Expression of 10 Sigma Factor Genes in Mycobacterium Tuberculosis. *Mol. Microbiol.* **1999**, *31*, 715–724, doi:10.1046/j.1365-2958.1999.01212.x.

141. Van Kessel, J.C., Hatfull, G.F. Mycobacterial Recombineering. *Methods Mol. Biol.* **2008**, *435*.

142. Kong, D.; Kunimoto, D.Y. Secretion of Human Interleukin 2 by Recombinant Mycobacterium Bovis BCG. *Infect. Immun.* **1995**, *63*, 799–803, doi:10.1128/iai.63.3.799-803.1995.

143. Balasubramanian, R.; Kenney, G.E.; Rosenzweig, A.C. Dual Pathways for Copper Uptake by Methanotrophic Bacteria. *J. Biol. Chem.* **2011**, *286*, 37313–37319,

doi:10.1074/jbc.M111.284984.

144. Bobrov, A.G.; Kirillina, O.; Fetherston, J.D.; Miller, M.C.; Burlison, J.A.; Perry, R.D. The Yersinia Pestis Siderophore, Yersiniabactin, and the ZnuABC System Both Contribute to Zinc Acquisition and the Development of Lethal Septicaemic Plague in Mice. *Mol. Microbiol.* **2014**, *93*, 759–775, doi:10.1111/mmi.12693.

145. Worrall, J.A.R.; Vijgenboom, E. Copper Mining in Streptomyces: Enzymes, Natural Products and Development. *Nat. Prod. Rep.* **2010**, *27*, 742–756, doi:10.1039/b804465c.

146. Chairatana, P.; Sassone-Corsi, M.; Edwards, R.A.; Raffatellu, M.; Perez-Lopez, A.; George, M.D.; Zheng, T.; Nolan, E.M. Siderophore-Based Immunization Strategy to Inhibit Growth of Enteric Pathogens. *Proc. Natl. Acad. Sci.* **2016**, *113*, 13462–13467, doi:10.1073/pnas.1606290113.